Delft University of Technology

Graduation Project

The impact of Marine and Offshore Renewable Energy on the European Energy System Evolution

By

Eleftherios Mezilis

Student Number: 5633761

Master thesis submitted to the TU Delft Repository to obtain the diploma of Master of Science on Offshore and Dredging Engineering

Chair & Supervisor: **Dr. George Lavidas**
Examination Committee: **Jannis Langer MSc, PhD Candidate**

April, 2024

Acknowledgements

I would like to express my gratefulness
to my family and friends for their unwavering support throughout this journey,
especially to Kostas Krachtopoulos not only for his valuable assistance
on the programming part but also for his moral support,
and of course to Dr. George Lavidas
whose knowledge and guidance made this project possible.

Contents

List of Figures

List of Tables

Abstract

The European energy transition policies aim to mitigate the effects of climate change by moving away from fossils and promoting both onshore and offshore renewable energy technologies. Although onshore renewables are driving the transition so far, policymakers believe that in order to achieve the targets, the power grid must have access to the theoretically abundant energy present in the oceans. More specifically, these targets suggest that by 2050, around the continent there should be at least 340 GW of marine and offshore renewables for EU member-states, in addition with 125 GW for the UK.

The present study investigates the role of marine and offshore renewable technologies in 100% renewable energy scenarios, inspired by the European targets of 2030, 2040 and 2050. The assessment of their role is based on he upgraded version of the open-source PyPSA-Eur (Python for Power System Analysis - European Sector, v0.25.1) energy system modelling tool developed within the Marine Renewable Energies Lab (MREL) of TU Delft, the PyPSA-MREL-TUD. This version is designed to have access on wave and farshore wind resources. The PyPSA framework utilizes an extract of the entire ENTSO-e transmission network and ERA5 climate data. By using time-series of 2018 for both the energy demand and weather data, this energy system model attempts to find cost-optimal solutions for the configuration of the different components of the power system. The developments include the addition of three wave energy converters and two types of floating offshore wind turbines to the existing generators and their associated costs, as well as the upgrade of the spatial resolution of the GEBCO bathymetry dataset of the model. For wave power, the model can access shallow water, nearshore and farshore wave resources, while for wind power both bottom fixed and floating generators are sub-categorized according to their distance from shore. Two significant constraints of the model include minimum generator capacity constraints for wind and wave power, and 70 % energy equity per country.

The analysis of the results focuses mainly on the generator and storage system configuration of the system. An emphasis was also given on the required expansion of the transmission grid, and the objective's investment and operational costs. What is initially observed is the impact of the spatial resolution of the ERA5 dataset on wave energy converter installations, which underestimated the energy potential profiles. Capacity constrained versions of the scenarios showed that wave energy has a higher average hourly market value, but is highly susceptible to seasonal patterns. Although the performance is better during colder periods, wave converters suffer the most during the warmer periods and are also the first generator type to be curtailed. While offshore wind turbines were installed all around the continent, with the best candidates being France, Baltic and Scandinavian countries, Greece and Romania, wave converters were installed mostly in Portugal, Ireland and Italy. However, the accessibility of every country to the sea basins varies. Country-specific analysis of the model implies that, for the 2050 horizon scenario, there is still a high level of dependability of landlocked countries on solar energy, on their neighbours and on storage systems. The overall line capacity must increase by a factor of two.

1 Introduction

1.1 Overview

Controlling the extend of Global Warming for future generations' quality of life is an environmental target highly prioritized by all European countries. The European Climate Law (European Commission, March 2020 [1]) dictates that nations must decrease greenhouse gases net emissions by 55% until 2030 compared to 1990's emissions, and continue to achieve carbon neutrality by 2050. Since the Paris Climate Change Agreement, the global community accepts a 2°scenario as the upper limit on temperature growth for 2050, to prevent substantial climate changes to the planet.

As anticipated, this objective is accompanied by several challenges related with societal, financial, political and geopolitical factors. Over the years governments created policies with views to substitute conventional sources of electricity (i.e. petroleum, natural gas, coal etc) with renewable ones, mainly relying on hydro, solar and wind resources, making these technologies the focal points of the energy transition.

While onshore wind farms dominate Europe's overall wind power share, they come with significant drawbacks, with terrain roughness being a major one. The irregular landscape distorts the wind flow, posing challenges to the stability and reliability of electricity supply. In response to Europe's ambitious climate goals, there is a growing emphasis on expanding offshore energy solutions. This strategic shift includes both wind and ocean energy and is aimed at overcoming the limitations associated with energy discontinuity.

Europe has turned its attention to the vast oceanic energy resource. After deploying the first full-scale commercial open-sea wave testing facility in 2003, Europe gradually began to explore marine technologies by incorporating 42.9MW of tidal and wave energy into the mix. While marine power has not yet reached the same level of development as other types of power, Europe aspires to position it as a significant contributor to its energy network.

The global wave energy potential is estimated to be 32,000 TWh/year (Vannucchi et al., 2016 [2]), which is very close to the average annual energy consumption of the entire planet. With more than 1000 registered wave devices, and a large amount of energy contained in the waves, marine renewables remain relevant in the transition. They can play an important role in a multi-renewable zero-carbon future energy system.

One more benefit of marine renewables, is their reduced visual impact. Concerns arise from land-use restrictions, limiting suitable areas for renewable energy infrastructure. Specific regions, including forests, cultivated areas, protected zones, and urban fabric, are excluded from hosting renewable energy installations, posing challenges in overcoming obstacles related to public acceptance.

The technical and economical challenges associated to the development of a high-share renewable energy system have a significant impact on the deployment of offshore and marine renewables. Identifying regions conducive to this deployment is crucial for establishing energy trajectories. This involves specifying the resource availability, understanding variability patterns, determining the required anti-variability measures, and estimating the necessary transmission expansion.

The renewable energy field has attracted extensive research attention, particularly focused on exploring power conversion principles and enhancing efficiency. While wind and solar energy have received significant research interest, wave energy remains promising but less explored in the context of integrating it into a power system. Most of the research on wave energy has focused on the assessment of the theoretical potential and the energy contained in the waves with some of the research investigating site-specific performances of different wave energy converters. Additionally, research has been made on the optimization of the hydrodynamics and the array layouts of potential wave energy farms. In this project, the aim is to explore the role of marine renewable energies as part of a power system.

1.2 Objectives

All of the financial, sociopolitical, and technical challenges add multiple layers of complexity to the successful deployment of offshore and marine renewable energy technologies. A complete energy system should be the result of a well-combined tuning of the aforementioned considerations, ensuring a harmonious integration of diverse energy sources and storage units, while addressing the constraints and opportunities presented by each. A useful tool that allows us to have a needs-based view of the future system and suggests an optimized path to achieve it is power system modelling. By introducing the challenges as variables in a modelling environment and configuring them with respect to valid assumptions and limitations, we can analyze potential scenarios and identify possible constraints. This way we can propose strategies for overcoming the hurdles that arise in the development and integration of offshore and marine renewable energy technologies. This modeling approach could facilitate decision-making, providing useful insight for policymakers, investors, and stakeholders to navigate the complexities of the energy transition.

Understanding the dynamics of a multi-source energy system is a key factor in the design of that solution. All the more so when this system involves an international electricity network, with different weather and geomorphological conditions from one region to another, and is required to be converted into a 100% "clean" system. The objective of this research is to assess the ability of marine and offshore wind renewables to be a considerable and possibly the leading option for the transition of the 2050 European energy system. To meet Europe's 2050 energy needs, deploying high-capacity marine renewables requires careful planning. This plan necessitates upgrading the energy transmission network, involving the installation of higher-capacity lines to transfer electricity from sea to shore and meet growing demand.

The use of an energy system model can be highly helpful as it can examine the feasibility of the target, give an idea of the economic framework, incorporate the necessary parameters on which the planning is based, such as weather conditions and the available area for development, and narrow down the options by providing a set of pathways. This thesis will make use of the upgraded version of the open-source PyPSA-Eur (Python for Power System Analysis - European Sector, v0.25.1) energy system modelling tool developed within the Marine Renewable Energies Lab (MREL) the PyPSA-MREL-TUD. This model is a dynamic energy system model generated from datasets of the European power system built on PyPSA, coupled with metocean climate data.

The aim is to simulate an energy system and create an optimized scenario with a determined share of power from specific technologies and regions. The end result of such a model is expected to provide an energy system that integrates renewable technologies to form a future high-share and multi-renewable European grid.

The overall objective of this research is to further explore the potential of renewable energy sources in order to solve the continuing problem of environmental pollution in the sector of electricity production. Since the Paris Agreement, a legally binding international treaty on climate change, Europe is committed to being a pioneer in fighting Global Warming, thereby all additional knowledge and research could accelerate the achievement of its targets.

1.3 Research Questions

In order to address the objective of this thesis with clarity, we will attempt to provide insight in the following research points and questions:

- How does the modeling of a power system vary with different spatial and temporal resolutions, considering time as the iterations of the optimization process and space as the spatial resolution of the network and the bathymetry?
- Validating 300GW of wind and 40 GW of marine capacity in Europe, plus 150GW of offshore and marine technologies for the UK.
- What is the role of Wave and Offshore Wind energy technologies in the context of a 2050 carbon-neutral scenario?
- What is the role of anti-variability measures on a fully-renewable energy system and its contribution on electricity supply stability?
- Economic assessment of a Renewable Power System.
- What are the geographic constrains that affect the deployment of Marine and Offshore technologies?

2 Literature Review

The literature review of this thesis begins with a listing and review of the commitments of Europe regarding the transition, and an overview of the achieved targets so far. It is followed by an analysis of the European Transmission Grid and the feasibility of an all-renewable energy system. Subsequently, the main offshore and marine Renewable technologies used in the work are introduced and explained. Finally, a brief description of the model's software and its functionalities are provided.

2.1 Commitments and Policies of Europe towards the Energy Transition

Assuring European citizens of a smooth transition to a carbon-neutral energy system is challenging. The Paris Agreement sets a goal to limit global warming to no more than 2°C. It aims to enhance the global response to climate change, encouraging countries to mitigate its effects. The Treaty on the Functioning of the European Union (TFEU) has long proposed Article 191 [3], promoting environmental goals such as preserving and improving the environment, safeguarding human health, responsible resource use, and global climate action.

Developing an inclusive European policy requires considering regional environmental variations and the economic and social conditions of each country. Many nations, both within and outside the EU, have enacted long-term climate legislation. By February 2020, ten EU Member States had climate laws, with seven having set long-term objectives [4]. Additionally, seven more Member States are contemplating climate legislation. Beyond the EU, five European and several non-European countries have passed climate laws since 2015 [5], the year of the Paris Agreement.

In October 2017, the European Parliament urged the European Commission (EC) to develop a zero-emission strategy for the EU by mid-century following COP23 [6]. The European Parliament reinforced the 1.5°C target in October 2018, mandating a target of reducing net greenhouse gas emissions by at least 55% by 2030, compared to 1990 levels ("Fit for 55")[7]. To legally bind EU states, the EC proposed a European Climate Directive on March 4^{th}, 2020. This enhances the long-term EU climate action, aiming for at least 55% greenhouse gas reduction by 2030 and 95% by 2050. A key component of the "Fit for 55" package is the revision of the 2009 Renewable Energy Directive (RED I) to RED II [8], pushing for at least 32% renewable energy (RES) in total energy consumption by 2030.

The REPowerEU plan [9], which was a response to the Russian-Ukrainian conflict, seeks to further raise the RES target to 45% by 2030. It emphasizes the need for Europe's independence from Russian fossil fuels and foresees a total renewable energy capacity of 1,236 GW, exceeding Fit for 55's projection of 1,067 GW. According to EC [10], the total energy demand of Europe rises more than 36% between 2020 and 2050.

To achieve these goals, Europe aims to tap into diverse sustainable sources. The continent is surrounded by five sea basins, where offshore technologies offer energy production opportunities. In an effort to harness the ocean's theoretical boundless energy, the policies concern mostly offshore wind and wave energy technologies. Like every renewable source, marine energy faces challenges: variable energy sources due to weather fluctuations and high development and maintenance costs, impacting the levelized cost of energy (LCOE) and locational marginal electricity prices. These obstacles complicate the technology advancement.

The EU Offshore Strategy set deployment targets for ocean energy of 100 MW by 2025. The share of offshore wind and ocean energy grows rapidly by 2030, where the strategy aims to have at least 60 GW of offshore wind capacity constructed, along with 1 GW of ocean energy, and by 2050, 300 GW and 40 GW, respectively. These numbers do not include the UK which since it exited EU, developed similar plans for 2030 and 2050 as well with hopes to deploy up to 50 GW of offshore wind, 5 GW of which will be floating for the year 2030, and ambition to raise the capacity to 125 GW by 2050, together with 22 GW for marine energies [11].

Nonetheless, the share of renewables in the electricity mix is set to rise from 37% in 2021 to 69% in 2030. The European Commission's EU Offshore Strategy, detailed in a 2020 publication (COM(2020)741) [12], outlines steps for long-term sustainable offshore renewable energy development. The strategy foresees the installation of 116 GW of new wind farms in Europe from 2022 to 2026, fostering offshore energy growth.

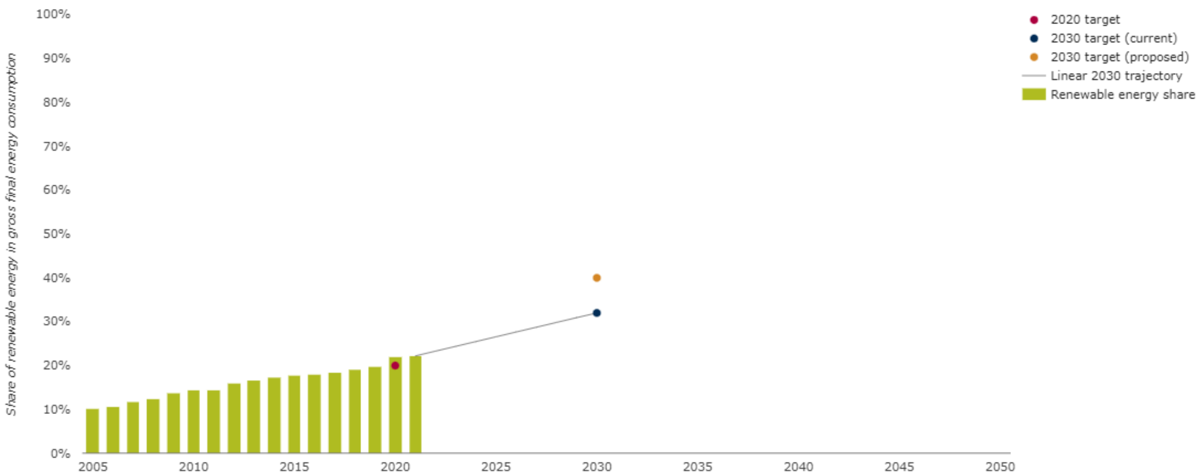

Figure 1: Projection of RES share in Europe, European Environment Agency [13].

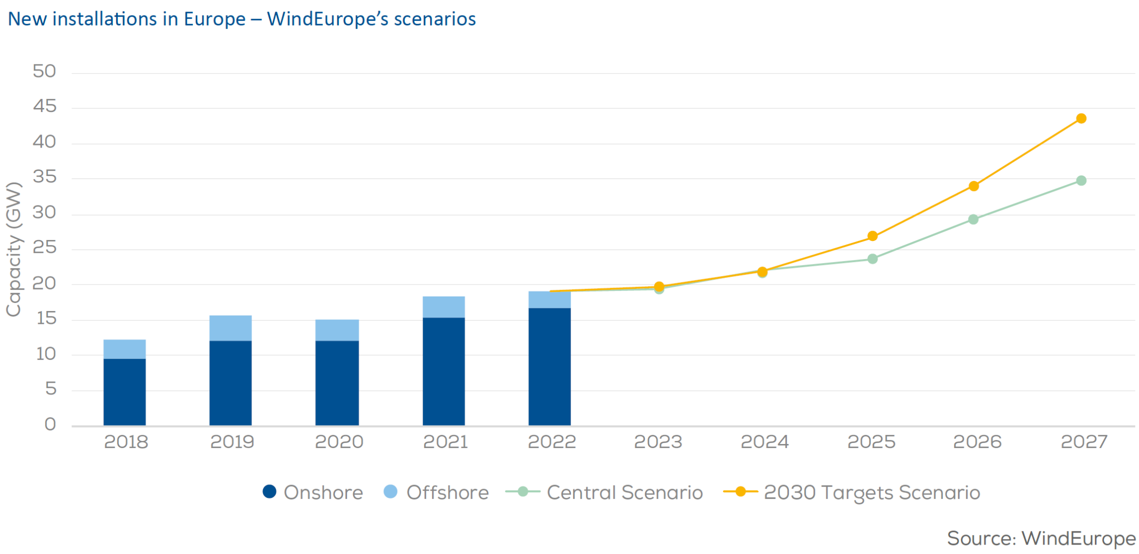

Figure 2: Scenarios of additional onshore and offshore wind installations for the 2023-2027 period in Europe, WindEurope [14].

The EU Member States, like many other nations, recognizes the need for integrating energy storage systems into the transition to a sustainable, multi-renewable energy system. To ensure a continuous energy supply, consumption must match production. Excess energy can be stored when production exceeds consumption. Two technologies that draw most of the attention are battery storage and hydrogen production via electrolysis using electricity. These technologies are employed when production falls short of demand. However, research on a highly renewable European electricity system (Schlachtberger et al., 2017 [15]) suggests that upgrading the transmission grid is more cost-effective than relying solely on storage. Integrated storage units within a complex transmission grid can help balance renewable energy variability. Each nation should tailor the capacity and dispatch of renewable energy plants according to geographic and weather conditions.

To further compensate energy stability, in the report of the EU Offshore strategy, there is a segment regarding hydrogen storing systems. More specifically, according to the EU Hydrogen Strategy, an ambitious 40GW of electrolyzers need to be installed in the EU by 2030 across all energy sectors, 6GW of which are planned until the end of 2024 [16]. Additionally, according to a report of the European Association of Storage of Energy [17], Europe needs to install at least 14 GW of battery storage units per year for the 200GW target capacity by 2030, and for 2050 this number must be increased to 600GW.

According to the Intergovernmental Panel on Climate Change (IPCC) special report on the impacts of global warming [18], managing total long-lived greenhouse gas emissions is a necessity for all 1.5°C pathways. Apart from the amount of non emitted GHG from electricity production there is also the possibility of greenhouse gasses removal. They insist on incorporating natural sinks that passively absorb carbon (forests, soils, wetlands) or negative emission carbon-capturing technologies consisting [19].

In a global scale, the International Renewable Energy Agency, IRENA, an intergovernmental agency devoted in the energy transition and carbon-neutrality, suggests a minimum action of tripling the globally installed capacity of renewables by 2030. In their Renewable Power Generation Costs in 2022 Report [20], IRENA claims that the average global LCOE of most of the renewable technologies has continued to decline until 2022. An exception is offshore wind which rose by 2% during 2022, driven by the simultaneous increase of offshore wind farm turbine sizes and optimization of the capacity factors, and the increase of wind farms' distance from the shore that require larger initial investment. The general increase of capacity factors and optimization of the technologies has shown their ability to be competitive in the energy market. IRENA believes that with the impending fuel crisis in 2022 and 2023, humanity should seize the opportunity and methodically turn its gaze to renewables.

2.2 Assessment of Renewable Power to date and the prospects of Marine Technologies

Europe's efforts to be a pioneering force in green transition, are reflected by the share of renewable energy in terms of consumed energy. More specifically, in Europe consumption provided by renewables more than doubled between 2004 and 2022, reaching 23% in 2022 share of its gross total energy consumption.

A smaller relative growth between 2020-2021 was due to a drastic deterioration of development caused by the COVID-19 pandemic. Energy consumption diminished in general in Europe during this period. At the same time, the share of RES appeared to slightly increase as these sources continued to produce electricity with almost the same rate as the previous year, when the non-renewable sources where used significantly less.

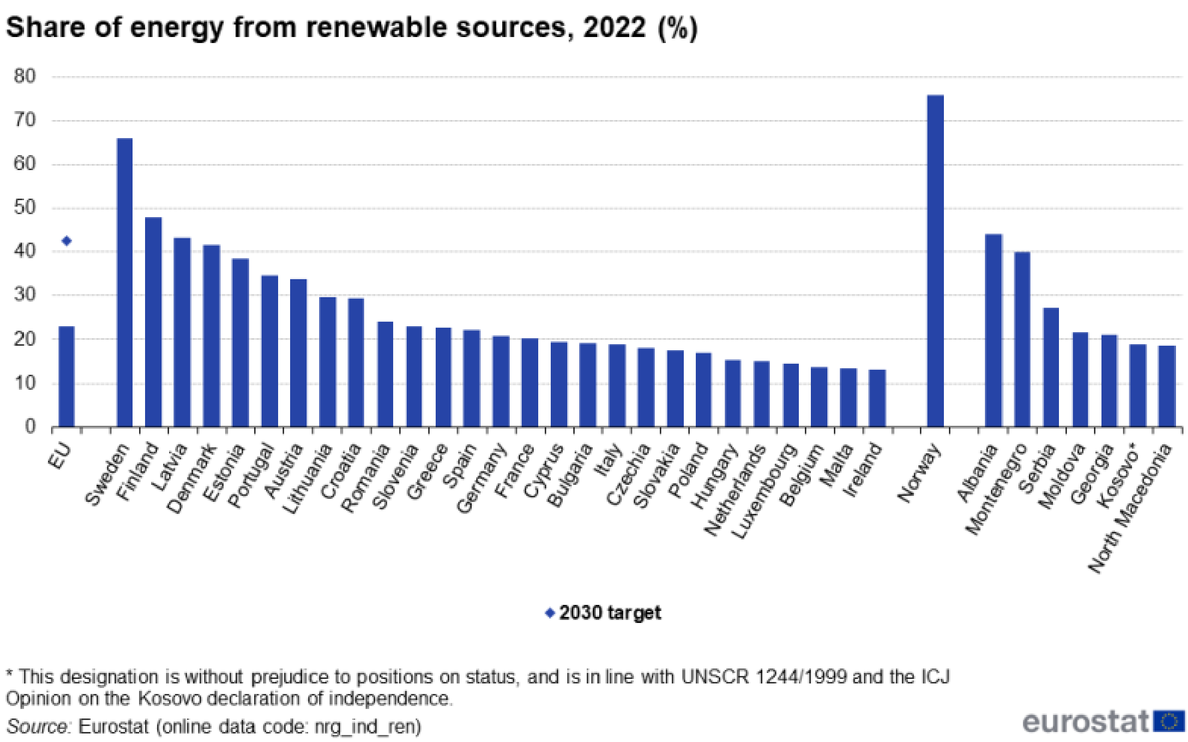

Figure 3: Share of energy from renewable sources, 2022 (% of gross final energy consumption), Eurostat [21].

As shown in Figure 3, Sweden (66%) had by far the greatest percentage of renewable energy in its gross final energy consumption among EU Member States (excluding Norway) in 2021, followed by Finland (47.9%) and Latvia (43.3%). The countries with the lowest percentages of renewable energy sources were

Malta (13.4 %), Belgium (13.8 %) and Luxembourg (14.4 %). Outside of EU, and on the top of the European leaderboard is Iceland and Norway reaching almost 100% of generation of their electricity by renewables, most of it being hydropower and wind.

As of 2022, Europe has installed 255 GW of wind turbines (WindEurope, [22]). Their share in the electricity production reached 489TWh, 18% of a total of 2,641TWh for Europe that same year. With the increasing demand for a stable power supply, wind farms have expanded to deeper and more remote locations since the generation seems more promising there. Figure 4 provides an overview of the potential energy yield in onshore and offshore regions of Europe according to the Global Wind Atlas wind dataset.

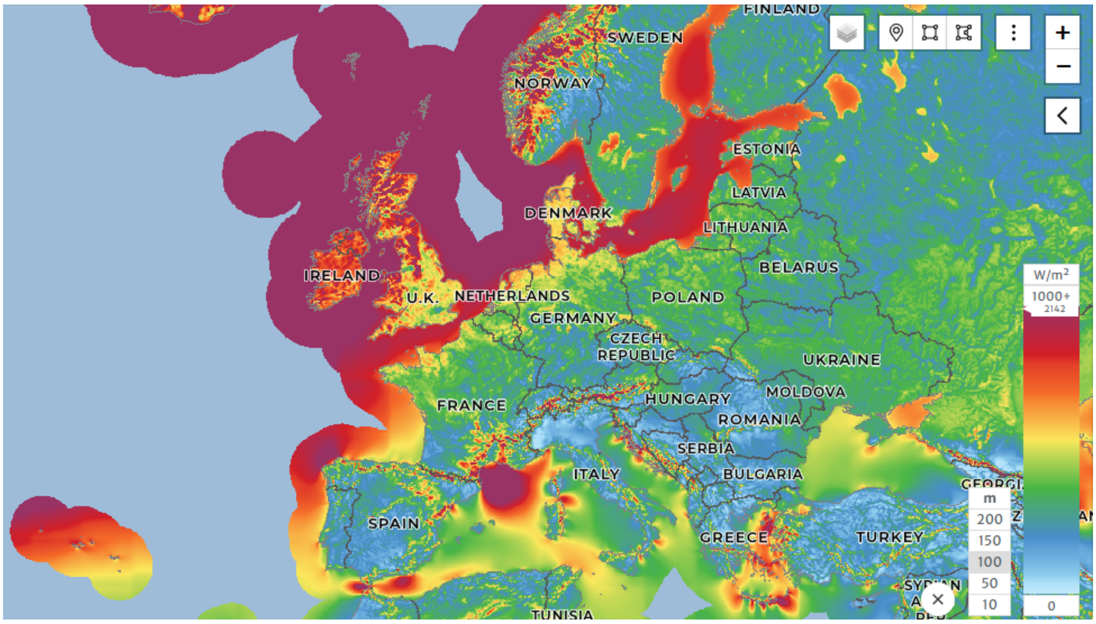

Figure 4: Wind energy yield in Europe according to wind speeds at 100m height above terrain, The Global Wind Atlas [23].

Offshore wind farms have already began to be installed in deeper seas, primarily utilizing bottom-fixed structures. These bottom-fixed turbines are typically cost-effective for water depths of 20–40 meters with some structure types, given the right conditions have reached 60 meters (Jian et al., 2021 [24]). In order to harness deep water wind resources, floating turbine technology needs to be integrated, capable of generating electricity in water depths exceeding 50 meters.

The EU plays a leading role in offshore technology and the renewable energy sector, as emphasized by the EU Offshore Strategy (Eurostat, 2020 [25]). In 2019, an impressive 93% of Europe's installed offshore capacity was fabricated within the EU, a testament to early decisions in establishing competitive markets for bottom-fixed offshore wind farms. The EU-27 offshore wind market represents 42% (12 GW) of the global market's total installed capacity, with the UK (9.7 GW) and China (6.8 GW) following. Eurostat also mentions that as of 2021, the EU's installed offshore wind capacity reached 14.6 GW and is projected to expand at least 25-fold by 2030. Figure 5 shows offshore installations around Europe and their stage of operation.

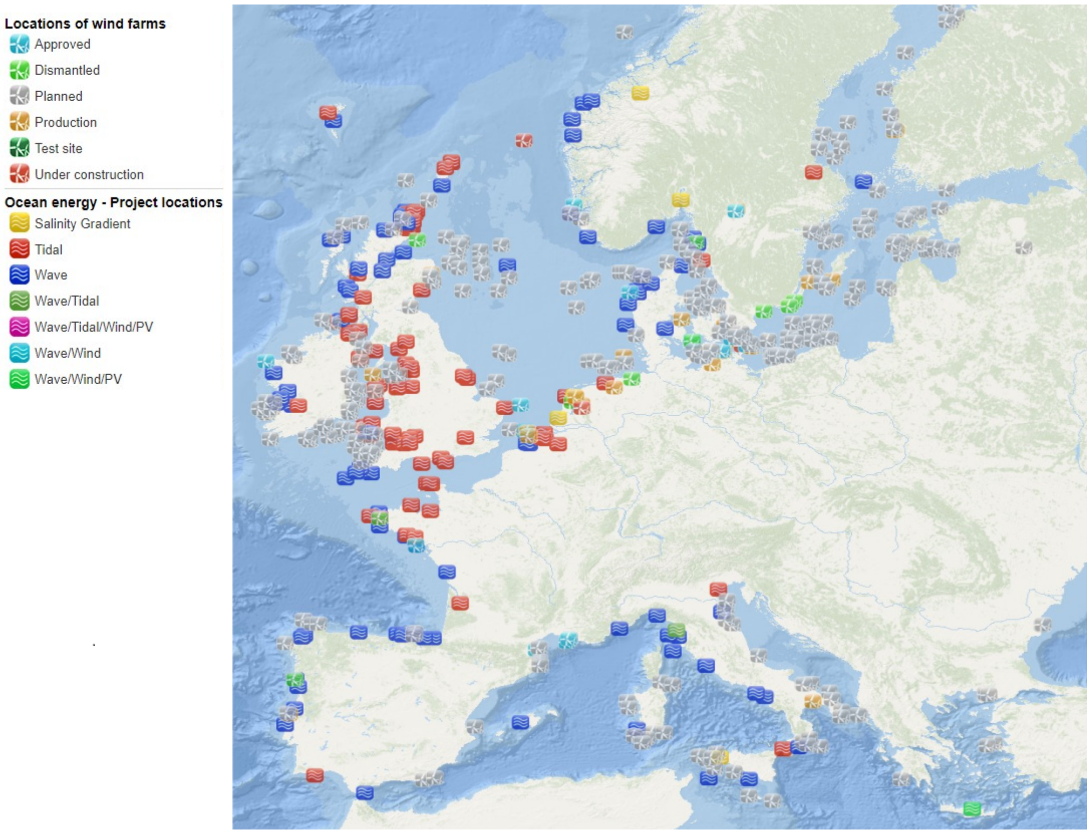

Figure 5: Offshore renewable powerplants in Europe and their stage of installation and operation, European Atlas of the Seas [26].

In general, according to WindEurope [27], 129 GW of new wind farms are expected to be installed between the years 2023-2027 in the European continent with a rate of around 20GW per year, 75% of which is estimated to be onshore. They mention that the installation rate of wind turbines should be raised to 30GW per year, if Europe was to meet its 2030 year targets. For offshore wind specifically, taking into account that 28GW is already installed, with respect to 2022, Europe needs to install around 9GW of turbines per year. Since the 2022 cumulative offshore wind installation reached only 2.5GW (figure 6), Europe needs to ramp-up the installation rate by a considerable amount. The average installation rate reaches 13.5GW per year, for target year 2050.

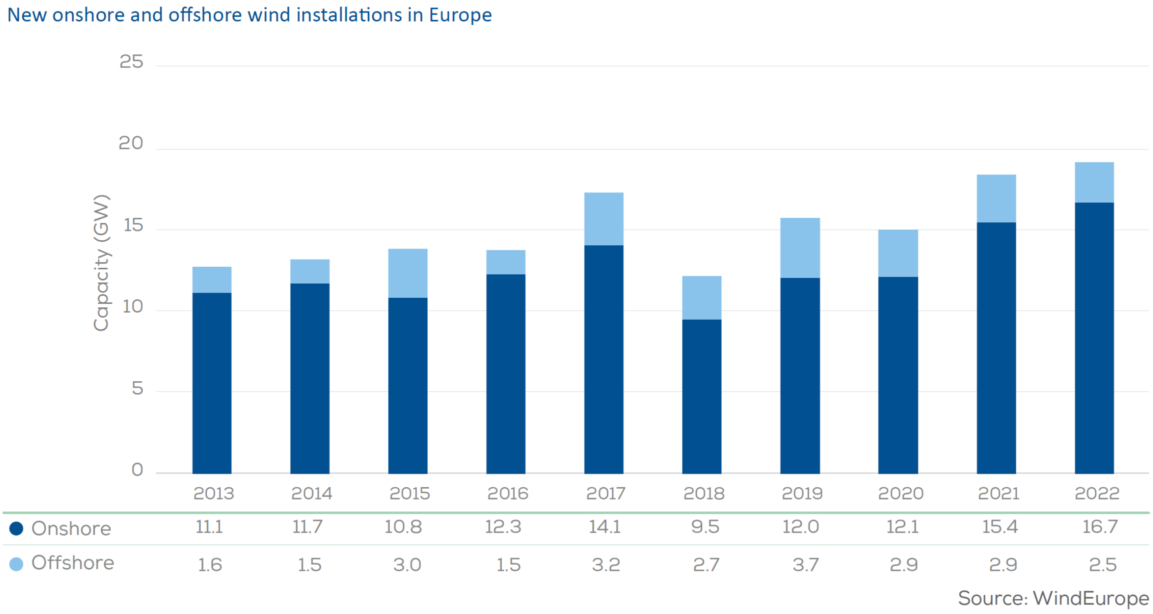

Figure 6: Annual onshore and offshore wind power installations in Europe, WindEurope [27].

While ocean energy technologies are not as advanced as the wind ones, the EU industry is still a global leader in the development of wave and tidal energy systems as well. 66% and 44% of wave and tidal energy patents in the industry are held by EU-based enterprises, according to Ocean Energy Europe (OEE) [28], with 12.7MW of wave energy converters installed around Europe since 2010 for testing and assessment. Currently only 400kW of wave converters is contributing in the production.

Figure 7 presents the average power density of waves around Europe based on NOAA WaveWatch III wave dataset, as calculated in Gunn et al., 2012. They observed a significant wave resource mainly available in the west coasts of land bodies.

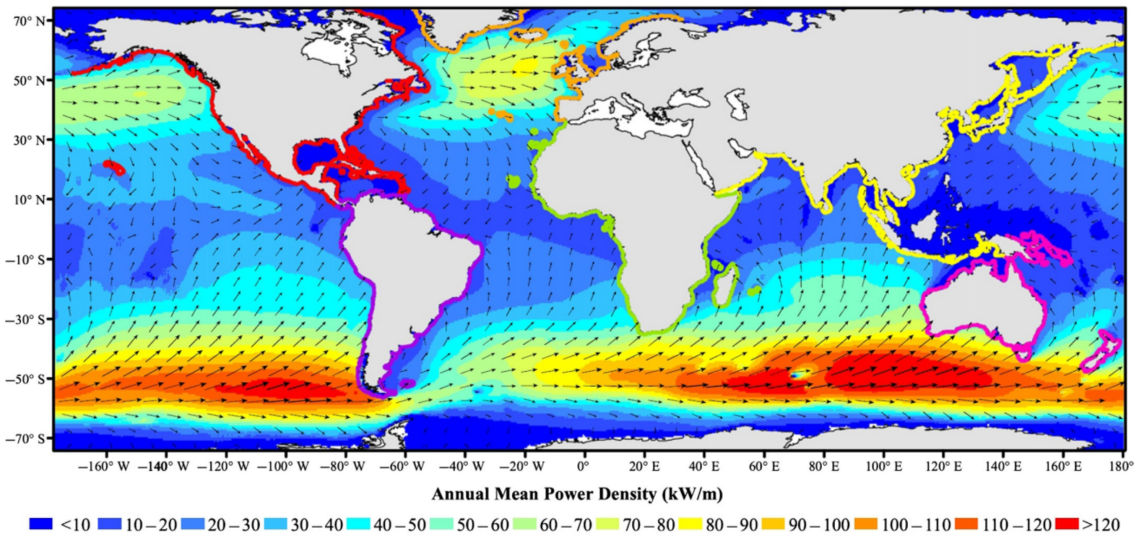

Figure 7: Global annual mean wave power density, Gunn et al., 2012 [29].

Tidal energy has an advantage, having reached 30.2MW, 13MW of which is operating. Other technologies being developed in Europe include floating solar systems, already deployed in landlocked waters but mainly at the research and demonstration stage at the sea with only 17 kW installed yet, ocean thermal energy conversion (OTEC), and algae biofuels (biodiesel, biogas, bioethanol).

Lastly, a widely exploited source of energy in Europe, already mentioned, is hydro-power with 258GW installed as of 2022. Hydropower is currently dominating in the share of renewable electricity worldwide and in Europe specifically mostly because it is a well known technique that has been applied for centuries. Some countries, Iceland and the Scandinavian countries for example, have the advantage of water abundance and suitable landscape, offering the circumstances for an effective power plant. Most of the regions however, suffer from insufficient river flow, precipitation and land elevation. The hydroelectrical power potential is in theory high, 15,000TWh per year according to IRENA 2022, but historical data show that the actual power output per year is significantly lower. This justifies the fact that, even though hydropower is more widely installed in Europe, its electricity consumption share was surpassed in the last years, falling behind by around 7.5% in 2022.

2.3 Power System Planning, Transmission Grid of Europe and Geographical constraints

The use of renewable energy sources depends to a large extent on the alignment of energy prices with their costs. Renewable energy provision faces challenges from natural factors, such as weather, terrain morphology, and human-made factors, such as technology progress and social acceptance. Overcoming these obstacles relies on the development of a cost effective and sustainable energy system.

For renewables, supply problems could be caused in days with low feed-in of energy due low intensity weather conditions. This can have an impact on the ability of countries to meet their energy demands consistently. Schlachtberger et al., 2017 [15] suggest addressing this issue by developing an interconnected transmission grid. Countries can share and balance their renewable energy resources, promoting a more equitable distribution of energy across the continent. This approach can enhance energy security but also contribute to the overall success of the European energy transition .

Additionally, in T. Brown's research on the European transmission network [30], it is found that offshore wind developments (based on 2050 targets) affected the transmission expansion the most compared to PV and onshore wind. The reason for this is the need of grid upgrades required to transfer power from the coast to the land.

Europe's electricity network is interconnected and allows the transfer of energy across borders. Transmission System Operators (TSOs) are the service managers of this infrastructure. An association that seeks to develop a pan-European transmission network with respect on the 2050 European targets, is the European Network of Transmission System Operators for Electricity (ENTSO-E). ENTSO-E represents 39 TSOs in 35 countries and aims to ensure a consistent, secure, and efficient electricity supply. ENTSO-E plays a crucial role in shaping energy policy and legislation by enabling Europe to become the first climate-neutral continent by 2050, promoting a pan-European electricity market, integrating renewable energy sources and promotes the cooperation among the TSOs.

Another key consideration affecting energy consumption is population numbers. Population projections for Europe in 2050 indicate stability, but increased accessibility and energy efficiency may increase energy consumption. This trend will most probably increase the load demands and call for improvements to the grid. Research on the relation between economic and population growth with carbon intensity in Dong et al. 2018 [32] confirms that there exists a large level of proportionality between the two.

Power system planning can help on recognizing challenges in energy transition and transmission upgrades, enabling realistic scenario creation and informed decision-making. Trondle et al. [33] emphasized the critical cost factor of mitigating variable renewable power, highlighting a trade-off between supply scale and infrastructure. Their study introduced a European transmission grid model, revealing that leveraging the grid for long-distance electricity transfers from Europe's ample resources to demand centers is cost-effective but requires substantial network expansion—potentially doubling the current infrastructure.

Conversely, balancing regional supply on a continental scale demands far less transmission capacity, roughly equivalent to today's system, if cross-border lines can transfer twice the energy. Meanwhile, Eriksen et al. [34] suggested interconnecting transmission between countries to balance wind and solar fluctuations, favoring it over excessive energy storage due to future cost concerns. Additionally, Brown et al. [35] supports that while expanding the grid is technically feasible, socio-economic factors such as public acceptance of overhead power lines may pose potential challenges.

The relationships among states participating in an integrated electricity network is equally crucial. This interconnected network spans between borders and water bodies to balance demand, requiring trading of energy among states due to unequal access to desired energy sources. Typically, TSOs, which are not all governmental, seek to find the region where generation is inexpensive, buy the energy and make revenue by transmitting it to another region with high energy demand. Some regions, like Hungary or Slovakia, face obvious disadvantages in an all-renewable energy power system that relies mostly on offshore technologies, as they do not have the access to high output offshore energy and could depend on

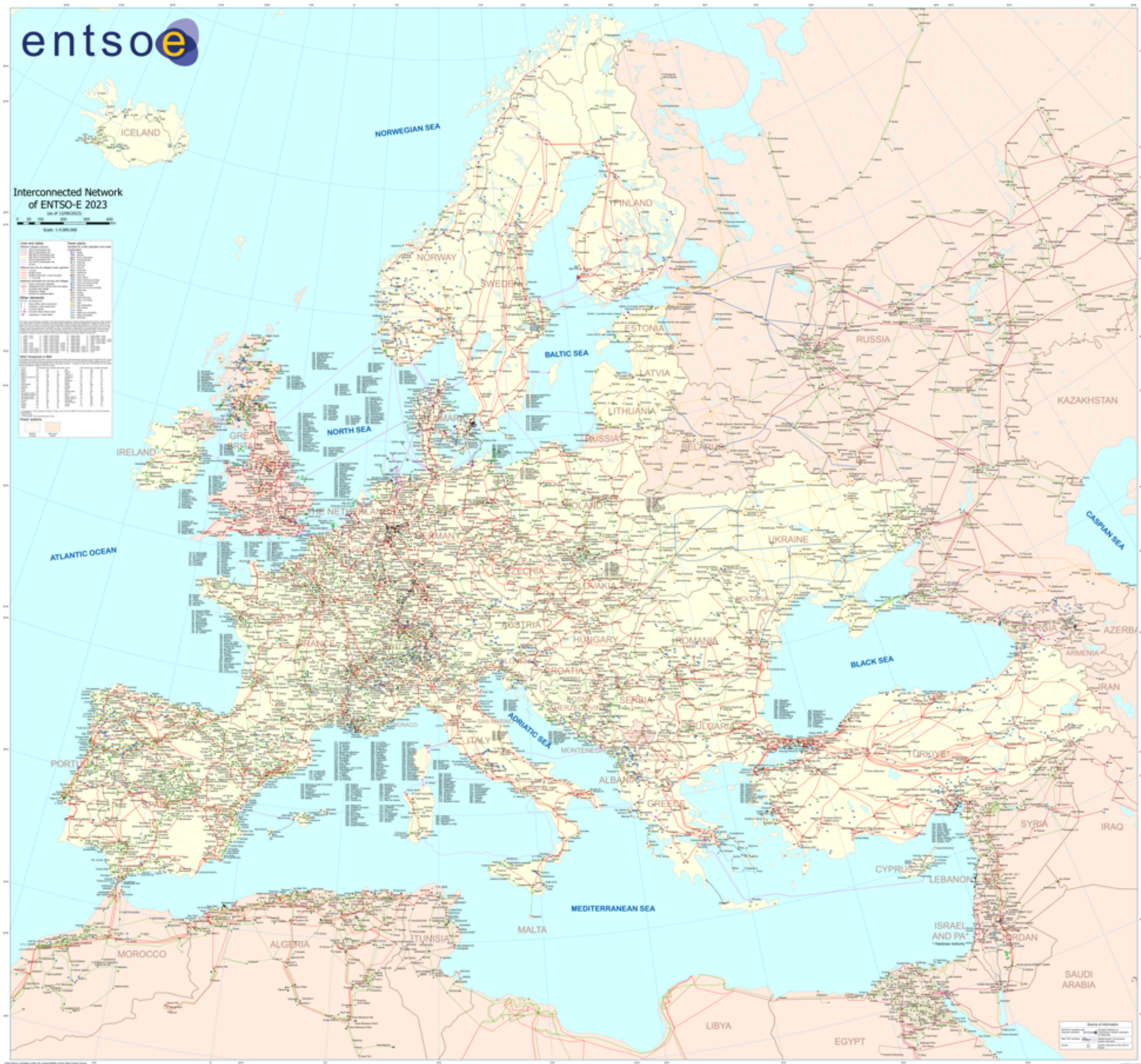

Figure 8: Transmission Grid of Europe, ENTSO-e [31].

buying the energy from foreign TSOs.

Moreover, operational challenges arise from varied legal and procedural standards for electricity management across nations, complicating energy trading due to its physical characteristics. Given ocean energy's potential to mitigate renewables' variability, system design must address geographical and economic barriers. A reliable energy system should eliminate supply shortages and align with regional energy market factors, seamlessly meeting energy demands.

What is concluded based on the model used in the research of T. Brown is that a development that aids the interconnection of cross-water regions is the installation of High Voltage Direct Current cables (HVDC). In general, High Voltage Alternating Current (HVAC) transmission lines are beneficial for long distance power transfer as by boosting the voltage and decreasing the current, a large amount of energy can travel through long distances. However, AC transmission lines come with alternating electromagnetic fields which generate inductive and capacitive losses between the lines and other nearby conductive elements such as the ground or water. This leads to reactive power losses, and when the cable is extended over large distances or is submerged, the accumulation of reactance currents decreases the overall efficiency of the system more than the equivalent HVDC system.

HVDC systems are used over large distances due to their advantages in these circumstances. They do not experience the cycles of charging and discharging that come with reactance currents and can have a more controllable power flow making them more versatile when connecting countries with different transmission line characteristics and electricity frequencies. In this research, the potential of the offshore wind energy generation is dependent on the distance that the marine power plant is placed from the shore. AC and DC technologies have different costs and are assumed as separate branches of carriers.

The feasibility of a high renewable share energy system is a topic that generates disagreement among researchers. Moriarty and Honnery [36] use the energy return on energy invested index (EROI) to investigate feasibility of a wind and solar energy system for Europe. This index is the ratio of the energy generated from a specific energy carrier to the amount of energy required to obtain that energy resource. An EROI value of less than one indicates that the energy carrier does not deliver energy any more and should be shut down. In their article, they compare EROI-assessment studies and find that there is a large variety of values among literature, implying a significant sensitivity of the index on geographical and environmental conditions, lifetime of projects and regional economic trends. He pinpoints the challenges of RES due to economic and population growth, declining optimal site availability, increasing distance from load centers and water sources and assumes the integration of storage systems to be inevitable. A global energy system solely reliant on wind/solar would likely have a lower average EROI than current values. This could necessitate substantial reductions in energy consumption. Lower economic growth scenarios could drastically reduce global energy consumption by 2040. The quest for a 100% green energy economy may require scaling down economic activity.

2.4 Marine and Offshore Renewables

This thesis focuses in the role of Marine Renewable Energy. Marine energy is a term used to describe any type of energy produced using the sea's kinetic, potential, thermal, and chemical energy in addition to the kinetic energy of the wind. As mentioned partly in section 2.1 offshore renewable systems, particularly wind and wave power, have the potential to significantly facilitate the transition to a carbon-neutral electricity system. These sources can provide a largely untapped resource for renewable power generation.

Considering the costs and economic viability of a technology the levelized cost of energy is additionally calculated for this report. The levelized cost of energy (LCOE) displays the technology-specific cost of electricity and is an essential metric for assessing the economics of any generating technology. It includes capital costs (CAPEX), such as equipment and installation, and operational costs (OPEX), such as maintenance and repair. It also takes into account financing costs, such as interest on loans, and other expenses such as taxes and insurance. The formula of LCOE calculation in this report, suggested by IRENA [20], is:

$$LCOE = \frac{\sum_{t=1}^{n} \frac{I_t + M_t + D_t}{(1+r)^t}}{\sum_{t=1}^{n} \frac{E_t}{(1+r)^t}} \tag{1}$$

where I_t is investment costs, M_t is maintenance, D_t decommissioning, E_t the sum of all electricity generated over the years of operation, r the discount rate of the project, n the life of the project.

What is noteworthy, is the fact that the software used for this research does not include LCOE calculations on its own, but rather takes economic factors such as CAPEX, OPEX, marginal costs, costs of expansion and more, to generate locational marginal prices. LCOE is used for this research as a representative first level of technology assessment, widely used in literature.

Another crucial concept of renewable energy assessment is capacity factors. A capacity factor is an index which represents the efficiency of a production farm. It is calculated as the ratio:

$$CF = \frac{\text{Actual power output}}{\text{Maximum power output}} \tag{2}$$

A higher capacity factor indicates a greater generational and financial benefit on the energy system by the technology. Apart from being directly influenced by the availability of the resource, capacity factors can be altered according to farm layouts, transmission line capacities, generator curtailment and more.

2.4.1 Wind Power

Wind power is generated when air passes through a WTG (wind turbine generator). A WTG is a device that converts kinetic energy from wind into electrical energy. Wind generators typically consist of a tower, rotor blades, and a generator. When wind blows over the rotor blades, they spin, causing the generator to rotate and produce electricity. There are two types of generators in the market, direct drive and gear wind turbines. While gear wind turbines use a gearbox to speed up the generator's rotational speed, direct drive wind turbines have matching blade and generator rotational speeds. The benefits of direct drive turbines are lower maintenance costs, greater dependability, and increased efficiency at partial loads as wind turbulence does not stress them as much as the gearbox ones. However, they are usually heavier and more expensive to produce. The decision between the two is influenced by variables such as the type of application, the wind speed and cost-benefit analyses.

The selection of an offshore wind turbine generally involves a number of different factors. Speed and direction of the wind, rotor size, hub height, durability of the structure, lifetime, operational, maintaining and decommissioning costs, distance of the wind farm site from the consumer sources, water depth of the site and the conditions of the ground material, are the main factors.

The layout of a wind farm also plays a catalytic role in the annual energy yield. Wind power generation is significantly impacted by wake effects, which refer to the decrease in wind speed behind a wind turbine caused by the drag and turbulence generated by the blades. Every wind farm has an optimal layout to minimize the implications of the wake effects. Wake losses can reduce the energy production by up to 15%. Hou et al., 2019 [37], mention that there are both computational and analytical methods to model and investigate wake effects.

Structurally, there are certain frequencies of loads that can cause danger. The natural frequency of the structure, floating or bottom fixed, should avoid matching any frequency that can induce resonance and cause fatigue damage. Regarding wind loads the natural frequency should lie in the range of 1P and 3P. Those frequencies refer to rotor rotational speed 1P load and blade passing frequency 3P, assuming there are 3 blades on the rotor. The in-between frequency ranges are the available design ranges. However, there are also wave loads that can cause resonance. Base on the two most used wave spectrums of fully developed (Pierson-Moskowitz) and developing seas (JONSWAP) the available ranges are narrowed down to the *soft-stiff* range region in order to achieve structural integrity and economic feasibility.

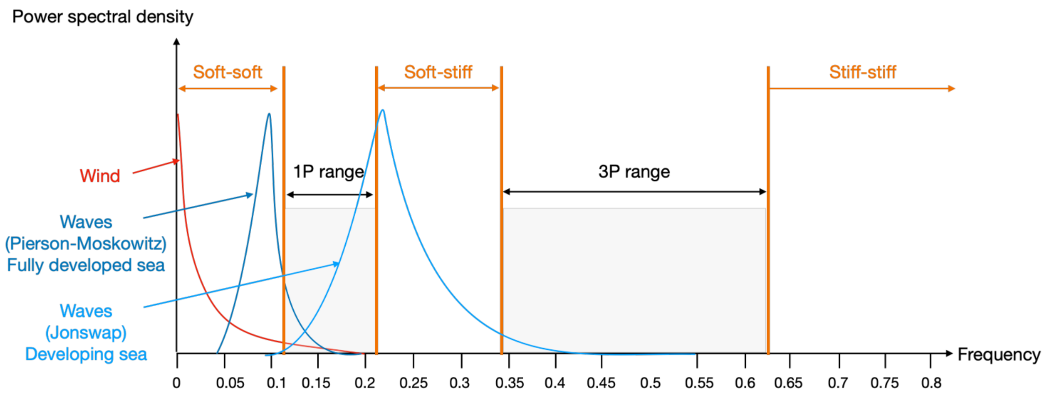

Figure 9: Wind turbine frequency ranges (Dr.ir. A.C. Viré, 2023, cource on Floating Offshore Wind Energy, MSc of Aerospace Engineering, TU Delft).

2.4.2 Wind power calculation

In the description of figure 4 it is mentioned that wind speeds are measured at a height of 100 meters. The most commonly used formula for wind speed calculation is the Hellmann exponential law that correlates the wind speed readings at two different heights

$$v = v_{ref}\left(\frac{H}{H_{ref}}\right)^{a} \tag{3}$$

in which v is the speed at height H, v_{ref} is the speed at height H_{ref} (frequently referred to as a 10-m height) and α is the friction coefficient or Hellman exponent. This coefficient is a function of the topography at a specific location roughness and generally assumed to be equal to $1/7$.
Once the wind speed is acquired the real power produced by a turbine can be expressed as such:

$$P = \frac{1}{2}\rho A v^3 C_p \tag{4}$$

where P is the real power in Watts, ρ is the air density in kg/m^3, A is the rotor area in m^2, v is the wind speed in m/s, and C_p is the power coefficient. Temperature, altitude, and, to a much lesser extent, humidity, all affect air density. The ratio of the power extracted by the wind turbine rotor to the power available in the wind is known as the power coefficient (Bañuelos-Ruedas et al, 2011 [38]).

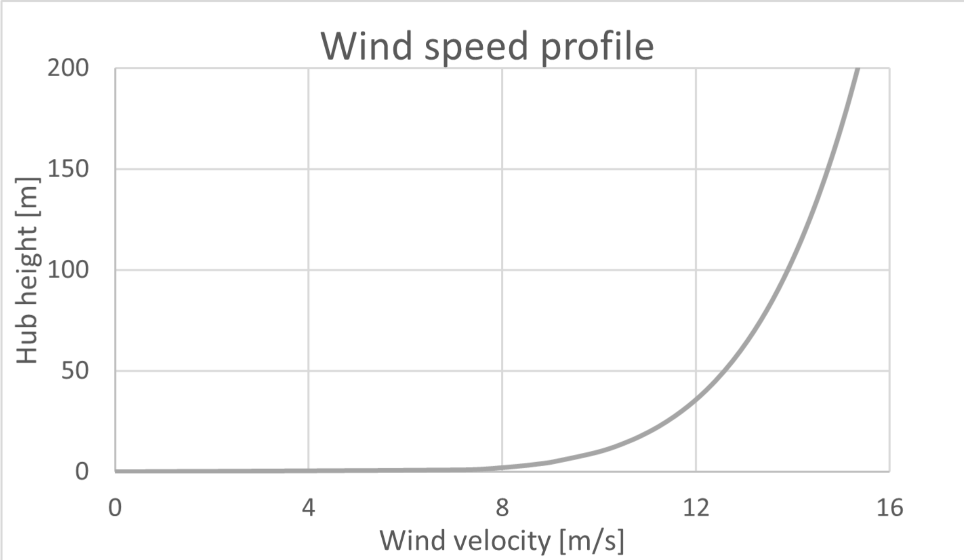

Figure 10: Wind speed profile depicted according to $v_0 = 10m/s$ at $H_0 = 10m$

In order to predict the the wind energy potential, the Weibull probability density function (pdf) is used. The acquired wind data of the chosen wind farm site are portrayed in a Weibull distribution fit type. This pdf is expressed as:

$$f(v) = \frac{k}{c}\left(\frac{v}{c}\right)^{k-1} exp\left[-\left(\frac{v}{c}\right)^{k}\right] \tag{5}$$

where v is the wind speed, k is the shape parameter, and c is the scale parameter. Once the mean $E(v)$ or $\overline{v}$ and the variance of wind speed are known, the following approximation can be used to calculate the Weibull parameters c and k and the pdf can be applied at the correct hub height (Lu et al., 2002 [39]). Both parameters are estimated based on a wind speed data-set. The scale parameter is related to the average wind speed:

$$c = \frac{\overline{v}}{\Gamma(1 + 1/k)} \tag{6}$$

or

$$\overline{v} = c\Gamma(1 + 1/k) \tag{7}$$

The result is a graph that looks similar to the following:

Next, it is necessary to know the rated power output of the WTG and its operational wind velocity, namely cut-in v_i, rated v_r and cut-out v_o speed. These indexes refer to the velocity range at which the blades start to rotate and generate energy, the velocity range at which the generator is at maximum production and the velocity at which the rotor stops revolving for safety reasons accordingly. Currently in the market there are installable and cost-efficient 15MW WTGs with a wind-swept area of more than 40,000 m^2 (diameter of around 230m) and the technology is advancing towards even larger capacities. There is an vast progress compared to the first wind farm turbines that had a rated power of around 450 kW. Turbines are able to access more stable wind flows as they become larger, i.e. taller with a larger rotor diameter and larger drive. Below at figure 12 is presented the power curve of the typical operational wind velocities of a 15MW WTG.

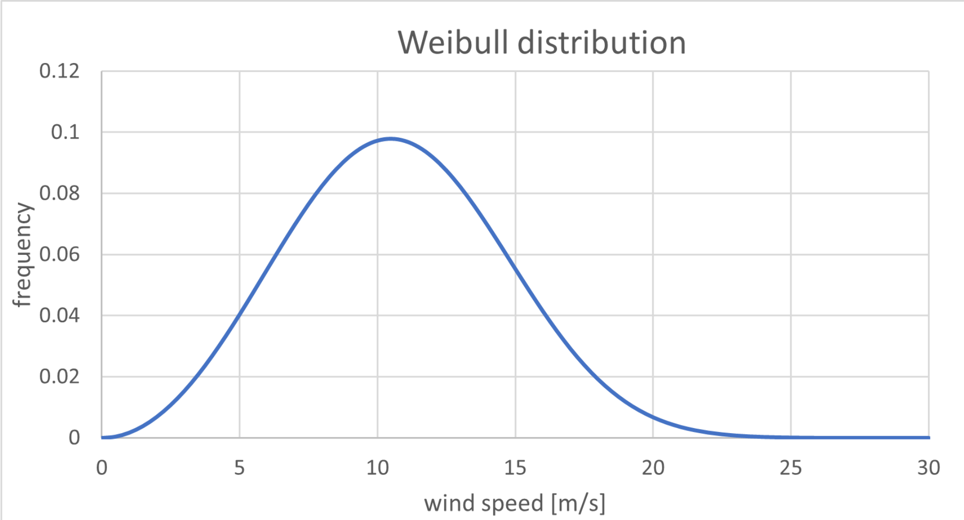

Figure 11: Typical Weibull distribution of wind speed probability.

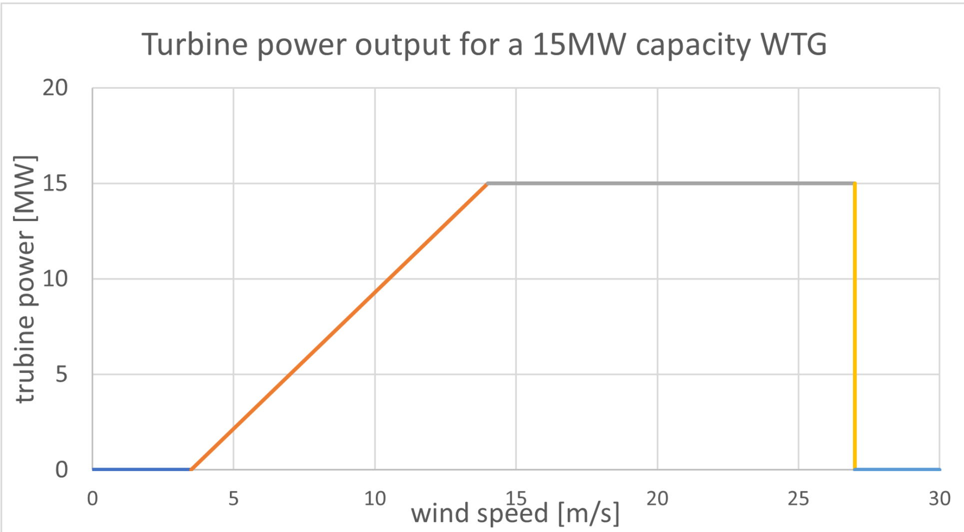

Figure 12: Power curve for a 15MW rated power WTG. $v_i = 3.5m/s$, $v_r = 14m/s$, $v_o = 27m/s$. These values roughly represent the current technology.

The power curve is ultimately the input on the model. A list of available turbines have their power curves expressed as a one-to-one correlation of speed to nominal power output.

Because wind speed and direction can vary, wind power generation may be sporadic, which will result into wind power output fluctuations. Production of wind energy is also influenced by the weather and seasonal patterns, which can further decrease its consistency. Due to this unstable nature, it is quite challenging to integrate wind energy into the electrical grid and guarantee a steady and consistent supply of electricity. However, improvements in weather prediction, grid management techniques, and energy storage technology are helping to lessen the effects of wind power intermittency and boost the overall performance and reliability of wind energy systems.

2.4.3 Wind turbine offshore structures

There are two types of WTGs structures, Bottom Founded and Floating structures.

2.4.3.1 Bottom founded structures

Bottom-founded offshore wind turbines are structures that can be installed at depths of up to 60 meters. The choice of foundation structure is determined by factors such as the seabed's soil composition

Figure 13: Types of offshore wind turbines, illustration by Josh Bauer, NREL.

and water depth. Monopile foundations, which are cost-effective due to the simplicity of manufacturing and installation, are commonly selected for creating offshore wind farms. These foundations consist of a single pile embedded into the seabed, with the depth proportional to the pile's diameter. Jacket structures, which are more complex structure can also be used, especially for deeper water locations. Tri-Pods, Gravity-based, and Suction Caissons are other options of substructures.

2.4.3.2 Economics of Bottom founded Wind Turbines

When it comes to costs, approximately 55% of the total CAPEX in bottom-fixed offshore wind projects is allocated to the turbine and substructure costs. Operation and maintenance (O&M) costs account for around 25% of the total life cycle costs (Martinez and Iglesias, 2022 [40]). O&M costs have both fixed and variable components, covering expenses like component repairs, staff, port facilities, equipment, and travel costs (Johnston et al., 2020 [41])

According to observations by Santhakumar et al. [42], improvements in technology, economies of scale, and supportive policies have led to a decrease in LCOE for offshore wind. CAPEX has reduced from 5.4 M€/MW in 2011 to 3.3 M€/MW in 2020, causing LCOE to drop from 150€/MWh in 2010 to 69€/MWh in 2020. Favorable financing, increased capacity factors, and lower technology costs contributed to this decline. The declining LCOE signifies the positive growth of offshore wind technology. Most operational offshore wind farms are part of national initiatives connected to the coast, a trend expected to continue. National grid operators are building cross-border interconnectors for energy trading and supply security.

The LCOE decreasing trend above is an index that offshore wind technology is positively growing. Most offshore wind farms that are currently in operation are part of national initiatives that are radially connected to the coast. This approach to producing offshore renewable energy is anticipated to continue, especially in areas where offshore development is still in its infancy. Furthermore, it is anticipated that national grid transmission system operators will continue building cross-border interconnectors for the purpose of energy trading and supply security.

The available and optimal oceanic area that can accommodate bottom founded structures is limited. Site selection for bottom founded wind farms is mainly affected by the depth of the seabed. Since more and more near shore sites, the majority of which are located in the North Sea, the Baltic and the Irish coasts, are occupied or are under development, there is a need to find suitable sites that overcome the barrier of water depth if the European goals are to be achieved. This, in addition to the increased wind resources of further offshore locations, justifies the slow but steady shift of the interest towards floating structures.

2.4.3.3 Floating structures

Literature on floating wind turbines has developed over the years. Based on articles and reports [24][43][44], bottom fixed structures show unacceptable levels of possibility of failure at depths greater than 50-60 meters, floating WTGs have the advantage of not being affected by water depth as much as the bottom fixed ones in terms of structure integrity.

Most offshore areas with high wind resources of Europe have a depth of more than 60 m and this makes the use of floating structures imperative regarding the transition of the energy system of the EU. The technology of floating WTGs is relatively new and the figure below presents the main concepts of structures so far:

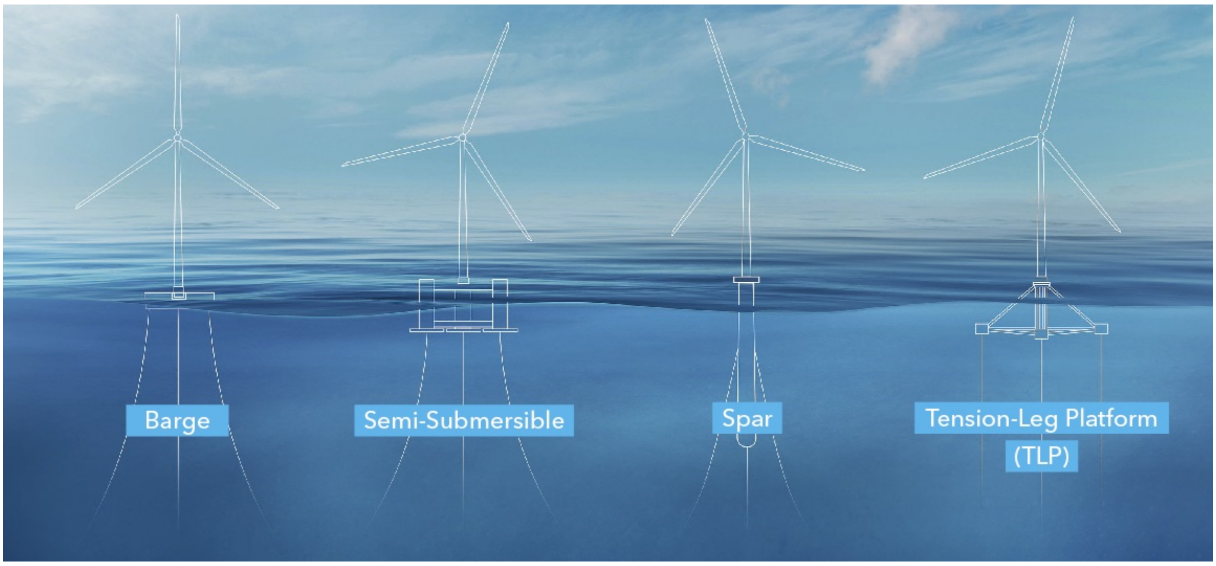

Figure 14: Floating WTG concepts, DNV GL Tom Buysse - Shutterstock.com.

To support the wind turbine and its tower on a floating foundation, it needs to be both buoyant and stable. These floating foundations are typically made of concrete hulls or steel cylinders with added support. They rely on mooring lines to keep them stable, and what's different from fixed foundations is that they are affected by second-order loads and currents, which are caused by the motion of the sea. This requires complex modeling of the aero-hydro-dynamic system.

Looking at the figures, there are different types of floating substructures for wind turbines. The Tension Leg Platform (TLP) features a wind turbine on top of a spaced tri-floater with columns and pontoons. It stays submerged and uses its buoyancy and taut mooring lines for stability.

The Barge, Semi-Submersible, and SPAR substructures follow a similar principle. They have a wind turbine on top, and their position is maintained by catenary mooring lines. The barge is a simple rectangular platform that supports the tower but is sensitive to waves and drift.

The Semi-Submersible consists of pontoons and columns that provide an amount of stability, similar to the TLP but with catenary mooring lines.

The SPAR is a large, deep-draft buoyant cylinder that can control its position well, even in rough conditions. SPAR substructures are typically preferred in deeper waters and far offshore due to their limited hydrodynamic response on the environmental loads.

2.4.3.4 Economics of Floating Wind Turbines

One of the first floating wind demonstration was the Hywind Scotland Project in 2017, which offers insights into a small floating wind farm's logistics, estimating a cost of approximately 7 M€/MW. This price is notably high for installed power, resulting in an LCOE ranging between 150€ and 200€/MWh for operational projects. However, cost reductions are expected as the technology advances, approaching global bottom-fixed offshore wind costs of 50€ to 100€/MWh in the near future, with an average wind turbine price of 1.6 M€/MW ([43]). Evaluating O&M costs for floating wind remains unclear due to the limited number of floating offshore projects, but they should align with those of bottom-fixed systems. An optimistic scenario from Enerdata ([45]) in December 2022 suggests that in the coming years, floating WTGs may reach costs comparable to current bottom-fixed WTGs, potentially falling below 100€/MWh and targeting 45€/MWh by 2035. The cost assumptions for Floating Wind turbines are obtained from the Marine Renewable Energies Laboratory (MREL) of TU Delft [46].

In the European region, 113 MW of operational floating wind turbines currently exist, with numerous larger projects underway. Notably, the world's largest floating wind farm, Hywind Tampen (88 MW), is already operational in Norway. Within the next two years, France plans to launch four modest projects, each with a capacity of around 30 MW. Europe aims to increase floating wind power to 330 MW by 2024. However, the unique substructures pose challenges for the supply chain, requiring significant investments in manufacturing facilities and related infrastructure [27].

According to the technology trend analysis in the report Floating Offshore Wind Market Technology Review of Carbon Trust organisation [47] in 2015, platform type and size is the main cost driver, followed by turbine control and mooring systems. The researchers used the re-introduced Technology Readiness Levels (TRL), an assessment parameter that scales from 1-9 originally used by NASA for risk management regarding the aviation and space industry. A TRL is an index that describes the maturity and the feasibility of a technology.

Level	Description
TRL 1	basic principles observed
TRL 2	technology concept formulated
TRL 3	experimental proof of concept
TRL 4	technology validated in lab
TRL 5	technology validated in relevant environment (industrially relevant environment in the case of key enabling technologies)
TRL 6	technology demonstrated in relevant environment (industrially relevant environment in the case of key enabling technologies)
TRL 7	system prototype demonstration in operational environment
TRL 8	system complete and qualified
TRL 9	actual system proven in operational environment (competitive manufacturing in the case of key enabling technologies; or in space)

Table 1: Technology readiness levels (TRL).

By reviewing most of the existing concepts with a variety of TRL, with respect to 2015, they derive cost reductive concepts. Platforms do not necessarily need to be steel-made as the much more economical concrete can achieve similar support targets. Floaters can drop the need of braces facilitating the fabrication process, and more aerodynamically shaped towers can be installed. Additionally, different hull sizes and ballast concepts, which allow the platforms to accommodate higher power rating turbines can increase production and lower LCOE.

2.4.4 Wave Power

Wave energy is potential energy contained into the waves. Global wave energy potential is estimated to be 32,000 TWh/year [2], which is very close to the average annual energy consumption for the entire planet. Wave energy also happens to be the renewable energy source with the highest energy density. Despite seasonal and short-term variations, waves can be well forecasted and are usually regarded as a reliable energy source.

Waves are generated when the wind imparts its kinetic energy to the ocean's surface. As long as the wind persists, pressure disparities create uneven sea surfaces. Waves carry both kinetic and potential energy, which can be computed when wave height (H) and period (T) are known. Wind waves and swell waves are distinct. Wind waves result from wind interaction with the ocean's surface, featuring short wavelengths and high amplitudes. In contrast, swell waves originate as wind waves but propagate over long distances, having longer wavelengths and smaller amplitudes.

Waves are most energetic in latitudes between 30 and 60 degrees, influenced by factors such as wave height, speed, wavelength (or frequency), and water density. Europe benefits from its vast coastline which is mostly within this range. Despite being less popular than other renewable sources, wave energy holds promise due to its uninterrupted motion.

To harness wave energy effectively, one must evaluate wave conditions in a specific area. However, challenges arise from irregularities in wave characteristics, making it difficult to maintain device efficiency across different frequencies. High forces and low speeds during power conversion can lead to reliability issues. Extreme weather conditions can subject structures to extremely high loads.

Despite these challenges, wave energy is considered beneficial. It can meet seasonal electricity demands, and wave power devices have a high availability rate, exceeding 90% for power generation. Moreover, offshore wave energy devices and ocean energy in general have a relatively low environmental impact. This justifies the European Union's goal of having 40 GW of marine energy technology by 2050, alongside 300 GW of offshore wind energy.

2.4.5 Wave power calculation.

The first step of wave energy assessment is the establishment of the metocean conditions. This includes wave wavelength, wave amplitude, and direction. Selecting a site for a wave power plant involves considering several parameters. Apart from the wave power resource in a specific region, water depth and seabed anomalies can significantly affect wave energy. As waves move into shallower regions they lose some of their speed and their linearity [48]. Those waves, also called transitional waves, start to experience bottom friction and water particles start to change their orbital patterns, making them narrower compared to the circular pattern in deep water disrupting the motion of the conversion device. Seabed variations can also cause refraction effects, that can be calculated with Snell's Law, altering the direction of wave crests.

Guillou et al. [49], expresses the wave energy potential per length unit of crest, measured in W/m, as the integral of the energy wave spectrum:

$$P = \rho g \int_0^{2\pi} \int_0^{\infty} c_g(\sigma) E(\sigma, \theta) \, d\sigma \, d\theta \tag{8}$$

where ρ is the density of seawater, g is the acceleration due to gravity, E is the wave energy density distribution σ and propagation directions θ, and c_g is the group velocity of the propagating waves.

The wave energy distribution is not simple to obtain as most studies were carried out with experimental parameters such as significant wave height H_{m0} and period T_p. There are simplified approaches to formulate wave power density. These include the assumption that the study is performed in deep waters. In deep water conditions the dispersion relation:

$$\omega^2 = gk \tanh(kd) = gk \tag{9}$$

as the term kd is a lot larger than 1 (k is the wavenumber and d is the water depth). Then the group velocity of the waves can be approximated as

$$c_g = g/(4\pi f) \tag{10}$$

where f is the wave frequency. The formulation above is then proportional to ${H_{m0}}^2$ ($H_{m0} = 4m_0$) and T_p ($T_p = m_1/m_0$)

$$P = \frac{\rho g^2}{64\pi} {H_{m0}}^2 T_p \approx \left(0.5 \frac{kW}{m_3 s}\right) {H_{m0}}^2 T_p \tag{11}$$

where m_i is the i^{th} moment of the spectrum

$$m_i = \int_0^{\infty} f^i E(f) \, df \tag{12}$$

Wave energy devices consist of the structure and the prime moving part that activates when the wave occurs, the foundation that keeps this structure in place, a power take-off (PTO) system that includes a generator to convert trapped energy in the waves into usable energy, and a control system to ensure a safe operation under alternating conditions [50].

The significance of a PTO system is directly related to effectiveness of the WEC, shaping its capacity factor, and eventually the cost of wave energy generation. As a PTO and depending on the wave conversion principle, a device can use a variety of mechanical systems such as turbines, hydraulic systems and electrical linear generators. In his research, Sheng [51] finds the PTO systems are highly dependent on the hydrodynamics of each device and highlights the need for maximizing the PTO's optimisation. A way to achieve this is to further investigate PTO control mechanisms that will boost the device's efficiency, by adapting its operation on the rapid change of the sea state.

2.4.6 Power Matrix of a WEC device

As mentioned before, WEC technologies are developing thus assessment data can be limited. According to Ahn et al., 2019 [52], analyzing the wave resource involves three types of assessments: theoretical, technical, and practical. A theoretical resource assessment, which often relies on numerical modeling with the use of usually limited historical datasets, calculates the annual average energy production for a given wave resource.

In contrast, the technical resource is defined as the percentage of the theoretical resource that can be captured using a certain technique. Therefore, it addresses device specifications and limitations. A method for evaluating the technical resource in wave energy modelling, suggested by Guillou et al. [49] and used in this research, includes the use of a specific power matrix for the chosen technology. For a given sea condition with a set of wave height (Hs) and wave period (Tp), power matrices are the equivalent of power curves used for wind energy and they quantify the device's potential power production. They correlate a distinct combination of wave height and wave period to power output. The used power matrices for this research are provided in a chapter 3.3 and figures 23, 24 and 25.

Extreme conditions like storms can occasionally generate in theory more than 500kW/m. Energy resource in kW/m expresses the amount of energy deliverable for every meter of wave crest. However, seasonal and inter-annual variability, as it is in the nature of every renewable source, limits the common power levels of developed devices up to 100kw/m at maximum, a power rating already considered optimistic and rare according to Ahn.

So far in Europe, the UK seems to have the advantage over the rest of the countries achieving a 50kW/m median power level compared to the 10-15kW/m that the Mediterranean Sea can deliver, according to Lavidas [53]. Even though UK seems to be the optimal region for WEC installation in terms of output, variability complicates the site selection and makes it difficult to be evaluated.

The remaining elements of the resource assessment, after taking into account all limitations including socioeconomic and environmental considerations, is the practical resource. Low power density places, areas far from electrical infrastructure, navigational channels, maritime protected areas, etc. are not included in the practical resource.

2.4.7 Wave energy systems and conversion principles

There are over 1000 registered device patents. Neil and Reza Hashemi [54] categorize them by technology type in the following groups:

- Attenuators
- Surface point absorbers
- Oscillating water columns
- Oscillating bodies converters
- Overtopping devices

An attenuator is a long, free-floating object that faces the direction the wave will go. By limiting certain motions along the wave's length, the device is able to capture the energy. The Pelamis is the most popular example of an attenuator, that consists of long beam sections connected with power converting joints. In principle, this device relies on its pitch motion and can actively adapt to the shape of the water surface which naturally has wave induced elevations. As it transitions from one shape to another, it generates motion to the conversion joints. Each joint has two hydraulic pistons, in other words a hydraulic PTO, one at the top and one at the bottom of each conversion module, that use the oscillation to pump water through a power generator drive system [55]. The first Pelamis device was developed in 2004 and managed to have capacity factor increase during a decade of simulation at a particular location of 22%, which is optimistic as it is closing the gap between the other renewable technologies (Ahn et al., 2019 [52]). The model of this research includes the 750kW Pelamis device as its far-shore wave energy converter.

Surface point absorbers in principle utilize the vertical motion of a floating buoy that is hinged to the seabed. Waves that pass over this buoy change its elevation and activate the PTO system in the absorbing unit section. In late year developments point absorber researchers explore new types of PTOs. Those transitioned from high-speed rotating hydraulic turbines to more resilient direct drive generators such as air pistons and permanent magnet electricity generators (Bozzi et al., 2013 [56]). A 400kW point absorber developed by MREL of TU Delft [46] is used in this thesis as a near-shore wave energy converter.

Oscillating water columns (OWC) are partially submerged devices that are open to the sea below. As the water surface rises or drops, air is compressed and drives a pneumatic PTO system, in other words an air turbine generator.

Next are oscillating bodies converters (OBC), that is an inverted pendulum or also known as a wave surge converter, is a bottom-hinged flap that changes its pitch with the arrival of waves. This rotation activates a hydraulic piston that pumps water into the PTO system, consisting of a Pelton wheel and an electrical generator. The top of the device is typically exposed above the surface. In the current model, a 290kW wave surge converter is used for shallow water wave energy exploitation.

Lastly, overtopping devices use the potential energy of water that spills into a closed reservoir to subsequently drive a hydraulic turbine. The incoming waves create a head of water which is released back to the sea through a low-head turbine PTO.

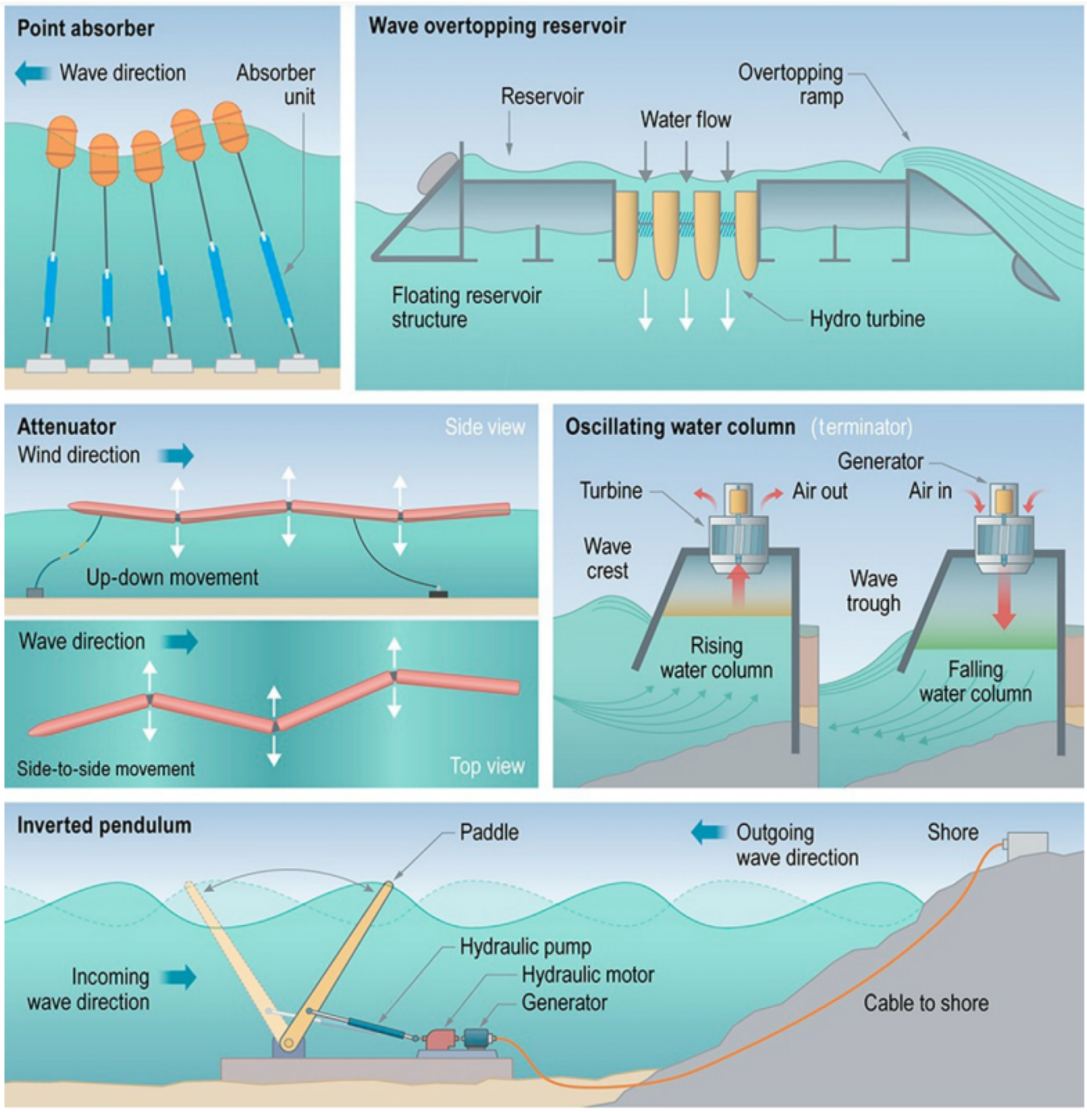

Figure 15: WEC types, photo by the US Department of Energy (DOE) Office of Scientific and Technical Information (OSTI) [57].

2.4.7.1 Economics of WEC technology

CAPEX and OPEX for wave energy includes a variety of factors. Initial costs of a WEC refer to design, construction and installation of it, cost of mooring system and installation, cost of cables and substation. The PTO system alone could have portion of 20–30% of the total capital cost. What characterizes WEC's OPEX, apart from general operational and maintenance costs, is the sensitivity to higher failure rates of the device's parts mostly the PTO, power transmission and generator.

Astariz and Iglesias [58] examined and compared various studies and sources. They concluded that the cost of equipment and installation ranges between 2.5 and 6.0 M€ per installed MW . For shallow water and nearshore plants, the levelized cost of energy varies from 90€/MWh to 140€/MWh, while for offshore energy farms, it varies from 180€/MWh and up to 490€/MWh. Along the capital costs, they find significant early stage developments or pre-operational costs up to 10%CAPEX. LCOE values vary between nations and even within one, depending on the location, equipment, proximity to the coast, and other factors.

A study of the LCOE for ocean energies was produced in 2015 by the IEA's OES Ocean Energy Systems Energy Technology Collaboration Programme [59] attempted to assess the current costs and goals in the wave energy industry. For their wave energy assessment they considered technologies with a minimum of TRL 7 (TRL 7 – system prototype demonstration in operational environment. The assessments were updated in 2020.

According to publicly available data, wave technologies will be able to meet the cost goals outlined in the European Strategic Energy Technology Plan (SET-Plan). They also highlight the significance of the early stage developments costs and how unreliably projects which have not upgraded into full scale prototypes (TRL lower than 5) and tested in the ocean yet can represent realistic capital and operational costs. Investment costs range from a high 14M$/MW for small scale projects (based on data referring to 2013), to as low as 4 and ideally 3M$/MW.

The report pinpoints the importance of scaling-up wave industry similarly to solar and wind in order to achieve an attractive cost reduction. These studies showed that in the most optimistic scenario and at a commercial scale, OPEX can be as low as 70-170$/kW per year and the LCOE could be reduced to 150$/MWh by 2030 and 100$/MWh by 2035. However, a more conservative short term prediction for commercial scale projects indicate an LCOE in the range of 120-480$/MWh, implying that the site resources is a major factor.

For the model under investigation and under the guidance of the MREL [46] of TU Delft the WECs used have an investment cost assumption of 2.012 €/W for the year of 2030 and for the years 2040 and 2050 it is assumed to follow the same decreasing trend that is applied for wind turbines that model uses by default.

2.5 Power System Analysis

Shaping the EU's trajectory towards a sustainable, carbon-free electricity system involves understanding the intricacies of the power system's components and interactions. This system comprises of various technologies, infrastructure, and institutions collaborating to generate, distribute, and consume energy. The EU's energy goals for 2030 and 2050 highlight a shift towards offshore energy production, envisioning the installation of at least 340 GW of new offshore wind and marine energy, excluding the UK, which aims to add approximately 150 GW into the grid.

Power system analysis models are comprehensive tools that blend various factors affecting an energy system. They aim to simulate and optimize the complex network of technologies, infrastructure, and energy usage. These models encompass energy sources, storage units, transmission networks, and specific load requirements across different locations. By integrating various exogenous and endogenous factors such as weather, geography, technology costs, and transmission details, these models configure the system variables to create an operational energy model. Ensuring cross-border integration requires considering individual country policies and requirements. As renewable energy sources dominate the model, anticipating production fluctuations becomes crucial. The model's role is to estimate:

- which technologies can facilitate the achievement of the goals
- where these technologies can be installed
- their availability and deployment
- the potential of expansion of the transmission network
- the variability of the sources and how the production of different energy sources is capable to meet the energy demand
- the amount of anti-variability measures, especially for renewable energy based systems, such as CCS, H_2 and storage, that can be integrated to the network
- the costs of expansion, installation and operation
- the possible economic growth, future energy market and energy prices trends depending on different scenarios of technologies and grid configurations

- the environmental and social constrains of such a development

Critical for evaluating and improving modern energy systems, power system analysis helps decision-makers navigate towards a cleaner and more efficient energy future. It provides insights into energy production and consumption patterns with precise geographical and temporal accuracy, aiding in understanding infrastructure needs and optimizing resource management.

This analysis enables the integration of renewable energy sources, aligns with sector-specific goals, and addresses CO2 reduction targets. Additionally, it assists in cost optimization and bottleneck management, considering various energy scenarios and constraints.

The following sections explain the reasoning behind the selection of PyPSA-Eur (Python for Power System Analysis - European Sector) as the software for modelling the European Energy System and its workflow strategy.

2.5.1 PyPSA-Eur

PyPSA-Eur (Hörsch et al., 2018 [60]) is a python based open model dataset of the European energy system at the transmission network level that covers the full ENTSO-E area. It is a suitable tool for generation and transmission expansion planning studies. In brief, it uses year specific electricity demand time series from the OPSD platform (Open Power System Data [61]), an electricity distribution network derived from the already mentioned ENTSO-e, a custom-made database of conventional power plants [62] created by the collection of data from various official sources.

It estimates the variable renewable generator availability, by default, according to ERA5 (ECMWF Re-Analysis) weather data [63], SARAH-2 (Surface Radiation Data Set - Heliosat) optionally for solar energy, and GEBCO (General Bathymetric Chart of the Oceans) bathymetric data [64] for on-land and underwater elevation. Finally, the geographical potentials for the renewable generators are restricted according to land use (CORINE, Coordination of information on the environment), excluding nature reserves (Natura2000), ship traffic density and are computed with the "atlite" python library (Hofmann et al, 2021 [65]), a tool created by the developers of PyPSA. The data inputs are explained in more detail in subsections 2.5.3 and 2.5.4.

Once this is done, a baseline network of lines and links is created, in which the technology costs are factored in and later the network is simplified and clustered according to optimization strategy, type of energy carrier and its ability for expansion, geographical potential of carriers, investment costs, system constraints, line voltage and expansion and the number of buses the researcher chooses to include, in order to facilitate the process of solving.

The PyPSA-Eur workflow employs the PyPSA framework (Brown et al., 2018 [66]) and it attempts to solve and optimize a multitude of linear problems. The PyPSA-Eur workflow process stops when an annual total-network cost objective function is minimized.

2.5.2 Linear Optimization and Software Solvers

There are two levels of system modelling, simulation and optimization. A simulation model is a representation of a system that is used to model and predict how the system would behave in a specific set of circumstances (Lund et al., 2017 [67]). In general, the word "optimisation" refers to a modelling method in which a set of decision-variables are determined to minimise or maximise a final objective function under certain constraints. These variables are components of the design of the energy system. Optimization models aim to move one step ahead by predicting a system's performance under specific assumptions (Savvidis et al., 2019 [68]).

By setting these decision-variables the researcher can examine specific scenarios that better represent reality. The more variables are introduced into the system, the more accurate and valuable the model becomes. However, a more complex system needs higher computational power which is not always available. It is inevitable that assumptions and simplifications would have to be made, according to the limitations of time and computational power while at the same time with respect to an acceptable representation of the scenario.

PyPSA framework employs an optimization function methodology to achieve the optimal solution. It uses linear optimization functions to solve an overall annual system's costs objective function. In short, the network is initially modified by the user. When this is completed, linear optimization functions that involve multiple inputs are used for creating, solving, modifying the optimization problem of power flow management into the network (linear optimal power flow, LOPF). LOPF process sends feedback to the network which then re-initiates this process until certain convergence criteria are met.

LOPF is eventually used to evaluate the configuration and economics of the combined network, the energy generation and demand for meeting the highest European peak-load hour, among other features. This assessment aims to ensure that the system can sustain the most extreme demand while keeping line-loading under 70% of its heat-rating. This constraint approximates an established stability requirement.

PyPSA passes the network model to an external solver to perform the optimization process. This solver can solve linear optimal power flow problem for a group of snapshots and extract results as the PyPSA-Eur solving environment calls its built-in optimization functions at each part of the workflow. Some of those solvers suggested by the designers are GLPK, HiGHs and Cbc for free-to-use ones and Gurobi or CPLEX for commercial ones, freely available with an academic licence. It is also noted that high complexity networks with a large amount of components might cause reliability issues on the solutions if the users performs a solution with a non-commercial solver.

For this research, the Gurobi [69] solver was used applying the "barrier" algorithm method, a method suitable for quadratic programming models which ensures that every iteration runs until the end and restricts the commencing of the next one.

2.5.3 Network Topology

This transmission network used by PyPSA-Eur was generated based on the ENTSO-e extract from March 2022. The system has 6001 High-Voltage Alternating Current (HVAC) lines with a volume of 345.7 TW km, with 17 TW km under construction. There are also 46 High-Voltage Direct Current (HVDC) lines with a volume of 6.2 TW km, and 2.3 TW km are still being built.

Figure 16 shows the unofficial extract of the ENTSO-E interactive map of the European power system that has been processed with the GridKit tool [70] to form complete topological connections. It includes 3657 substations and 1320 auxiliary buses like junctions and power plants, used to connect the network lines. This setup forms a network for efficient power distribution, using both HVAC and HVDC technologies to deliver electricity across various areas.

The technical characteristics of the transmission lines, which constitute the default configuration on the scenarios under investigation, have multiple associated metric components. Voltage levels represent the most common high-voltage lines used around Europe, wires give a set of connections per line, series resistance provides the resistance of the cables (Ohm) per kilometer and series ind. reactance represents the per kilometer inductive reactance (derived from AC line properties) of the lines. Shunt capacitance refers to the per kilometer capacitance (in nanofarads) between the lines and the ground, current thermal limit is the maximum current that a transmission line can carry within safety restrictions, and apparent power thermal limit is the maximum allowable apparent power that a transmission line can carry without exceeding its thermal limits. These terms will be explained at the methodology section 3.1.

Voltage level [kV]	**Wires**	**Series resistance** [Ω/km]	**Series ind. reactance** [Ω/km]	**Shunt capacity** [nF/km]	**Current thermal limit** [A]	**App. power therm. limit** [MVA]
220	2	0.06	0.301	12.5	1290	492
300	3	0.04	0.265	13.2	1935	1005
380	4	0.03	0.246	13.8	2580	1698

Table 2: Electrical parameters of the transmission lines.

For computational reasons the model is simplified by being clustered down. The network already poses some limitations, notably due to:

- geographical coordinates obtained from the ENTSO-E map prioritize topological clarity over precise geographical accuracy, coordinates might not precisely correspond to real-world locations
- the network uses a conservative lower bound of the voltage level ranges provided by ENTSO-e voltage ranges
- conflicts related to line structures which are resolved by selecting the first structure within the set.
- transformers in the network which do not exist initially at ENTSO-e and are created in the software according to voltage difference from one node to the next
- the association between generators and buses determined by identifying the nearest station geographically at the lowest voltage level

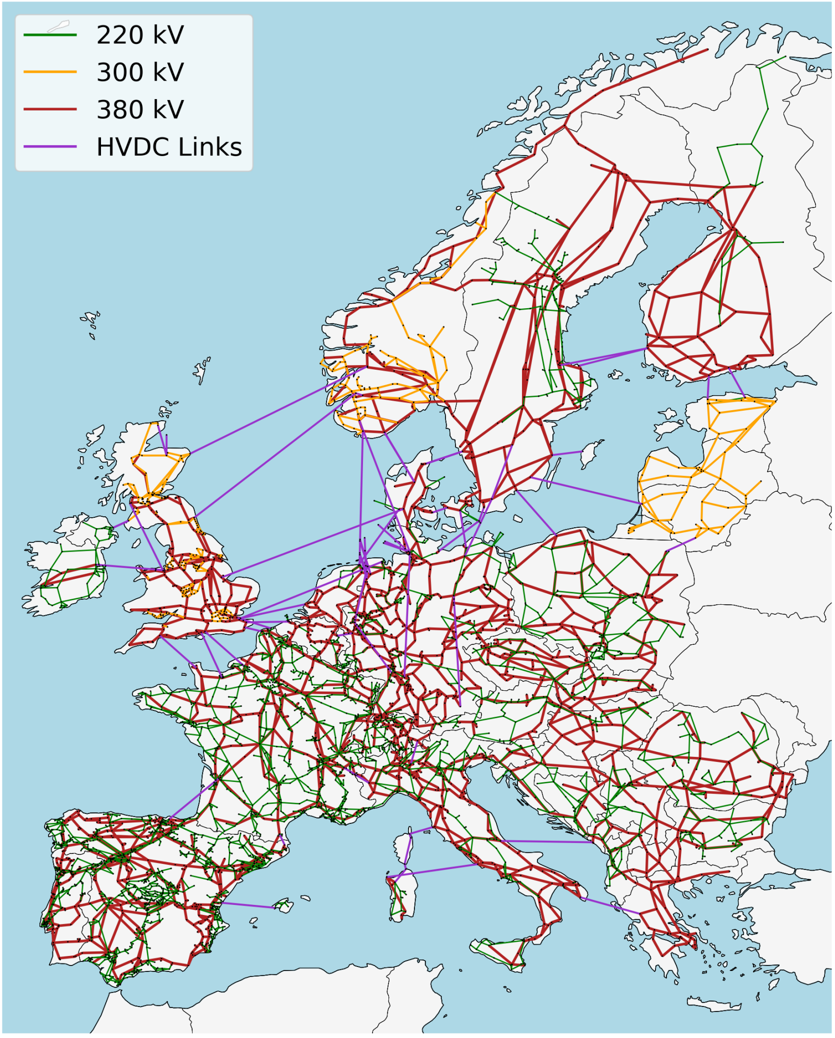

Figure 16: Simplified PyPSA-Eur network based on ENTSO-e.

During the simplification process of the baseline network, an equivalent transmission network (busmap) is created, in which all voltage levels are mapped to the 380 kV level. This happens in order to save time per iteration of solving, as the transition of voltage from one node to the next takes place only initially, before the power flow optimization is ready to be applied on the final network. Further simplification of the network is happening by grouping branches of it according to the onshore and offshore generation potential and their assigned costs.

Grid connection cost of offshore wind and wave generators are added to the capital costs of each generator. The database of cost assumptions for the generators has attributes such as discount rate, lifetime, investment (CAPEX), fixed operation and maintenance (FOM), variable operation and maintenance (VOM), fuel costs (for non renewable carriers) and efficiency for specific years from various official sources. However, this collective dataset does not include values regarding floating wind and wave energy carriers. In this project these costs are assumed according to literature review and research by the MREL of TU Delft [46].

The, next step to prepare the network topology is clustering it according to the researchers' selection of the resolution of clusters. Then, the offshore and onshore energy potential, as well as the relevant cost are aggregated and stored as resources for solution per node (cluster/bus) that is located in space according to weighting functions that take into account the transmission network geometry and the load per node.

The countries are divided into Voronoi cells, serving as catchment areas, with an assumption that each cell is connected to the substation through lower voltage network layers. Voronoi cells are polygons used in mathematics and computational geometric problems. Given a set of nodes, the construction of Voronoi cells involves connecting the midpoints of the line segments between each pair of neighboring nodes, shaping the area of effect of these particular nodes. These Voronoi cells play a role in associating power plant capacities, calculating potential renewable energy generation, and establishing the proportion of demand drawn at the substation. The system includes EU-27, Albania (AL), Bosnia and Herzegovina (BA), Switzerland (CH), Great Britain (GB), Montenegro (ME), North Macedonia (MK), Norway (NO), Serbia (RS), and excludes Cyprus (CY), Malta (MT) and Iceland (IS), making a total of 33 countries.

Applying Voronoi cells to establish load and generator data for transmission network substations disregards the existence of the underlying distribution network, potentially leading to assets being connected inaccurately to substations. A critical assumption of PyPSA-Eur is that the load time-series are applied at the substations within each country, with 60% of it allocated based on the gross domestic product (GDP), representing industrial demand, and 40% allocated based on population, representing residential demand within a Voronoi cell. This distribution is determined through a linear regression analysis of per-country data, resulting in the 60-40% split.

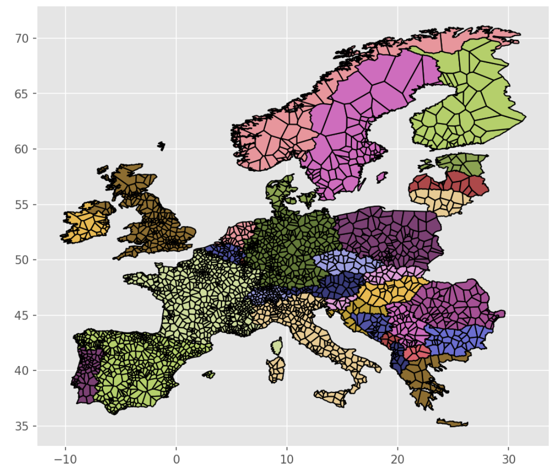

Figure 17: Onshore regions, PyPSA-Eur.

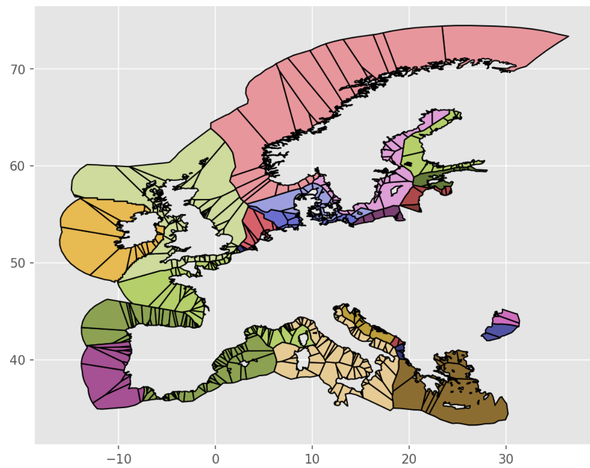

Figure 18: Offshore regions, PyPSA-Eur.

The minimum number of clusters for the entire European region model is 37, 4 more than the number of countries. This is mandatory as the 2022 updated ENTSO-e busmap considers Majorca (ES), Northern Ireland (GB), Sardinia (IT) and Zealand (DK) as separate nodes regardless. The user can select a higher number of nodes but this requires significantly larger computational power and probably can not be performed by local computers.

Figure 19: 37 clusters busmap.

Figure 20: 128 clusters busmap.

Last step of preparation concerns the time resolution and the application of constraints. The user can chose to set from 24 down to 1 hour level of temporal resolution in which the averaging of inputs and iterations will be happening. With time resolution applied, the model takes into account annual carbon emissions limit, level of line expansion in terms of costs or volume, and other types of constraints, explained in the next chapter, such as minimum capacity per carrier, percentage of energy equity per country, exogenous price per tonne emissions of CO_2 etc.

2.5.4 Weather and geographic datasets

PyPSA-Eur uses specific datasets of environmental conditions and geographical topography both for offshore and onshore regions to estimate the renewable generators' potential. Specifically it uses a regional slice of the ERA5 hourly data also referred to as the "cutout", the dimensions of which is determined by the user, for time periods up to 2022. The cutout is the product of raw ERA5 data that are extracted, aggregated, grouped and formatted in terms of features specified in the model (i.e. 'wind', 'wave', 'solar', etc). The workflow for weather data extrapolation and conversion and reformatting is managed by the "atlite" library.

By default, PyPSA-Eur does not process wave data as the technology is not implemented into the model. This is an additional development of the code, that makes it capable of processing wave data too.

ERA5 data are provided by the European Centre for Medium-Range Weather Forecasts (ECMWF) and they are the result of reanalysis. The most recent ECMWF reanalyses are generated under the EU-funded Copernicus Climate Change Service (C3S) (Hersbach et al., 2019 [71]). These reanalyses are available for free through the C3S Climate Data Store (CDS). The process of reanalysis combines historical short-term forecasts with observational data through data assimilation (combinations and numerical representations of observations from various sources), in order to replicate the generation of daily weather forecasts. It employs a consistent fusion of observations and short-term forecasts, usually at a resolution lower than that of contemporary weather forecasts. ERA5 data have a spacial resolution of 31 km, a number which translates to almost 0.3 degrees of longitude and latitude. For this project the full 1 hour resolution ERA5 2018 year data were used.

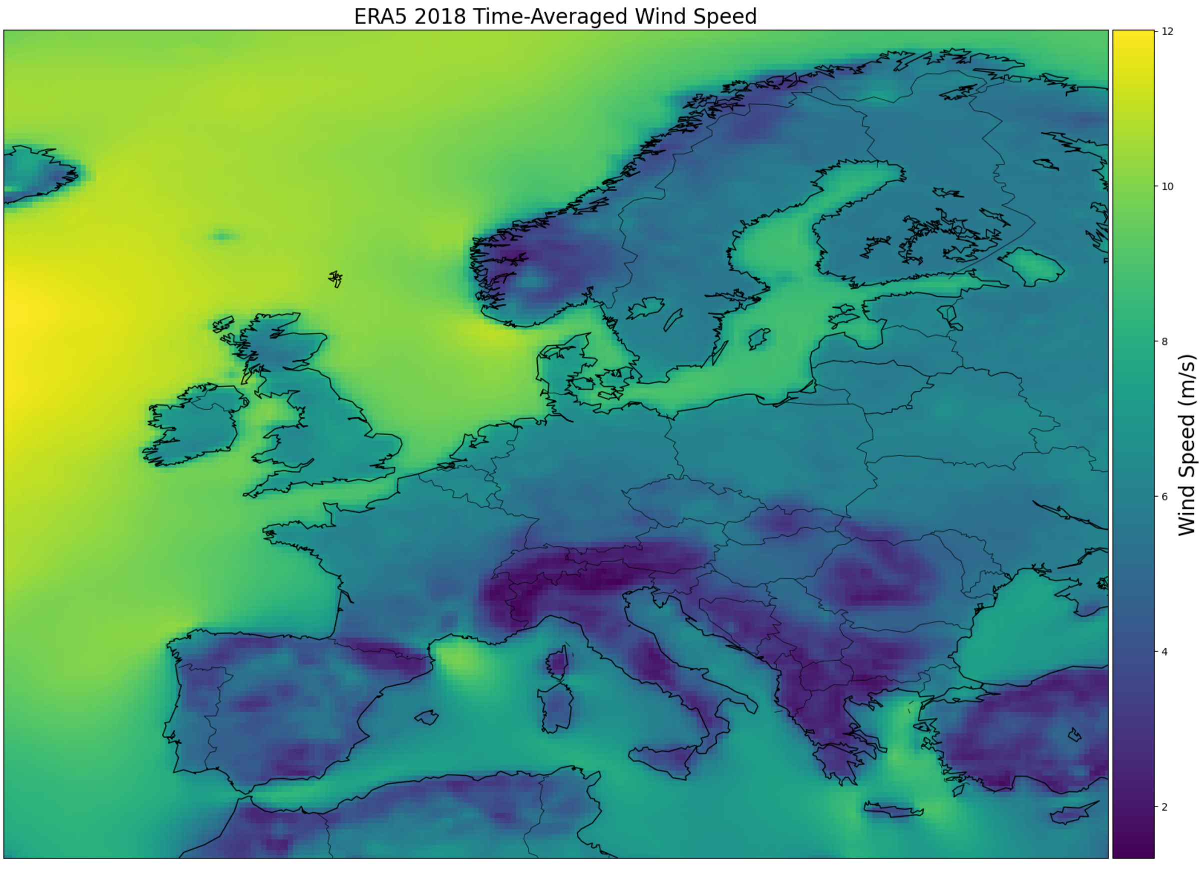

Figure 21: ERA5 2018 wind data.

Offshore renewable energy is highly dependent on the bathymetry of the installation region. PyPSA-Eur uses GEBCO 2014 bathymetry data to introduce the elevation of both offshore and onshore regions. GEBCO 2014 has a spatial resolution of 30 arc-seconds for longitude and latitude which is equal to a resolution of under 1 km for measurements around the equator. To further improve the resolution of the grid, the newest GEBCO 2023 dataset was used. This dataset has a 15 arc-seconds, which is equal to under 500m or around 0.004 degrees resolution and could depict measurable differences in regions with significant elevation fluctuations.

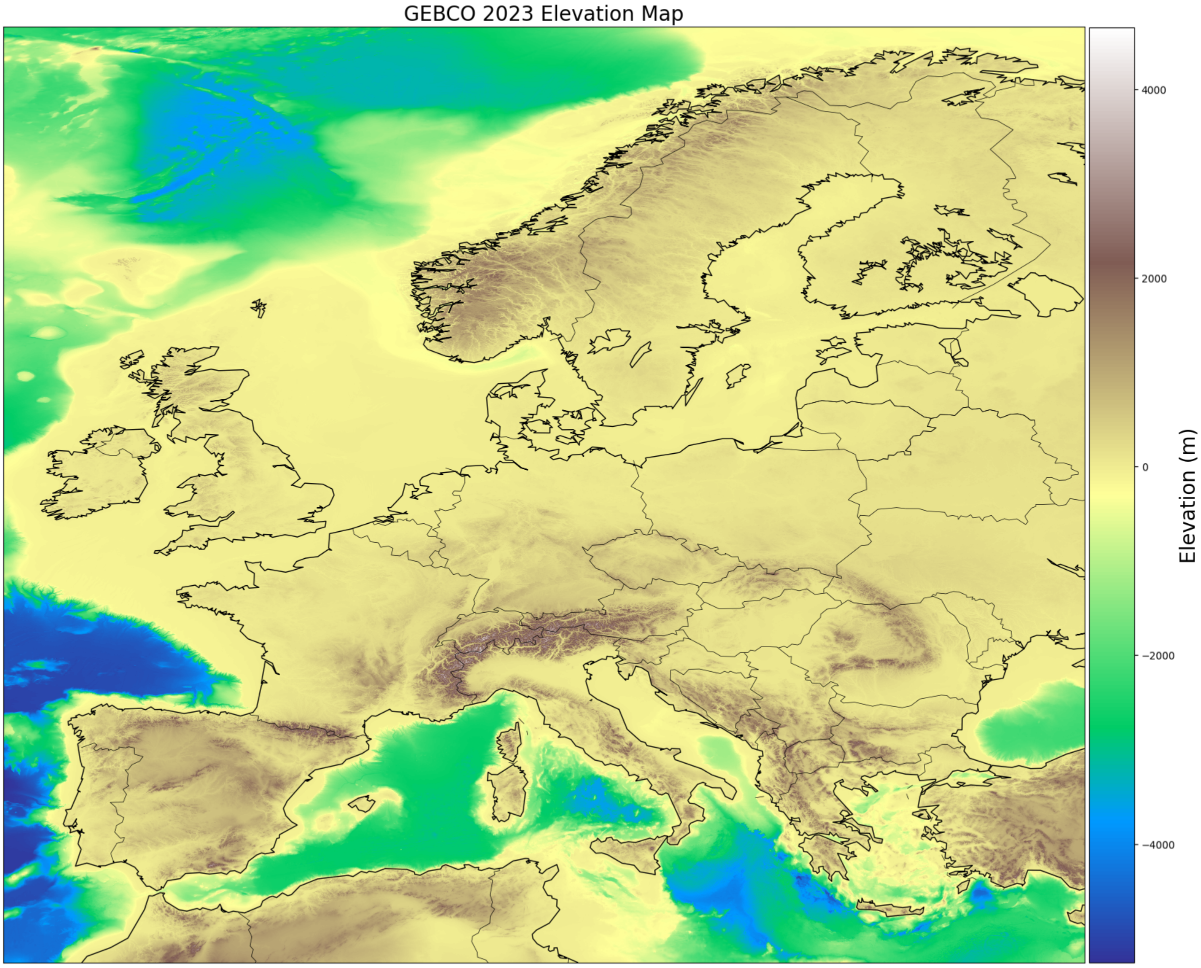

Figure 22: GEBCO 2023 data.

The technologies used in this power system model have maximum and minimum depth constraints, along with proximity to shore constraints, and a detailed bathymetry could provide a deeper view on the feasibility of each of those technologies. However, it is important to couple this highly detailed bathymetry dataset with an equally high resolution weather data package. The final renewable energy profile will have spatial resolution closest to the lowest resolution of the two datasets used to create it, and the benefit of extremely high resolution data might not be visible.

The 0.3 degrees resolution of the ERA5 dataset, limits the overall spatial resolution of power estimation significantly. An available option, not implemented into this project is the use of CERRA (Copernicus European Regional ReAnalysis) data package, which is a higher resolution weather reanalysis dataset with a horizontal resolution of 5.5km or around 0.05 degrees. Higher resolution datasets will potentially benefit offshore energy installation and availability, as the ocean-land contours follow a more realistic shape and less amount of surface is misrepresented. Unfortunately, the PyPSA framework does not support the different data configuration of CERRA, and in order to be utilized, "atlite" needs to include a new branch which will be developed according to the features and resolution of CERRA data.

By coupling the above-mentioned datasets of ERA5 and GEBCO with the land use and restriction datasets of CORINE Land Cover (CLC) the pan-European land cover and land use inventory, and NATURA2000, the network of nature protection areas in the territory of the European Union, PyPSA-Eur creates the renewable generators profiles. CORINE is a land cover dataset which provides a consistent and thematically detailed information on land cover and land cover changes across Europe, it being forests, farming regions, urban fabric etc. Natura2000 is the European network of protected areas that aims to preserve biodiversity around the continent. The final profiles include the generation potential per area, per unit hourly availability factors profile for each bus, the average distance of potentially installed units from the bus and other relevant features.

2.5.5 Validation of the model

Some of the validation points of the model regarding network topology are already mentioned in previous sections. Official statistics for Europe were used to compare total circuit lengths and literature values were consulted to assess renewable expansion potentials. Additionally, an optimal power flow study was conducted, and the network was compared with other network models. The following validation points are assessed by PyPSA-Eur designers.

Deviations on the lengths of the transmission lines are unavoidable as ENTSO-E is connecting the points linearly while in reality transmission lines follow contours and altitude changes. Furthermore, the PyPSA-Eur dataset indicates deviations from the ENTSO-E lengths of circuits as well. These deviations, on average, show a mean absolute error of 15% for 220 kV lines, 7% for 300 kV lines, and 9% for 380 kV lines and are due to the simplification of the network under the preparation processes, which make it even more linear in parts.

Another validation point concerns the renewable expansion potential. Comparing PyPSA-Eur results for Germany with other models it is found that in this model, the potential for onshore wind in Germany is estimated at 441 GW. Literature assessments present a varied range, spanning from 198 GW with a restriction to 2% of total land area, to 1190 GW utilizing 13.8% of the total land area, disregarding species protection and economic viability. Additionally the software finds an installable capacity of 87 GW for fixed-foundation offshore wind in Germany while estimates from literature sources vary, spanning from 38 GW to 85 GW. For solar energy the model estimates the expansion of 350GW which is rather conservative.

In the context of Power Flow, estimated with LOPF heuristic methods, load shedding appeared to be the most significant issue in the model. Load shedding happens due to grid bottlenecks in the model, while in real life network nowadays can manage them. By lifting capacity constraints for short lines the model can restrict load shedding capacity in 6GW from the initial 20.4GW, values compared according to the highest peak-load of 2013 load records. It is also found that clustering the network in a way that each cluster represents a larger area, smooths local load and supply errors

3 Methodology

This section, provides a detailed representation of the functions and the workflow of the PyPSA-Eur model in order to create the PyPSA network. This network contains all of the required components of the model in order to perform calculations. Secondly, the developments in the software regarding wave energy converters and floating wind power will be explained. The developments required for the research of this thesis were completed with the guidance of the Marine Renewable Energies Laboratory (MREL) of TU Delft, especially Dr. George Lavidas, and with the help of the 2021 software documentation of Felix Delgado Elizundia on his research on a Multi-Renewable European Power System.

3.1 Design Overview and model Components

PyPSA is a tool suitable for linearizing and calculating static power flow problems. In principle, the linear optimal power flow (LOPF) method attempts to find the least-cost configuration of a network based on generators and storage dispatch under specified constraints. It is using linear network equations over the amount of snapshots it is given, and applies them in an overall objective function. This way it calculates a least-cost investment plan on the generation, storage, transmission and other components expansion required to fulfill the demand with respect to the number of snapshots.

A network is formed from the combination of multiple sub-networks determined by PyPSA. PyPSA identifies sub-networks automatically, requiring no user input. These sub-networks consist of subsets of buses and passive branches (such as lines and transformers) that are interconnected. These subsets inherit a uniform energy carrier from the buses they are connected to. AC and DC sub-networks can include passive branches. Passive branches are branches whose power flow is not directly controllable, but is determined passively by their impedances and the nodal power imbalances, i.e. lines and transformers. Impedance Z is the resistance equivalent of AC electricity that is generated in parallel AC circuits. It is the product of the line's resistance R and reactance X and it is directly affected by the frequency of the electricity. PyPSA determines each line's impedance as complex numbers:

$$Z = R + jX \tag{13}$$

Impedance can be positive and negative, resulting to the removal or addition of energy to the branch. All other sub-networks must contain only a single isolated bus. In sub-networks, the power flow is governed by the passive flow through the passive branches, influenced by the impedances of these branches.

One of the sub-network components is transformers, which are assigned uniquely for every bus. Transformers are devices that convert AC current of usually a high Voltage level to a lower one. The PyPSA workflow uses transformers as a limiter on the amount of power that can pass through a branch. Transformers are not a component of the final network.

A bus can have as many components as the user desires and it is the energy equilibrium point in the network. Energy enters the model from various sources like generators, storage units, that initially hold a large amount of energy available for consumption. At this stage the components have an efficiency greater than 1 and as long as this is true, they continue to input energy into the system.

Conversely, energy consumption exits in the model through loads, storage units, or stores that draw energy from the generators. However, storage units can also serve as generators. Nodal power balance constraints ensure energy conservation for all elements that contribute to the system. In this system, energy can escape the model through lines, links, storage units etc. which have an efficiency less than 1. Resistance, impedance and other types of energy losses during the process of energy harvesting and transmission are all included in the power equilibrium. In order to achieve power balance, the passive components of the circuits i.e lines and transformers adhere to both the Kirchhoff Voltage Law (KVL) and Kirchhoff Circuit Law (KCL), which is a set of equations for power flow calculations.

Components like generators, links, stores, and storage units have both capital and marginal costs associated with them while transmission lines only have capital costs. Marginal cost represents the incremental monetary cost of adding one additional unit of power beyond the existing capacity. Each component type is uniquely named for each generated network. The output components that the final network consists of are the following:

- **Bus**: fundamental node of the network, on which all loads, generators, storage units, lines, transformers and links are attached
- **Carriers**: energy carrier titled as AC/DC (for lines), wind, pv (generators) etc., it tracks the properties regarding the global constraints

- **Generators**: power generators indicated at every bus differentiated according to carrier type
- **Global Constraints**: constraints on the optimal power flow that affect all of the components, in this thesis CO_2 emissions restrictions are the only global constraints
- **Lines**: distribution and transmission lines, overhead lines and cables
- **Links**: links between buses with arbitrary energy carrier and with controllable active power, links are assumed to neither produce nor consume reactive power, for this project links are overseas DC lines, cables for battery chargers and dischargers, and pipelines distributing energy contained in terms of H_2 for electrolysis and electricity generation via fuel cell technology
- **Load**: explained in section 2.5.3, time-varying datasets that determine the power consumption of the network for each bus, can be adjusted with scaling factors
- **Storage Units**: storage units with fixed nominal-energy-to-nominal-power ratio and maximum hours of continuous operation, in this project storage units consist of batteries, hydro reservoirs, pumped-up hydro storage, and H_2 storage
- **Storage**: generic storage units whose capacity may be optimised, in this case H_2 and battery storage

As it can be observed, every component in the system is conceptually different from the rest with the exception of 'Storage Units' and 'Storage'. In PyPSA, the term 'Storage Units' refers to units attached to a single bus that can be used to balance the power inter-temporally. They have the ability to shift electrical energy from one time period to another with regard to a maximum-time power feed in the power system set by the user. The more fundamental 'Storage', refers to storage units also attached to a single bus, but which simply store the excess energy of the generators, produced in high-output periods on the same bus and deliver it back to the system in periods of high demand via specific links.

3.2 Power System Optimization

3.2.1 Objective function

The goal of an objective function in linear programming is to include the relevant variables and constraints in order to minimize or maximize the objective under investigation. PyPSA is an optimal investment cost software that mixes capital costs for all components and operational costs for the generators to find the minimum solution for the following function:

$$\sum_{n,s} c_{n,s}\bar{g}_{n,s} + \sum_{n,s} c_{n,s}\bar{h}_{n,s} + \sum_{l} c_l F_{n,s} + \sum_{t} w_t \left[\sum_{n,s} o_{n,s,t} g_{n,s,t} + \sum_{n,s} o_{n,s,t} h_{n,s,t}\right] \tag{14}$$

where n, s are the bus and carrier notations, $\bar{g}_{n,s}$ is the nominal power of the generator s at bus n, $\bar{h}_{n,s}$ is the storage nominal power of unit s at bus n, $c_{n,s}$ is the capital cost of extending the capacity of that carrier by 1 MW, F_l is the the capacity of a branch l of components and c_l its associated capital cost, w_t is the function's weighting of time/snapshot t factor, $g_{n,s,t}$ and $h_{n,s,t}$ are the dispatch of the generators and storage systems at time t, and $o_{n,s,t}$ their operational costs. The term 'nominal' refers to the specified capacity of a generator which determines its performance under typical operating conditions. The objective function calculates the cost of the entire power system over the number of snapshots, and since in this project 8760 hourly snapshots where used, that makes a total of a full year. In other words in this project, the objective function represents the annual expenses of the power system.

3.2.2 Software Constraints

The dispatch and nominal power inputs in Equation 14 subject to constraints. In order to optimize the generators nominal power and dispatch at every point in time, their values are contained into time-dependent restrictions. These related to aspects such as weather conditions or power plant de-rating. De-rating refers to a situation where a power plant operates at less than its maximum capacity or output and is quite common for renewable sources. The generators lie under the constraint:

$$\tilde{g}_{n,s,t} * \bar{g}_{n,s} \leq g_{n,s,t} \leq \hat{g}_{n,s,t} * \bar{g}_{n,s} \tag{15}$$

where $\tilde{g}_{n,s,t}$ and $\hat{g}_{n,s,t}$ are the time-dependent constraints applied per unit of nominal power and $\bar{g}_{n,s}$ is the nominal power of a generator. All of the generators used in the model are RES and have a time-varying availability expressed in time-series. Since the generators are extendable up to some extend, according to the land and resources availability, nominal power is additionally constrained between a minimum and maximum limit of installable capacity.

Similar constraints apply for storage units as well. For a storage unit the maximum power output is dependant to the maximum power input, creating a dependency between the rates at which energy is taken in and released by the storage unit. Moreover, the state of charge of the unit, in other words the highest amount of energy that can be stored, is also linked to the maximum power output. This linkage is established through the maximum hours variable, which influences how the storage unit operates. PyPSA offers the ability to build storage units via the more traditional 'store' and 'link' components.

Storage unit constraints have three time-dependent variables, first one being the dispatch $h_{n,s,t}$, where the state of charge decreases

$$0 \leq h_{n,s,t} \leq \bar{h}_{n,s} \tag{16}$$

the charging or uptake of the unit $f_{n,s,t}$, where the state of charge increases

$$0 \leq f_{n,s,t} \leq \bar{h}_{n,s} \tag{17}$$

and the state of charge $E_{n,s,t}$ it self constrained according to the number of hours $r_{n,s}$ the nominal power is available for

$$0 \leq E_{n,s,t} \leq r_{n,s}\bar{h}_{n,s} \tag{18}$$

where $\bar{h}_{n,s}$ is the storage nominal power. The state of charge can be calculated by aggregating all the relevant energy loses as the unit is operating:

$$E_{n,s,t} = \eta_{n,s}^{stand,w_t} \cdot E_{n,s,t-1} + w_t \left(\eta_{n,s}^{store} \cdot f_{n,s,t} - \eta_{n,s}^{dispatch,-1} \cdot h_{n,s,t} + h_{n,s,t}^{inflow} - h_{n,s,t}^{spillage} \right) \tag{19}$$

η represent the efficiency factors regarding thermal loses, increase and dispatch of power and general inflow $h_{n,s,t}^{inflow}$ and spillage $h_{n,s,t}^{spillage}$ of power.

Generic store systems of which nominal energy can be optimized for every snapshot only have two time-dependent constraints, store dispatch $h_{n,s,t}$

$$-\infty \leq h_{n,s,t} \leq +\infty \tag{20}$$

and real time energy $e_{n,s,t}$

$$\tilde{e}_{n,s} \leq e_{n,s,t} \leq \bar{e}_{n,s,t} \tag{21}$$

where $\tilde{e}_{n,s}$ represents a variability related constraint and $\bar{e}_{n,s,t}$ is the nominal energy. The relation of the variables are as such:

$$e_{n,s,t} = \eta_{n,s}^{stand,w_t} \cdot e_{n,s,t-1} - w_t \cdot h_{n,s,t} \tag{22}$$

Two additional constraints concern the passive branch flows, and utilize limits in the capacities of lines and transformers that determine the maximum allowed power flow inside a branch. These limits are employed in the nodal power balance equations.

3.2.3 Nodal Power Balances

Nodal power balance equations determine the energy conservation inside a loop or a branch. It ensures that supply and demand match and it has the following form:

$$\sum_s d_{n,s,t} = \sum_s g_{n,s,t} + \sum_s h_{n,s,t} - \sum_s f_{n,s,t} - \sum_l K_{nl} f_{l,t} \tag{23}$$

where $d_{n,s,t}$ is the load for every snapshot at each bus, $K_{nl} \in \{-1, 0, 1\}$ is an incidence matrix indicating the start or end of a branch l with respect to the bus. It has non-zero values $+1$ if branch l starts on bus n and 1 if branch l ends on bus n.

PyPSA uses Kirchhoff formulation to ensure energy conservation. The flows are bound to obey to the physical laws established by Kirchhoff. Kirchhoff's Circuit Law KCL suggests that the current injected at each bus must be equal to the current withdrawn by the networks branches attached to thee node.

$$\sum d_{n,s,t} = \sum p_i \tag{24}$$

KCL is applied into one branch at a time so for this case $\sum d_{n,s,t} = d_{n,t}$ and provides N amount of linear equations for the L unknown flows f_l. KCL provides a general set of equations but disregards the components inside a branch. Kirchhoff's Voltage Law (KVL) states that the sum of Voltage differences between the relevant branches and circuits must be zero. Graph theory principles, utilized by the software's designers, show that for a connected graph (electrical network in this case), there are $LN + 1$ independent cycles. These cycles, when expressed mathematically using a cycle incidence matrix C_{lc}, provide additional equations that help constrain and determine the unknown branch flows. KVL in terms of power flow is expressed as:

$$\sum C_{lc} x_l f_l = 0 \tag{25}$$

Other types of constraints that are applied in the entirety of the model are transmission volume and cost expansion limits, capacity per technology expansion limit and CO_2 emissions limit. In PyPSA, the user has the option to set an upper boundary of expansion of transmission lines, either in the context of volume or costs of it, but not both simultaneously.

This boundary allows up to 50% expansion for the PyPSA-Eur environment, but it can also be switched to a more broad cost-only expansion optimization. A risk associated of the last is that the final expansion might be very optimistic and infeasible in terms of time and resources. Capacity per technology refers to the "Business-As-Usual" concept, that utilizes predictions and trends in order to predetermine the minimum target for installation capacity per generator. Lastly, CO_2 emissions limit refers to the fraction of 1990's emissions for which the user aims to develop the model. These constraints are explained in section 3.4.

3.3 Developments

Developments in the PyPSA-Eur environment were performed in order for it to be able to estimate floating wind and wave energy together with the existing technologies.

For floating wind the amount of development was limited into using additional floating wind generator components in the existing 'wind' calculation methods. This required establishing a new notation for the technology, one for the AC and one for the DC technology, as well as creating branches in the code to include their unique capital costs.

Also, a new variable of minimum depth of installation was introduced to distinguish the different depths each technology can utilize. So far bottom fixed WTGs (wind turbine generators) are installed at a maximum depth of around 50m. Floating WTGs are set to be installed beyond this value but limited to 250m due to excessive costs of cabling and mooring investments. New entries which followed the software's format were added at the cost data. Those concern investment, operation and maintenance costs, lifetime of the structures, as well as costs regarding the cable connections and the substations.

Changes regarding capital costs that are applied for floating wind generators apply for wave energy converters (WECs) as well. Those have distinct values attributed to them. However wave technologies require additional developments as the features necessary to extrapolate the wave data did not exist. A new method 'wave' was introduced into the cutout and two new datasets were downloaded from the ERA5 data package, those being wave period T_p and significant wave height H_{m0}.

Wave energy uses the device's power matrix to estimate the power output of the generator, based on the operating conditions suggested by the cutout in a specific location and time. In other words the methods locates the combination of significant period T_p and significant wave height H_{m0} and assigns it to a specific generated power output. Similarly to the rest of the methods, a renewable profile is created, including the information about the availability of the the technology, the time-series generation, the average distance from the closest bus and the fraction of the underwater cabling required to install the offshore power plant.

As mentioned in chapter 2.4.6, WECs in this thesis are located in shallow waters from 0 to 20m, nearshore from 20 to 80m, and farshore from 50 to 150m. The shallow water WEC is a 26m wide and 13m tall Oyster inspired 290kW oscillating wave surge converter (Guillou, 2023 [72]), with a hydraulic pump PTO. The nearshore WEC is the 400kW CorPower and MREL-TUDelft (Alday et al., 2023 [73]) developed point absorber with a height of 18m, diameter of 9m, and a minimum installation depth of 40m. Lastly, the farshore device is a 180m long and 4m in diameter Pelamis P2, with a rated power of 750kW [74]. Below their power matrices are presented.

	Tp															
Hm0	1.0	2.0	3.0	4.0	5.0	6.0	7.0	8.0	9.0	10.0	11.0	12.0	13.0	14.0	15.0	16.0
0.5	0	0	0	0	0	0	0	0	0	0	0	0	0	0	0	0
1.0	0	0	0	0	0	0	0	0	0	0	1	3	0	0	0	0
1.5	0	0	0	0	20	30	38	42	44	44	45	47	3	0	0	0
2.0	0	0	0	0	80	85	92	97	102	103	104	100	45	0	0	0
2.5	0	0	0	0	140	147	152	158	155	155	160	161	104	0	0	0
3.0	0	0	0	0	192	197	208	202	203	209	211	201	156	0	0	0
3.5	0	0	0	0	241	237	237	241	243	230	236	231	204	0	0	0
4.0	0	0	0	0	0	271	272	269	268	267	270	260	235	0	0	0
4.5	0	0	0	0	0	291	290	290	280	287	276	278	260	0	0	0
5.0	0	0	0	0	0	291	290	290	280	287	276	278	277	0	0	0
5.5	0	0	0	0	0	0	290	290	280	287	276	278	277	0	0	0
6.0	0	0	0	0	0	0	290	290	280	287	276	278	277	0	0	0
6.5	0	0	0	0	0	0	290	290	280	287	276	278	277	0	0	0
7.0	0	0	0	0	0	0	0	0	0	0	0	0	0	0	0	0
7.5	0	0	0	0	0	0	0	0	0	0	0	0	0	0	0	0
8.0	0	0	0	0	0	0	0	0	0	0	0	0	0	0	0	0
8.5	0	0	0	0	0	0	0	0	0	0	0	0	0	0	0	0
9.0	0	0	0	0	0	0	0	0	0	0	0	0	0	0	0	0
9.5	0	0	0	0	0	0	0	0	0	0	0	0	0	0	0	0
10.0	0	0	0	0	0	0	0	0	0	0	0	0	0	0	0	0

Figure 23: Shallow 290kW WEC power matrix.

	Tp																															
Hm0	1.0	1.5	2.0	2.5	3.0	3.5	4.0	4.5	5.0	5.5	6.0	6.5	7.0	7.5	8.0	8.5	9.0	9.5	10.0	10.5	11.0	11.5	12.0	12.5	13.0	13.5	14.0	14.5	15.0	15.5	16.0	16.5	17.0
0.5	0	0	0	0	0	0	0	0	0	0	0	0	0	0	0	0	0	0	0	0	0	0	0	0	0	0	0	0	0	0	0	0	0
1.0	0	0	0	1	4	6	10	14	18	21	24	28	31	32	35	37	37	39	38	36	35	33	30	29	26	24	22	21	20	18	0	0	0
1.5	0	0	1	3	8	15	22	31	39	47	55	62	70	73	78	84	84	87	85	81	80	73	67	65	59	54	50	48	44	41	0	0	0
2.0	0	0	1	6	14	26	40	55	70	83	97	111	124	130	139	149	148	155	151	145	142	130	119	115	105	97	88	86	79	72	0	0	0
2.5	0	0	2	9	22	40	62	85	109	130	152	173	193	202	217	232	232	241	236	226	221	204	186	180	164	151	138	134	123	113	0	0	0
3.0	0	0	3	13	32	58	89	123	158	187	218	249	278	291	312	334	334	348	340	325	319	293	268	260	237	217	199	193	178	163	0	0	0
3.5	0	0	4	18	43	79	121	167	214	254	297	339	379	397	400	400	400	400	400	400	400	399	365	353	322	296	271	263	242	222	0	0	0
4.0	0	1	6	24	56	104	158	218	280	332	388	400	400	400	400	400	400	400	400	400	400	400	400	400	400	387	354	343	316	290	0	0	0
4.5	0	1	7	30	71	131	200	276	354	400	400	400	400	400	400	400	400	400	400	400	400	400	400	400	400	400	400	400	400	367	0	0	0
5.0	0	1	9	37	88	162	247	341	400	400	400	400	400	400	400	400	400	400	400	400	400	400	400	400	400	400	400	400	400	400	0	0	0
5.5	0	1	11	45	107	196	299	400	400	400	400	400	400	400	400	400	400	400	400	400	400	400	400	400	400	400	400	400	400	400	0	0	0
6.0	0	1	13	53	127	233	356	400	400	400	400	400	400	400	400	400	400	400	400	400	400	400	400	400	400	400	400	400	400	400	0	0	0
6.5	0	1	15	62	149	273	400	400	400	400	400	400	400	400	400	400	400	400	400	400	400	400	400	400	400	400	400	400	400	400	0	0	0
7.0	0	2	18	72	173	317	400	400	400	400	400	400	400	400	400	400	400	400	400	400	400	400	400	400	400	400	400	400	400	400	0	0	0
7.5	0	2	21	83	198	364	400	400	400	400	400	400	400	400	400	400	400	400	400	400	400	400	400	400	400	400	400	400	400	400	0	0	0
8.0	0	2	23	94	226	400	400	400	400	400	400	400	400	400	400	400	400	400	400	400	400	400	400	400	400	400	400	400	400	400	0	0	0
8.5	0	0	0	0	0	0	0	0	0	0	0	0	0	0	0	0	0	0	0	0	0	0	0	0	0	0	0	0	0	0	0	0	0
9.0	0	0	0	0	0	0	0	0	0	0	0	0	0	0	0	0	0	0	0	0	0	0	0	0	0	0	0	0	0	0	0	0	0
9.5	0	0	0	0	0	0	0	0	0	0	0	0	0	0	0	0	0	0	0	0	0	0	0	0	0	0	0	0	0	0	0	0	0
10.0	0	0	0	0	0	0	0	0	0	0	0	0	0	0	0	0	0	0	0	0	0	0	0	0	0	0	0	0	0	0	0	0	0

Figure 24: Nearshore 400kW WEC power matrix.

	Tp																												
Hm0	1.0	1.5	2.0	2.5	3.0	3.5	4.0	4.5	5.0	5.5	6.0	6.5	7.0	7.5	8.0	8.5	9.0	9.5	10.0	10.5	11.0	11.5	12.0	12.5	13.0	13.5	14.0	14.5	15.0
0.0	0	0	0	0	0	0	0	0	0	0	0	0	0	0	0	0	0	0	0	0	0	0	0	0	0	0	0	0	0
0.5	0	0	0	0	0	0	0	0	0	0	0	0	0	0	0	0	0	0	0	0	0	0	0	0	0	0	0	0	0
1.0	0	0	0	0	0	0	0	0	0	22	29	34	37	38	38	37	35	32	29	26	23	21	0	0	0	0	0	0	0
1.5	0	0	0	0	0	0	0	0	32	50	65	76	83	86	86	83	78	72	65	59	53	47	42	37	33	0	0	0	0
2.0	0	0	0	0	0	0	0	0	57	88	115	136	148	153	152	147	138	127	118	104	93	83	74	66	59	0	0	0	0
2.5	0	0	0	0	0	0	0	0	89	138	180	212	231	238	238	230	218	199	181	183	146	130	118	103	92	0	0	0	0
3.0	0	0	0	0	0	0	0	0	129	198	260	305	332	340	332	315	292	266	240	219	210	188	187	149	132	0	0	0	0
3.5	0	0	0	0	0	0	0	0	0	270	354	415	438	440	424	404	377	362	326	292	260	230	215	202	180	0	0	0	0
4.0	0	0	0	0	0	0	0	0	0	0	462	502	540	546	530	499	475	429	384	366	339	301	267	237	213	0	0	0	0
4.5	0	0	0	0	0	0	0	0	0	0	544	635	642	648	628	590	562	528	473	432	382	359	338	300	266	0	0	0	0
5.0	0	0	0	0	0	0	0	0	0	0	0	739	726	731	707	687	670	607	557	521	472	417	369	348	328	0	0	0	0
5.5	0	0	0	0	0	0	0	0	0	0	0	750	750	750	750	750	737	667	658	586	530	476	446	395	355	0	0	0	0
6.0	0	0	0	0	0	0	0	0	0	0	0	0	750	750	750	750	750	750	711	633	619	558	512	470	415	0	0	0	0
6.5	0	0	0	0	0	0	0	0	0	0	0	0	750	750	750	750	750	750	750	743	658	621	579	512	481	0	0	0	0
7.0	0	0	0	0	0	0	0	0	0	0	0	0	0	750	750	750	750	750	750	750	750	676	613	584	525	0	0	0	0
7.5	0	0	0	0	0	0	0	0	0	0	0	0	0	0	750	750	750	750	750	750	750	750	686	622	593	0	0	0	0
8.0	0	0	0	0	0	0	0	0	0	0	0	0	0	0	0	750	750	750	750	750	750	750	750	690	625	0	0	0	0
8.5	0	0	0	0	0	0	0	0	0	0	0	0	0	0	0	0	0	0	0	0	0	0	0	0	0	0	0	0	0
9.0	0	0	0	0	0	0	0	0	0	0	0	0	0	0	0	0	0	0	0	0	0	0	0	0	0	0	0	0	0
9.5	0	0	0	0	0	0	0	0	0	0	0	0	0	0	0	0	0	0	0	0	0	0	0	0	0	0	0	0	0
10.0	0	0	0	0	0	0	0	0	0	0	0	0	0	0	0	0	0	0	0	0	0	0	0	0	0	0	0	0	0

Figure 25: Farshore 750kW WEC power matrix

Each device has a generation time series and the energy potential can now be calculated by factoring in bathymetry, land use and land restrictions data. The 9 renewable technologies, excluding hydro generations which is not considered to be extendable, that are used for the model under investigation are:

Official name	Model name
Floating Offshore Wind AC	`offwind-fl-ac`
Floating Offshore Wind DC	`offwind-fl-dc`
Bottom fixed Offshore Wind AC	`offwind-ac`
Bottom fixed Offshore Wind DC	`offwind-dc`
Onshore Wind	`onwind`
Onshore Solar	`solar`
Wave Converter Farshore	`wavefarshore`
Wave Converter Nearshore	`wavenearshore`
Wave Converter Shallow	`waveshallow`

Expanding PyPSA involves adding new features. By default, PyPSA includes geothermal and biomass in its carriers. Additional options like tidal energy, ocean thermal energy, and offshore solar energy can be integrated. This diversification is expected to enhance the model by limiting system variability and promoting stability. Figure 26 illustrates the energy potential for each scenario in this thesis, representing the maximum installable capacity at each node multiplied by an average capacity factor.

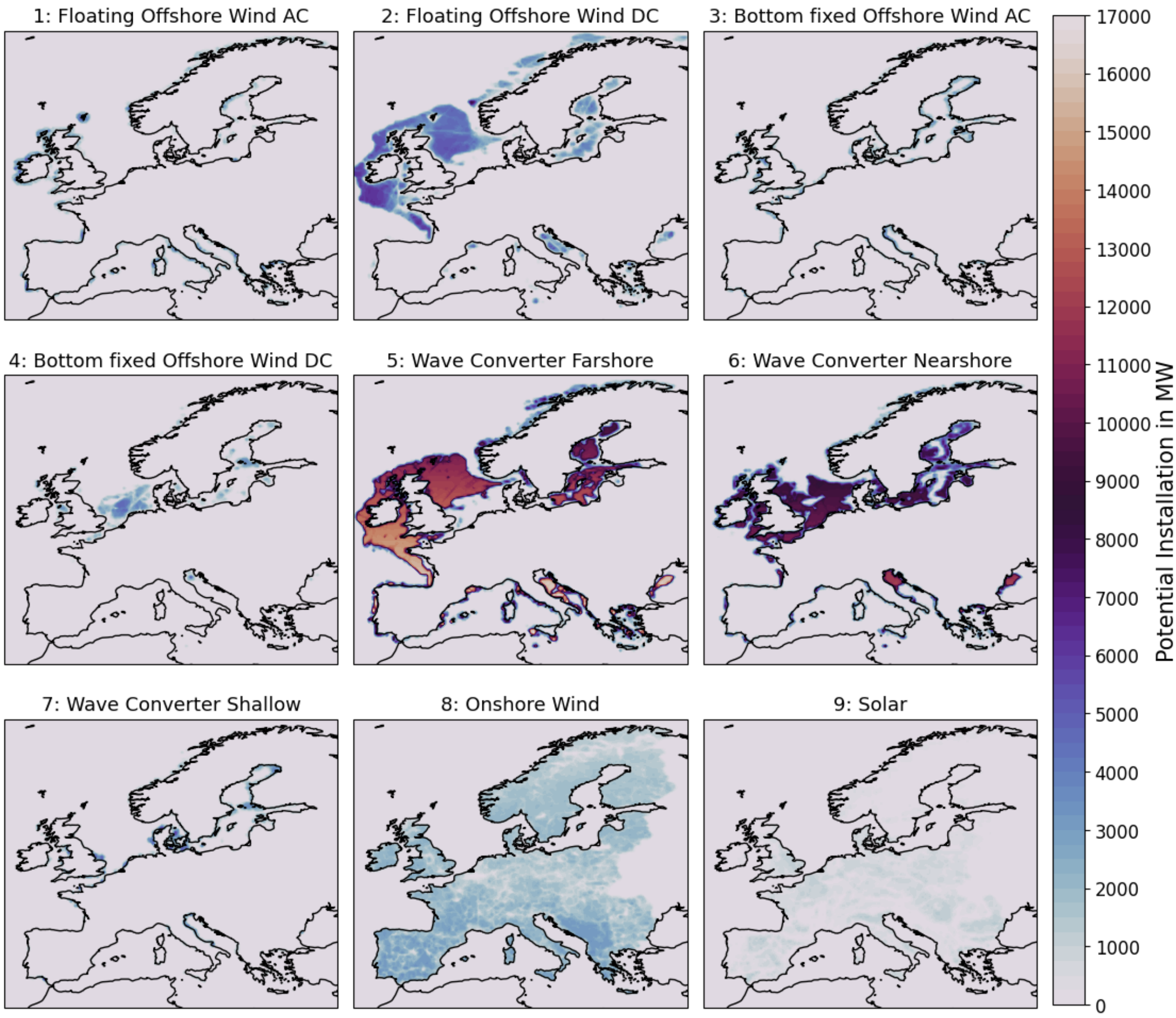

Figure 26: Renewable energy generation potential.

This potential is highly dependent on the technical configuration of the renewable capacities. All of the types of carriers have their potential calculated according to generators with specific rated power and geometry characteristics.

3.4 Model Configuration

The model configuration involves temporal resolution and network geometry, technology characteristics and land use, capacity and expansion restrictions and capital costs.

The model can calculate the power flow for snapshots with a resolution of as small as 1 hour. Most of the runs of the software were performed in a 1 hour resolution. In the initial stage however, for limit testing and different configuration comparison, runs of 24 and 6 hour resolutions were also performed, together with tests of different bus numbers.

Increasing the resolution and the number of buses increases computational time and requires more computing resources. The PyPSA capabilities appear to be more dependant in computing memory availability than processing availability and configurations of 1 hour resolution with more than 50 buses were unable to be performed. The available tools to generate the model limited the final tests network to 50 buses for a 1 hour resolution run. Below, the 50-bus network configuration.

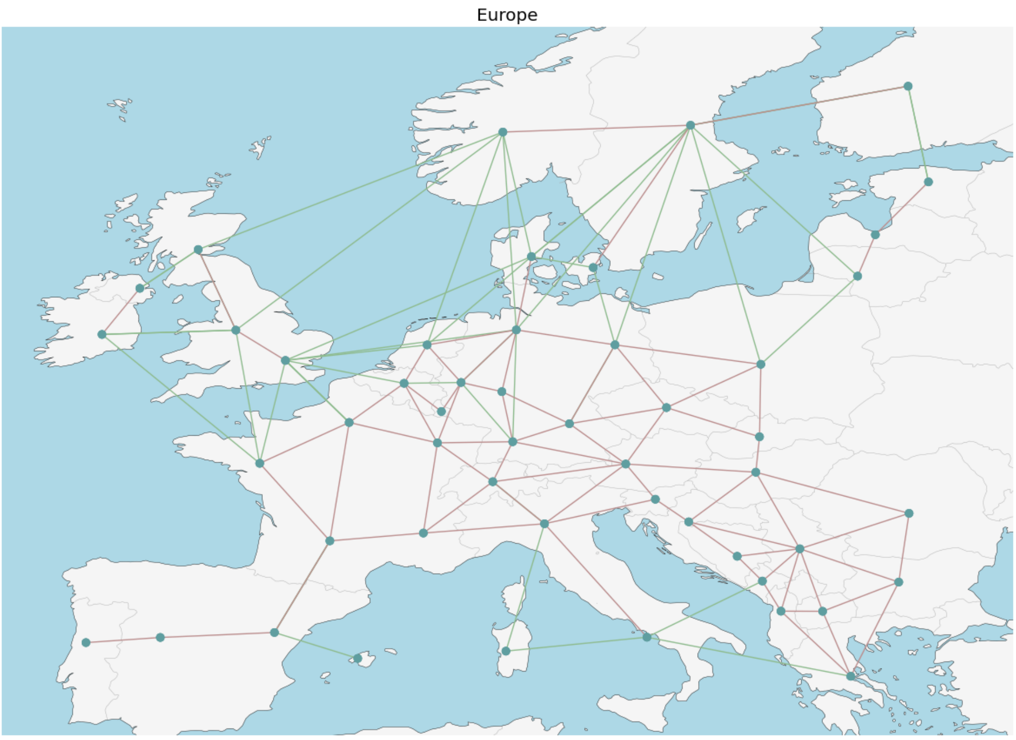

Figure 27: 50 buses map.

Red lines indicate the HVAC transmission lines while green ones indicate the HVDC ones. Comparing this busmap with the 37 one, one can spot differences regarding the high consumption or highly industrial regions of Europe, previously represented by only one bus. Great Britain, France, Spain, Italy and Germany all use the available extra buses to split each country's demands while the rest of the countries still comprise of one bus. Restriction-wise, the transmission lines are expanded and optimized according to their capital costs. This includes separate costs for both overhead and underwater sections different for HVAC and HVDC lines. In order to meet transmission line safety standards, in PyPSA lines have a maximum flow set to 70% of their rated capacity. Since the model is carbon-free, CO_2 emission limits and costs were not required. The scenarios include only 2030, 2040 and 2050 target years.

3.4.1 Wind power

The renewable energy system under investigation has specified technical characteristics that shape the generation of energy. The user can chose CORINE Land-use Codes (CLC) on which every technology will be installed. The CLC documentation and classification of regions can be found in literature. For the onshore wind technology:

	Onshore Wind
Device	Vestas V90 3MW [75]
Capacity MW/km^2	4
Rotor diameter [m]	90
Hub height [m]	80
Cut-in/rated/cut-out wind speed [m/s]	4/12/25
CORINE codes	[12, 13, 14, 15, 16, 17, 18, 19, 20, 21, 22, 23, 24, 25, 26, 27, 28, 29, 32]

Table 3: Onshore wind energy.

For bottom fixed and floating offshore wind turbines with both AC and DC transmission line connections, with CORINE [44, 255] which refers to the oceanic regions of each country the tables are, for bottom fixed:

	Offshore Wind AC	**Offshore Wind DC**
Device	NREL 2020ATB 12MW	NREL 2020ATB 12MW
Capacity MW/km^2	8	8
Rotor diameter [m]	214	214
Hub height [m]	136	136
Cut-in/rated/cut-out wind speed [m/s]	4/11/25	4/11/25
Min. depth [m]	0	0
Max. depth [m]	50	50
Min. distance from shore [m]	0	30000
Max. distance from shore [m]	30000	-

Table 4: Bottom fixed wind energy.

and for floating wind turbines:

	Offshore Fl. Wind AC	**Offshore Fl. Wind DC**
Device	NREL 2020ATB 15MW	NREL 2020ATB 15MW
Capacity MW/km^2	9	9
Rotor diameter [m]	240	240
Hub height [m]	150	150
Cut-in/rated/cut-out/wind speed [m/s]	4/11/25	4/11/25
Min. depth [m]	50	50
Max. depth [m]	250	250
Min. distance from shore [m]	0	30000
Max. distance from shore [m]	30000	-

Table 5: Floating wind energy.

The offshore wind turbine parameters, power curves and dimensions used in this model were provided by the National Renewable Energy Laboratory (NREL) repository [76].

Capacity per km^2 for wind power is derived from the horizontal spacing between the turbines which is calculated according to the turbines rotor diameter D multiplied by a factor, in this case:

$$5 \times D \tag{26}$$

based on rule-of-thumb calculations broadly used in wind farm design concepts. This distance affects the amount of wake loses from the disturbance of the air flow as it passes through a wind farm and actively changes the capacity factor. This calculation is then decreased to the closest integer for convenience and a conservative measurement. In order to calculate this integer small scale wind farm grids were used in which the wind devices were placed in a square pattern and the sum of installed capacity was divided by the area in which this amount was supposed to be installed. It was found that the numbers start to converge for grids of 4×4 and greater.

For the onshore wind turbines, 3MW turbines with a diameter of 90m can allow in theory more than $15MW/km^2$ installed. There are two assumptions for why its capacity density is decreased to only $4MW/km^2$. Firstly, since the turbines are installed on land, they need to follow certain building protocols in order to be accepted from the local communities which they affect. Considering information from operating sites in the European region, a lot of wind farms on land are typically placed in a line layout, since they are installed on mountain ridges, in order to take advantage of the wind resource.

Secondly, production-wise, placing the devices too close to each other can drastically diminish the capacity factor due to wake effects, in the case of which installing more turbines probably does not benefit the production. Even though the model "reads" a high input value on the technology, the overall system might only manage to achieve a disproportional cost increase with respect to the energy increase.

The distance from shore also has a conservative assumption logic. AC cables can transmit power for distances up to 50km due to capacitance phenomena, as mentioned in the literature review. In this project, however, 30km ones were chosen to compensate inter array cabling distancing and to balance the installation of DC and AC generators, as the first one has significant potential advantage over the second one. A maximum shore distance constraint is not applied, mostly to estimate the overall potential of the installable capacity around the European sea basins. Since the connection costs for the production sites to the nodes have their own high values, the final model will filter out production zones with high associated electricity costs.

From onshore to floating offshore wind, the devices get larger in power rating. This happens in order for the model to be able to harvest the larger power resources that the open sea can deliver, while onshore or closer to shore resources rate lower. Larger equals more expensive and the overall design should balance the trade of cost over power production. In other words, installing 15MW WTGs onshore, while being possible, might not be quite feasible.

3.4.2 Wave power

For wave technologies:

	Farshore WEC	**Nearshore WEC**	**Shallow WEC**
Device	750kW	400kW	290kW
Capacity MW/km^2	20	15	10
Min. depth [m]	50	20	0
Max. depth [m]	150	80	20

Table 6: Wave energy.

The EU's strategy outlines targets for 2030, aiming for a minimum installed capacity of 60 GW for offshore wind and 1 GW for ocean energy, with aspirations for 300 GW and 40 GW, respectively, by 2050. In addition, the UK aims to deploy up to 50 GW of offshore wind, including 5 GW in floating wind by 2030, with projections suggesting a potential demand of 125 GW by 2050. Moreover, there are ambitions for a total installed capacity of 22 GW for marine energies by 2050, considering wave and tidal, however in absence of suitable high fidelity tidal data, waves are considered.

Capacity per km^2 for wave energy normally varies per device as the concepts use different wave energy principles thus there exists a variety in geometry and in the spacing between them. According to Lavidas and Blok, 2021 [77], who studied the cost-effectiveness of multiple configurations of wave energy farms, and compared those to ones found in literature, wave energy installation can be as dense as $20 - 40MW/km^2$, depending on the quality of calibration of the wave farm. Their safer assumption suggests that, at this level of research, wave farms can be feasible in the range of $10 - 20MW/km^2$. For this reason, the same range is kept in the modelling of wave energy, it being 20/15/10 MW/km^2 for farshore, nearshore and shallow waters respectively. Farshore WEC device in the model is the Pelamis P2 devices which is 180m long but has a width of only 4m meaning devices can be placed close to each other with minimum effects from the motion of one to the neighbouring ones. A research on the optimal layout of point absorbers was performed by Bozzi et al. 2017 [78], where their findings suggest the highest power output can be achieved with a spacing in the range of 10-20 times the diameter of the device. They also highlight the significance of layout shape and orientation of the devices, according to which the combination of a rhombus shaped layout with a site specific orientation of the wave farm delivers the most. Lastly, a study of a wave surge device layout from Benites-Munoz et al. 2024 [79] using computational fluid dynamics to model the devices in a variety of spacings found that for a range of wavelengths and according to the width of the devices, there is an power enhancement possibility that derives from the diffracted waves which amplify the movement of the neighbouring ones. Nonetheless, the devices maximize the power output in a combination of two ratios of dimensions, specifically the lateral distance should be 1.5 to 5 times the width of the panel and the horizontal distance between 0.5-1.1 times the design wavelength. A very optimal layout could achieve $40MW/km^2$, however production is assumed to be quite lower due to the proximity to the shore.

3.4.3 Business As Usual

All of these capacities are passed as minimum capacity restrictions in the model for the 2030, 2040 and 2050 target years. The capacity of each carrier is set according to assumptions influenced by literature on the availability of each technology. The following table shows these capacities, only for the marine RES, that are passed as the built-in "Business As Usual" or "BAU" argument in the software. In other words a baseline starting scenario. Once the minimum capacities are installed, the rest of the demand is distributed according to the functions of PyPSA.

	2030 [GW]	**2040** [GW]	**2050** [GW]
Offshore Wind AC	10	34	40
Offshore Wind DC	30	40	55
Offshore Fl. Wind AC	25	50	80
Offshore Fl. Wind AC	45	115	230
Farshore WEC	1	7	17
Nearshore WEC	2	15	25
Shallow WEC	3	10	20
Minimum capacity ('wind' &'wave')	110 & 6	249 & 32	405 & 62

Table 7: Minimum BAU capacities set in the model in GW.

3.4.4 Solar power

Solar energy was included with the original PyPSA-Eur settings. Similarly to the rest, in PyPSA-Eur, the calculation of solar energy entails various factors, resulting in an influx of irradiation onto solar panels. This influx is determined by multiple aspects including the orientation and position of the panels, considering their tilt and azimuth angles relative to the sun's path. The solar panel model incorporates both direct and diffuse influx, accounting for direct sunlight and scattered light from the atmosphere. Additionally, it considers the influence of albedo, which refers to the reflective properties of the surface on which the solar panels are installed. The result is a photovoltaic generation time-series, converted from the total radiation flux and ambient temperature.

	Solar
Device	CSi
Capacity MW/km^2	1.7
Slope	35°
Azimuth	180°
CORINE codes	[1, 2, 3, 4, 5, 6, 7, 8, 9, 10, 11, 12, 13, 14, 26, 32]

Table 8: Solar energy.

Theoretically, solar power could be installed in variety of surfaces. PyPSA by default includes more CORINE grid codes than the ones used in the model. Permanent cropland, heterogeneous agricultural areas, pastures for animals and forests were not included in this model.

3.4.5 Hydro-power

Hydro-electric generation relies on typical hydro-electric dam turbine generation and with Run-of-River plants (RoR). The difference between the two is that in RoR the flow from a river is diverted through canals or pipelines and enters a turbine facility. The force of the water as it flows downhill through the turbine is enough to generate power, and then the water is returned to the river. On the other hand, hydro-electric dam requires a large reservoir to create a significant amount of potential energy, used to turn a large turbine. RoR is friendlier to the ecosystem but its power generation is largely affected by seasonality.

Climate-induced changes in stream-flow temporal patterns, reservoir siltation and evaporation, deforestation, all could affect levels of hydroelectricity in the following years. For this reason, only the existing infrastructure of hydro-related power plants is considered making hydropower a non-extendable energy carrier in contrary with the rest RES.[RES feasibility] In this model, RoR power generation time-series from ERA5 are included to calculate daily power generation, but hydro power is mostly used as a storage unit method, utilising reservoir's and pumped hydro storage (PHS) ramp up potential to fill in for energy shortages due to power supply variability. PHS is set to have a maximum output capacity of 6 hours.

3.4.6 Storage Units and general Storage

Storage Units in the model, apart from Hydro reservoirs and Pumped-Hydro storage, include Battery and H_2 storage units. Regarding Hydrogen, the model employs an H_2 storage and pipeline network of efficiency 46%. Hydrogen systems can generate power for up to 168 hours. Battery systems consist of storage systems operating for a maximum period of 6 hours with an efficiency of 97.9%.

In the context of model components, the two aforementioned types of storage lie in the 'Storage Units' category of the model. They operate as inter-temporal power-shifting devices. There are also generic 'Storage' units included into the model. Those are additional battery and H_2 storage units for every bus and their integration into the system is simplified into reserving excess energy for future use. Those need to be attached to links in order to deliver this energy. Hydrogen links comprise of H_2 electrolysis and fuel cells, with efficiencies 80% and 58% respectively, and for battery systems the links are battery chargers and dischargers with an efficiency of 97.9%.

3.4.7 Loads and Costs

Loads and costs for every year have differences as expected. As technology progresses, its cost tends to decrease but electricity loads follow a rising trend. The load time-series were retrieved from the Open Power System Data platform (OPSD) for the year of 2018 due to convenience as they were the latest load data that had entries for all of the countries included in the model.

Load time-series are assumed to scale up by a factor of 1.1, 1.2 and 1.3 for 2030, 2040 and 2050 years accordingly, with respect to the 2018 load records, which follows closely EU predictions. According to official data from EU, the UK government and The Norwegian Energy Regulatory Authority, for 2018, the European mix of energy demand consisted of around 2,900TWh for EU, 336TWh for UK, and 106TWh for Norway, making a total of approximately 3,342TWh. According to PyPSA's 2018 load data, for the scenario's combination of countries, the total amount of load reaches around 3,300TWh, and since the model includes, all non-EU Balkan countries and Switzerland, and excludes Cyprus and Malta, this is assumed an acceptable approximation.

Moreover, an additional constraint was introduced regarding energy generation equity per country. In other words, it is mandatory for every country to be able to produce at least 70% of its energy demand, regardless of the buses that comprise it in the model.

Costs, on the other hand, can be entered into the model manually depending on the user's estimations either from literature or their own research. As mentioned previously, PyPSA has its own repository of cost data and technical assumptions per technology used, which is created by a compilation of data from various valid sources. These sources are the Danish Energy Agency Technology Database for most of the technologies, Vartiaien et. al. 2019 [80] for solar pv, Fraunhofer ISE Studie for gas and pipelines, older PyPSA database, the European Technology and Innovation Platform for solar pv and solar rooftop installation, and other sources regarding conventional energy carriers excluded from the model such as fuel, coal etc. As mentioned in section 2.4, the costs for floating wind and all wave energy converters were assumed according to research of the Marine Renewable Energies Laboratory (MREL) of TU Delft for the year 2030 and 2050. Their 2040 values followed a similar reduction trend as the rest of PyPSA's assumptions. Bellow the costs for every scenario are presented:

2030	**Investment [€/kWe]**	**FOM [%/year]**	**VOM [€/MWe]**	**Efficiency**	**Lifetime [years]**
Wave Energy Converters	2012	8	0.10	-	25
Onshore Wind	1035.56	1.22	1.35	-	30
B. Fixed Offshore Wind	1523.55	2.32	0.02	-	30
Floating Offshore Wind	2408	15	0.39	-	30
Hydro-electricity dam	2208.16	1	-	0.9	80
Pumped-Hydro storage	2208.16	1	-	0.75	80
Run-of-River	3312.24	2	-	0.9	80
Solar	492.11	1.95	-	0.01	40
Solar-rooftops	636.66	1.42	-	-	40
H2 electrolyzer	314443.31	0.63	-	0.7	30
H2 fuel cell	343278.72	0.58	-	0.49	30
H2 storage	4329.35	0.43	-	-	30
H2 pipeline	267 [/km]	3	-	-	40
Battery charger/discharger	160	0.34	-	0.96	10
Battery storage	142 [€/kWh]	-	-	-	25
HVAC overhead	432.97 [/km]	2	-	-	40
HVDC inverter pair	162364.82 [/km]	2	-	-	40
HVDC overhead	432.97 [/km]	2	-	-	40
HVDC submarine	471.16 [/km]	0.35	-	-	40

Table 9: 2030 cost assumptions.

2040	**Investment [€/kWe]**	**FOM [%/year]**	**VOM [€/MWe]**	**Efficiency**	**Lifetime [years]**
Wave Energy Converters	1950	8	0.10	-	25
Onshore Wind	977.57	1.19	1.24	-	30
B. Fixed Offshore Wind	1415.08	2.18	0.02	-	30
Floating Offshore Wind	2300	15	0.38	-	30
Hydro-electricity dam	2208.16	1	-	0.9	80
Pumped-Hydro storage	2208.16	1	-	0.75	80
Run-of-River	3312.24	2	-	0.9	80
Solar	407.87	2.04	0.01	-	40
Solar-rooftops	525.16	1.56	-	-	40
H2 electrolyzer	314443.31	0.63	-	0.7	30
H2 fuel cell	343278.72	0.58	-	0.49	30
H2 storage	4329.35	0.43	-	-	30
H2 pipeline	267 [/km]	3	-	-	40
Battery charger/discharger	100	0.54	-	0.96	10
Battery storage	94 [€/kWh]	-	-	-	25
HVAC overhead	432.97 [/km]	2	-	-	40
HVDC inverter pair	162364.82 [/km]	2	-	-	40
HVDC overhead	432.97 [/km]	2	-	-	40
HVDC submarine	471.16 [/km]	0.35	-	-	40

Table 10: 2040 cost assumptions.

2050	**Investment [€/kWe]**	**FOM [%/year]**	**VOM [€/MWe]**	**Efficiency**	**Lifetime [years]**
Wave Energy Converters	1822.8	8	0.10	-	25
Onshore Wind	963.07	1.18	1.22	-	30
B. Fixed Offshore Wind	1380.27	2.17	0.02	-	30
Floating Offshore Wind	2181.5	15	0.37	-	30
Hydro-electricity dam	2208.16	1	-	0.9	80
Pumped-Hydro storage	2208.16	1	-	0.75	80
Run-of-River	3312.24	2	-	0.9	80
Solar	370.19	2.07	0.01	-	40
Solar-rooftops	475.38	1.61	-	-	40
H2 electrolyzer	314443.31	0.63	-	0.7	30
H2 fuel cell	343278.72	0.58	-	0.49	30
H2 storage	4329.35	0.43	-	-	30
H2 pipeline	267 [/km]	3	-	-	40
Battery charger/discharger	60	0.9	-	0.96	10
Battery storage	75 [€/kWh]	-	-	-	25
HVAC overhead	432.97 [/km]	2	-	-	40
HVDC inverter pair	162364.82 [/km]	2	-	-	40
HVDC overhead	432.97 [/km]	2	-	-	40
HVDC submarine	471.16 [/km]	0.35	-	-	40

Table 11: 2050 cost assumptions.

4 Results

The results of this thesis divide into software capabilities results and scenario results. As software capability results we assess the performance of several key tunable parameters assessing their impacts. These are, the time resolution, network configuration and dataset results. Scenario results refer to the cost-optimization forecast of the energy system as related to the research questions concerning the role of marine and offshore wind renewables into the European energy system. Those results are assumed to provide a comprehensive level of understanding on the system dynamics.

4.1 GEBCO bathymetry dataset

The first set of results will compare installation capacities of the model under the GEBCO 2014 and the GEBCO 2023 bathymetry data for the 2030 target year. What distinguishes one from the other, is the spatial resolution of each dataset. GEBCO 2023 dataset's resolution has increments of 15 arc-seconds, half of what GEBCO 2014 has. The tests have an 1-hour time resolution and a network of 37 buses that does not include BAU minimum capacities. Existing installed capacity according to PyPSA's repository is included.

Carrier	Existing [GW]	GEBCO 2023 [GW]	GEBCO 2014 [GW]	Difference [GW]
Offshore Wind AC	9.62	10.17	10.14	-0.03
Offshore Wind DC	15.37	43.23	41.2	-2.03
Offshore Fl. Wind AC	-	12.69	15.01	2.31
Offshore Fl. Wind DC	-	173.12	173.31	0.19
Onshore Wind	184.65	515.68	514.8	-0.89
Solar	152.97	904.75	907.11	2.36
WEC Farshore	-	-	-	-
WEC Nearshore	-	-	-	-
WEC Shallow	-	-	-	-
Total	412.53	1709.58	1711.49	1.52

Table 12: Installed capacities for the total system according to different GEBCO datasets and their differences in GW.

The results of figure 14 show that the differences in installation are very minimal but still existent. The actual differences in capacities are most probably not visible in the setup of this model. While bathymetric data have a resolution a of around $460m \times 460m$, weather data represent a grid of around $31,000m \times 31,000m$. Power generation profiles are falsely presented as the nearshore-to-onshore contours are underestimated. Figure 28 shows how the model views weather data. It is clear that, while there is a trade off for land and ocean in the dataset (i.e. overlapping wave data on land), that will affect minimum depth constraints of the model and make it unable to exploit higher fidelity coastal data. The part of the rectangles that extends onshore is filtered out by the model. This representation (of South Portugal and Spain in this occasion) misses an amount of optimal installation sites of nearshore energy technologies such as AC offshore wind and nearshore/shallow water WEC devices.

Using GEBCO2023 shows that grid transmission expansion is larger by only 0.7%, less storage units are installed but there is an emphasis on the use of battery carriers, while the objective cost is slightly decreased by 70 million €. The following figures 29 and 30 show that the installation of each generator distributed is almost identically among the two configurations.

The piecharts on every bus represent the share of energy technology on the bus while the vectored lines represent the average trade of energy from one bus to another.

Bellow at table 13, the theoretical maximum capacity per generator is presented. The values of each generator are calculated individually and they do not represent the cumulative total installable capacity. This means that, while for example the farshore WEC can obtain 30.8TW of devices, those devices will occupy the available room of installation, hence the rest of the technologies will need to be installed somewhere else. What can be confirmed by this table, is that wave energy has indeed a vast potential of generation compared to the rest of the technologies.

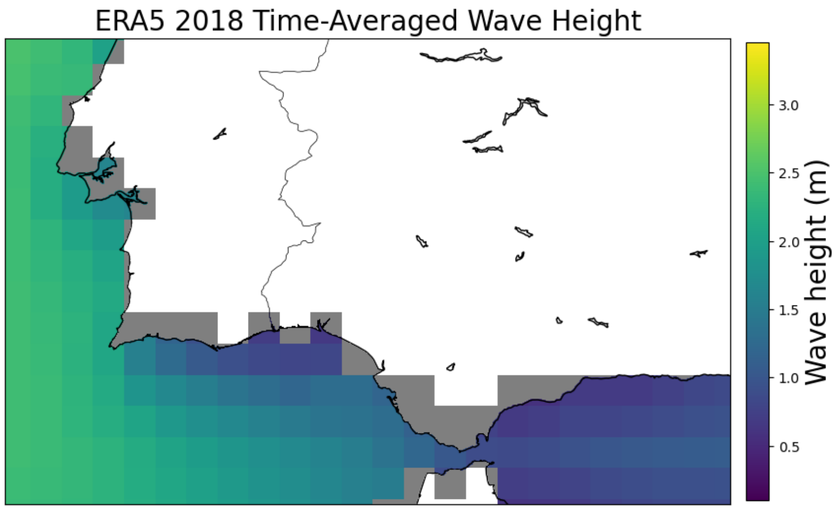

Figure 28: ERA5 resolution. Grey parts of the grid represent the lost potential due to resolution limitations.

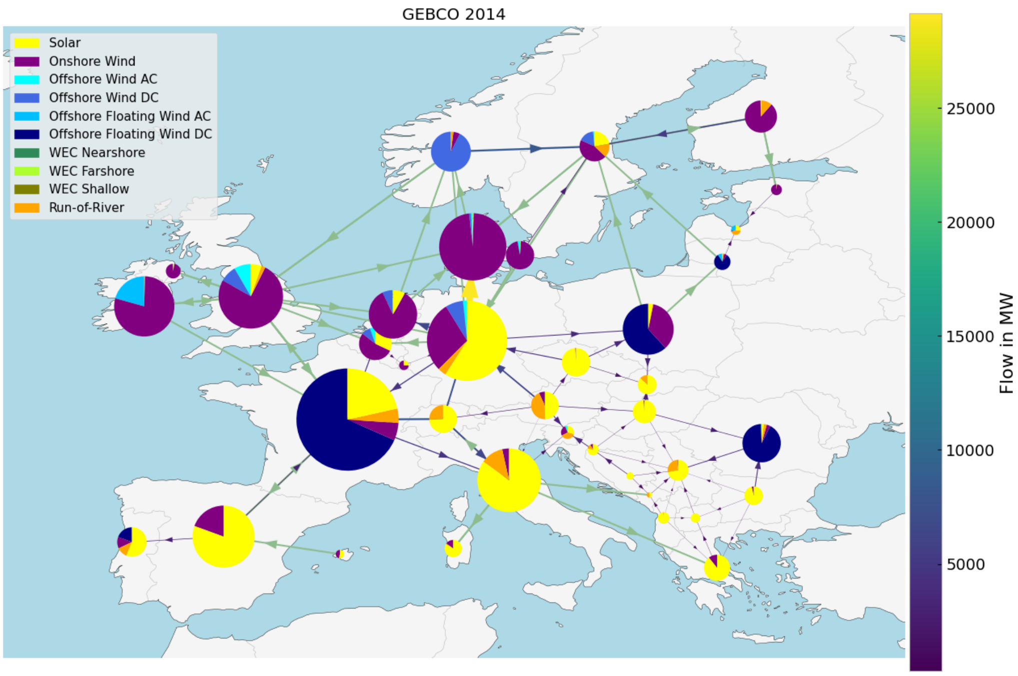

Figure 29: Share of energy carriers per bus for GEBCO 2014 bathymetry.

4.2 Time resolution and Network configuration

We compare different temporal and spatial configurations under the updated GEBCO 2023 dataset. Initially, these tests comprise of 37 buses and only time resolution changed for every test with 3 different time-steps: 24-hour, 6-hour, and 1-hour for target year 2030. In figure 31 the difference in loading time series is firstly presented between February 1 and 14 of 2018.

The 6 and 1-hour resolution shows a significant improvement on the samples of electricity demand. The 24-hour one disregards the minimum and maximum load and has no fluctuation during a 24 hour period. This has a considerable impact on the model as the following tables 14 and 15 will show. Hourly time series can provide entirely different results as the input, conversion and aggregation of the data is more detailed. For example, figure 32 presents the solar and onshore wind generation of the bus of Germany and shows how a small resolution can over/under-estimate the generation of power. Especially solar energy, which has obvious differences in generation during daylight and night-time is highly affected by time resolution.

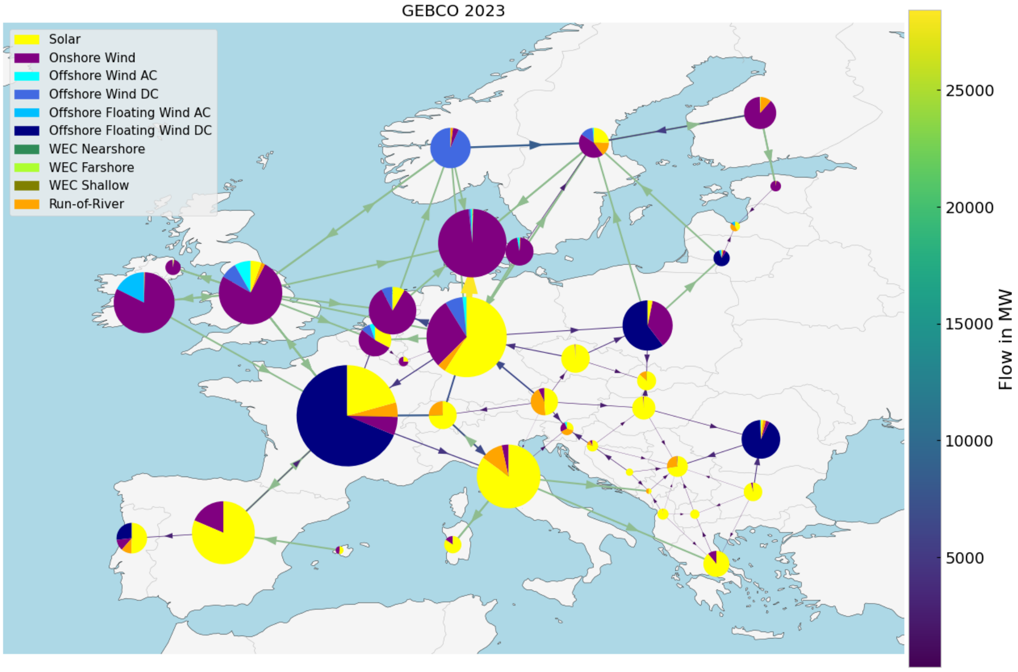

Figure 30: Share of energy carriers per bus for GEBCO 2023 bathymetry.

Carrier	Maximum capacity [GW]
Offshore Wind AC	1445
Offshore Wind DC	871
Offshore Fl. Wind AC	1371
Offshore Fl. Wind DC	5509
Onshore Wind	11561
Solar	2406
WEC Farshore	30810
WEC Nearshore	22363
WEC Shallow	3809

Table 13: Theoretical maximum capacity per generator based on the technology configurations.

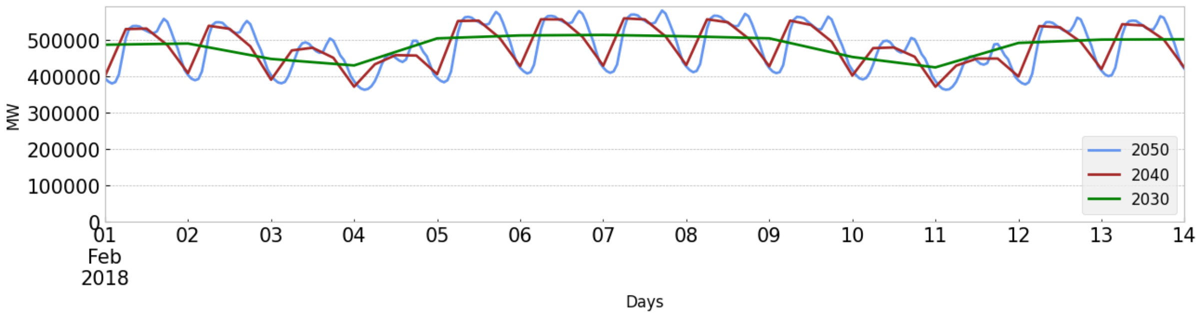

Figure 31: Load profile of each time resolution.

Table 14 shows the sensitivity of the model in time resolution.

What can be immediately observed, is that the model does not install wave energy converters in any of the time-resolution scenarios. The 1-hour time resolution benefits Offshore wind carriers over solar ones, while the 6-hour and 24-hour one does not. Instead, these ones choose to install more solar energy while both roughly maintain their onshore and offshore wind installation. The reason for this is the fact that 24-hour resolution time-series, and to some extend the 6-hour one, create unrealistically linear approximations of the profiles of the generated power. For wind and wave energy this does not appear

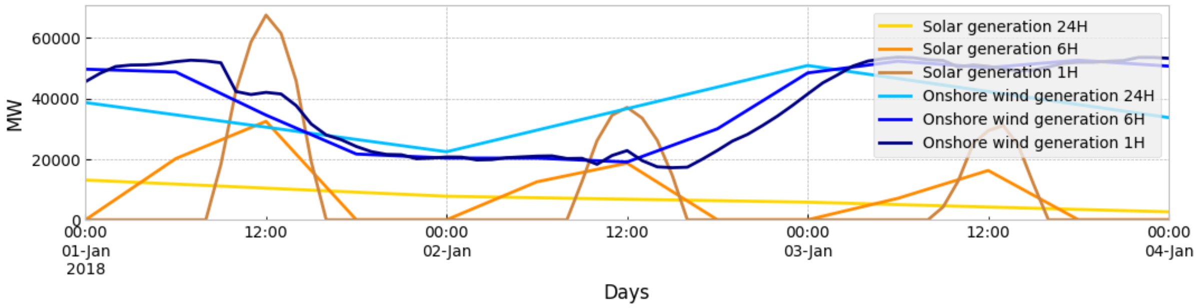

Figure 32: Generation of Onshore Solar and Wind power at the bus of Germany.

Carrier	24H [GW]	6H [GW]	1H [GW]
Offshore Wind AC	10.16	10.16	10.17
Offshore Wind DC	38.74	44.40	43.23
Offshore Fl. Wind AC	7.88	1.03	12.69
Offshore Fl. Wind DC	133.11	131.99	173.12
Onshore Wind	488.55	515.31	515.68
Solar	1057.00	1073.22	904.75
WEC Farshore	-	-	-
WEC Nearshore	-	-	-
WEC Shallow	-	-	-
Total	1785.37	1826.04	1709.58

Table 14: Installed capacities for the total system according to different time resolutions and the additional capacity of each one scenario in GW.

to be a large issue, as there already exists some consistency in the power output. For solar however, the same effect implies that solar power is constant as well. Solar power becomes more attractive as it is less expensive and has a falsely presented minimized variability, hence a broader selection of such generators. The 1-hour resolution trades some of this theoretical solar energy with more offshore wind energy and adds AC and DC lines and storage components into the model. Eventually, there is a large difference in total capacity installed, which for the 1-hour resolution is equal to at least 75 GW less than the one of 24-hour resolutions and around 117 GW less than the 6-hour one. The table below shows the differences in the rest of the components and verifies the preference of higher temporal resolution models to the installation of more storage units.

Similarly to the generators, what can be noticed is the large difference between most of the components between the 24-hour and the other two time resolutions. Apart from significant differences regarding transmission lines and links of DC lines and H_2 carriers, the daily resolution creates a model that completely ignores battery storage while the 6-hour one uses them to a limited extent. This is due to the increased variability of generation for high resolution models. Batteries typically activate when power production from the energy sources is not adequate. In a model that has a continuous power supply, there is no need for battery systems. Performing low resolution simulations can lead to models that are inapplicable in reality.

In general, there is a correlation between the time resolution and the overall objective cost of the power system. The higher the resolution, the higher the investment costs. More specifically, 24-hour time resolution model has annual system cost of 133.72 billion €, for the 6-hour one this is 145.59 billion € and for the 1-hour one is 152.08 billion €. Ensuring that the high-res model is not susceptible to the variability of its nature requires greater expansion of the more prominent energy sources, those being the high output far offshore DC wind farms, and the installation of more transmission lines and storage units. In the 1-hour model, generators might have less of a share in the installed capacity compared to the 24-hour one, however those have a higher capital, operational and maintenance cost, they require larger underwater connections to link the wind farms to the grid and also include expensive battery systems with short lifetime. For this configuration, the difference in investment costs between 1-hour and 24-hour is 14% and implies that performing high resolution analyses is imperative for research on power system developments.

Computational power for this thesis was a limiting factor on exploring the capabilities of the network

Type	Metric	24H [GW]	6H [GW]	1H [GW]
Line	HVAC	412.71	421.49	428.86
	HVDC	124.79	150.22	156.47
Storage Unit	Battery Storage	-	0.46	65.8
	Hydrogen Storage	0.07	0.03	0.62
	Pumped Hydro Storage	54.33	54.33	54.33
	Reservoir & Dam	102.22	102.22	102.22
Link	H2 electrolysis	85.66	78.6	79.45
	H2 fuel cell	178.19	161.39	154.71
	Battery charger	-	87.66	76.54
	Battery discharger	-	89.47	78.12
Energy capacity of general storage		24H [GWh]	6H [GWh]	1H [GWh]
Store	Battery Storage	0.01	652.41	377.88
	Hydrogen Storage	23326.78	21415.33	19934.01

Table 15: Installed capacities of the rest of the components of the different time resolution scenarios in GW. As mentioned in the Configuration chapter, the repeating terms (i.e. Battery Storage and Hydrogen Storage) have fundamental differences in the software. 'Storage Units' are units attached to a single bus and are used for inter-temporal power balancing. 'Links' refer to the more generic type of storage unit that has a single functionality of storing excess energy generated in a single Bus on the system, and only if connected to a link (i.e. Battery charger or H2 fuel cell), can contribute to the system.

analysis. Including more buses to the network increases computational time disproportionately, as the number of components and sub-networks increases as well. As a result, increasing the model from 37 to 50 buses, more-than doubled the computational time and it was the limit according to the available computational resources. The differences imply that the larger the amount of interconnections, the larger the degree of optimization in the model. The objective cost drops by 1.78 billion €, while the total capacity installed increases by more than 24GW reaching 1734.78 GW. A more complex network can facilitate the accessibility of energy by dividing the deployment of generators between every sub-network cluster. This means that although the final network comprises of more components, those are better distributed within the network and the power is flowing in a more optimal manner. Table 16 again presents the breakdown of each technology in terms of installed capacity in GW.

Carrier	37-buses [GW]	50-buses [GW]	Difference [GW]
Offshore Wind AC	10.17	10.17	-
Offshore Wind DC	43.23	35.12	-8.11
Offshore Fl. Wind AC	12.69	31.78	19.09
Offshore Fl. Wind DC	173.12	111.94	-61.18
Onshore Wind	515.68	601.31	85.62
Solar	904.75	894.53	-10.22
WEC Farshore	-	-	-
WEC Nearshore	-	-	-
WEC Shallow	-	-	-
Total	1709.58	1734.78	25.2

Table 16: Difference in installed capacities for 37 and 50 buses network in GW.

Again what is observed is the lack of wave energy converters while the rest of the generators appear to be dominant in the production. Going from 37 to 50 buses resulted in 19GW more floating AC wind turbines but DC ones dropped by 61GW. The onshore wind had an 85GW increase. This is probably due to the fact that Central Europe now has more buses and thus the complete system has less access to offshore energy sources compared to the 37-buses network.

As expected, transmission line expansion is larger for more complex networks. For the 50 buses scenario the expansion reaches 64.8%, rising from 553GW to 909GW of HVAC lines, while for the 37 one this is 58.5%, from 270GW to 429GW. HVDC lines, seem to be closer on expansion since the overseas connections do not have a large difference between the two models. For the 37-nodes model they increased from 20.5GW to 153GW and for 50-nodes one they increased from 22.7GW to 160GW. The denser model showed around 7% less expansion of HVDC lines.

The final share of energy carriers per node is presented in figure 33, which can be compared to figure 30.

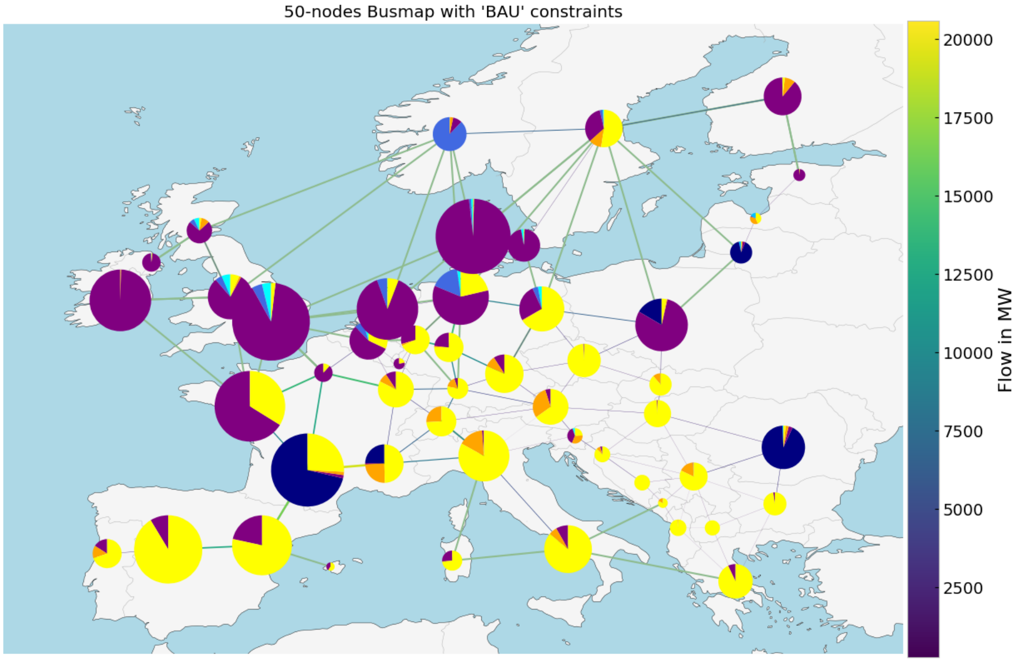

Figure 33: Share of energy carriers per bus for a 50-buses configuration.

4.3 Consideration of BAU minimum capacities

Since the model by itself dismisses wave energy generators, the installation of those is induced with the aforementioned BAU minimum capacity constraints, the values of which can be found in table 7. The following results show the differences of a 50-bus network with applied BAU constraints from the equivalent network without them.

Carrier	BAU [GW]	Non-BAU [GW]	Difference [GW]
Offshore Wind AC	10.17	10.17	-
Offshore Wind DC	34.96	35.12	-0.16
Offshore Fl. Wind AC	29.88	31.78	-1.9
Offshore Fl. Wind DC	112.85	111.94	0.91
Onshore Wind	598.63	601.31	-2.68
Solar	894.07	894.53	-0.46
WEC Farshore	1.00	-	1.00
WEC Nearshore	2.00	-	2.00
WEC Shallow	3.00	-	3.00
Total	1736.49	1734.78	1.71

Table 17: Installed capacities of generators according to BAU minimum capacity constraints and the differences of that compared with a model without them in GW.

As expected the model does not exceed the minimum capacity on Wave energy. The 6GW of total wave energy that were set in the BAU scenario replace some of the subtracted capacity by the most of the other carriers, and adds less than 2GW more to the overall system. Apart from that, offshore DC wind farms appear to be slightly more favourable while the rest of the non-marine technologies have very minimal capacity drops. The same case is true fro transmission lines, storage and link expansions which show almost no change as well.

As a result, the objective cost for the two scenarios is very similar. For the BAU scenario it is 151.84 billion € and for the non-BAU it is 150.30 billion €. The difference of +1.54 billion € is minimal

Type	Metric	BAU [GW]	Non-BAU [GW]
Line	HVAC	909.51	909.11
	HVDC	160.7	160.83
Storage Unit	Battery Storage	58.04	58.3
	Hydrogen Storage	0.73	0.58
	Pumped Hydro Storage	54.33	54.33
	Reservoir & Dam	102.22	102.22
Link	H2 electrolysis	84.58	85.18
	H2 fuel cell	147.64	148.5
	Battery charger	94.46	94.47
	Battery discharger	96.41	96.42
Energy capacity of general storage		BAU [GWh]	Non-BAU [GWh]
Store	Battery Storage	458.12	459.12
	Hydrogen Storage	19583.15	19850.51

Table 18: Installed capacities of the rest of the components of BAU and non-BAU scenarios in GW.

compared to the magnitude of investment in a project as big as the upgrade of the European power system.

4.4 Results of 2030-2050 scenarios

The following section presents the results for the target years 2030, 2040 and 2050. Firstly however the difference in load time-series will be presented for a fraction of time in the year of 2018:

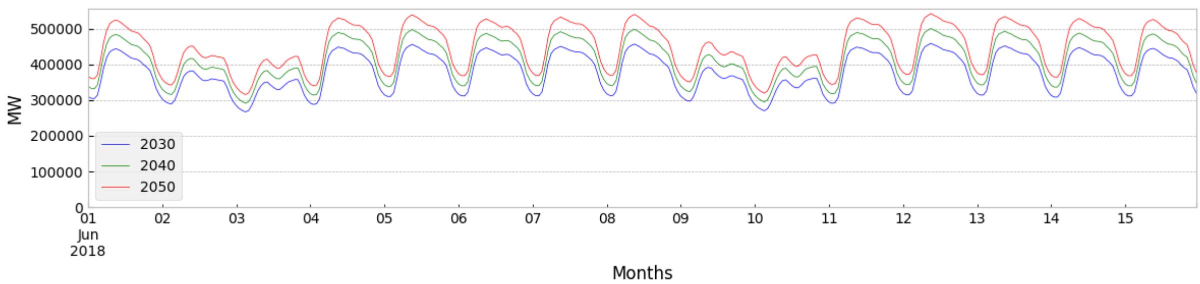

Figure 34: Load time-series

As mentioned in the configuration of the scenarios, loads in the model increase by a factor of 10% for every 10 years, compared to 2018's load data, meaning 110% for 2030, 120% for 2040 and 130% for 2050. Note that based on the International Energy Agency, in 2018 Europe's demand was higher than in 2020 due to the COVID-19 pandemic which drooped the energy demand in a global scale. 2020 would normally be the 10-year incremental baseline, however 2018 is assumed to be more representable of the natural trend that the energy growth would have. The effect of this load scaling can be seen in the following results, where it is clear that total capacity installation has an increasing trend.

4.4.1 General results overview

This growth trend is not linear neither in capacity nor in capital costs. As the following tables will show, from 2030 to 2050 there seems to be a lack of proportionality, even though the energy demand in the system is assumed to be linearly increasing. There are several factors which affect installation capacity and objective cost. First of all, regarding cost assumptions, it is difficult to estimate the exact dynamic between inflation, cost reduction of CAPEX and OPEX and project discount rates. These factors affect cost predictions as initially inflation is influencing the overall increase in prices over time, and developers aim to predict this currency price-shift in order calculate the discount rates of the projects, by factoring in assumptions on cost reduction of the technologies based on their availability. An other factor is the availability of the sources itself. Increasing the energy demand might be pivotal in the context of energy coverage by the system. If more capacity is demanded, this capacity might be available only far from shore, increasing water depth and underwater connection lines. What is also increased is the variability of the system. These might drive the software to lean towards the certainty of storage units, which apart from hydro dams and pumped-up hydro storage it can be battery storage systems with chargers and dischargers and H_2 pipelines with electrolysis and fuel cell units.

Carrier	2030 [GW]	2040 [GW]	2050 [GW]
Offshore Wind AC	10.17	30.00	40.00
Offshore Wind DC	34.96	40.00	55.00
Offshore Fl. Wind AC	29.88	50.00	80.00
Offshore Fl. Wind DC	112.85	115.00	230.00
Onshore Wind	598.63	537.65	368.06
Solar	894.07	1079.15	1104.92
WEC Farshore	1.00	7.00	17.00
WEC Nearshore	2.00	15.00	25.00
WEC Shallow	3.00	10.00	20.00
Total	1736.49	1933.72	1989.91

Table 19: Installed capacities of generator expansion for target years 2030, 2040 and 2050 in GW.

Again what can be realized is that the the capacities of the offshore technologies do not exceed their minimum ones set for these scenarios. A reason for this might be a combination of the low spatial resolution of the weather dataset together with the costs of each technology and with the limited amount of buses which represent the whole of Europe. Splitting the model into more buses means there are buses closer to the sea regions of each country. This might amplify the deployment of offshore technologies.

Type	Metric	2030 [GW]	2040 [GW]	2050 [GW]
Line	HVAC	909.51	920.32	970.02
	HVDC	160.7	141.28	165.52
Storage Unit	Battery Storage	58.04	116.17	122.55
	Hydrogen Storage	0.73	0.01	0.04
	Pumped Hydro Storage	54.33	54.33	54.33
	Reservoir & Dam	102.22	102.22	102.22
Link	H2 electrolysis	84.58	118.5	123.97
	H2 fuel cell	147.64	168.21	169.87
	Battery charger	94.46	93.91	103.5
	Battery discharger	96.41	95.85	105.63
Energy capacity of general storage		2030 [GWh]	2040 [GWh]	2050 [GWh]
Store	Battery Storage	458.12	607.09	601.73
	Hydrogen Storage	19583.15	25000.08	27110.4

Table 20: Installed capacities of the rest of the components for target years 2030, 2040 and 2050.

Overall expansion of the system has an increasing trend in the total year scenario. For the year 2040, some components drop in capacity, those being the inter-temporal power balancing hydrogen storage, battery charger and discharger and HVDC lines, but general battery storage seems to increase. However, one can observe that between 2030 and 2040, the generator expansion is almost 200GW or 11.2%, while for year 2050 this is around 56GW or around 2.9%. On the contrary, HVAC line expansion seems to increase in an opposite trend, 1.2% and 5.4% for HVAC lines, while HVDC line capacity appears to drop by 14% in 2040 and then rise by 17.4% in 2050. Tables with more detail on the specifics of the transmission expansion will be provided in section 4.4.5.

Next, each target-year scenario will be analyzed in more detail. Regarding the first scenario, figure 35 presents the 50-buses network scheme.

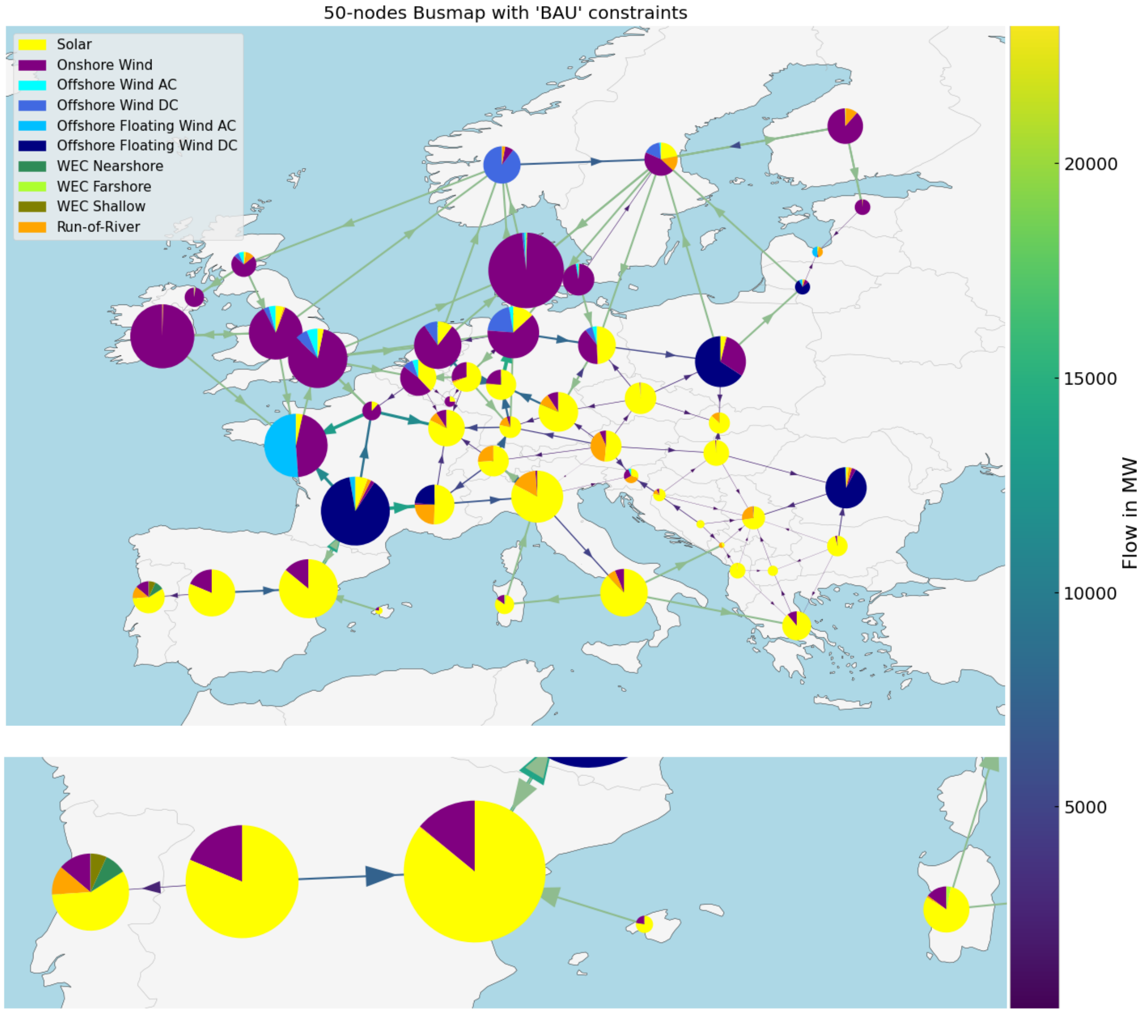

Figure 35: 50-nodes busmap with 'BAU' minimum capacity constraints for year 2030. The new wave capacities have been installed in Portugal for the shallow and nearshore WECs and in Sardinia (Italy) for the farshore one.

By observing figure 35 one can realize that the offshore technologies are mostly installed in coastal buses. All of the floating wind DC (dark blue color) installation is installed in four regions, south of France, Baltic Sea in Poland and Lithuania and on the Black Sea in the Romanian Economic Zone. The rest of the Offshore wind technologies are all installed in the northern part of Europe, with the greater part of floating wind AC being again in France, bottom fixed DC distributed in the countries that have access to the North Sea most of which accommodate AC bottom fixed too.

The lack of offshore wind technologies in the south comes from two factors. Firstly, the wind resource is quite lower compared to the northern one, probably due to terrain morphology and roughness of the region. Secondly, due to the bathymetry. The Mediterranean's seabed is not only significantly deeper than most of other European sea basins, but has rapid depth variations from low to high depths in very small distances. One can add the fact that the Mediterranean has more natural protected areas on which human intervention is limited, which hinders the deployment of offshore wind in reality. Wave energy devices however do not have as big visual or ecological impact as offshore wind energy and can be placed closer to urban or protected regions as they should have a greater social acceptance, since they are barely visible. Eventually, for target year 2030, south Europe is primarily electrified by onshore wind and solar energy, and the limited amount of wave energy.

4.4.2 Generator installations per country

The following table 21 shows the installation capacity of every technology per country. Small values of 1-10GW exist due to computational imperfections and numeric convergence limitations of the model and can be neglected.

Country	B.Fixed AC WTG [MW]	B.Fixed DC WTG [MW]	Floating AC WTG [MW]	Floating DC WTG [MW]	Onshore WTG [MW]	Solar [MW]	Fars. WEC [MW]	Nears. WEC [MW]	Shal. WEC [MW]	Total [MW]
Albania	-	-	-	-	-	9903	-	-	-	9903
Austria	-	-	-	-	3224	21438	-	-	-	24663
B. & Her.	-	-	-	-	87	2487	-	-	-	2574
Belgium	901	1411	-	-	12612	21198	-	-	-	36122
Bulgaria	-	-	-	1	703	15095	1	-	1	15800
Switzer.	-	-	-	-	86	27376	1	-	-	27463
Czech R.	-	-	-	-	339	42434	-	-	-	42774
Germany	1739	6990	-	-	66614	168069	-	-	1	243411
Denmark	1065	636	-	1	97897	1300	1	-	1	100899
Estonia	-	-	-	1	4954	130	-	-	-	5085
Spain	3	-	-	2	36878	158907	2	1	2	195792
Finland	42	31	-	1	29934	410	-	-	-	30418
France	4	1	28667	63072	51464	94389	4	1	2	237602
Great B.	5434	4948	3	6	112949	13463	2	1	2	136806
Greece	-	-	-	3	4113	28242	-	-	-	32358
Croatia	-	-	-	8604	788	4767	-	-	-	14160
Hungary	-	-	-	-	323	26703	-	-	-	27026
Ireland	25	1	2	1	80266	40	1	-	1	80336
Italy	1	-	1	1	10882	170265	985	-	4	182139
Lithuania	1	1	243	2235	539	148	-	-	-	3167
Luxemb.	-	-	-	-	2111	1095	-	-	-	3206
Latvia	-	1	-	2	78	272	-	-	-	352
Monten.	-	-	-	-	118	485	-	-	-	603
N. Maced.	-	-	-	-	37	3764	-	-	-	3801
Netherl.	129	2312	-	-	31651	10213	-	-	-	44305
Norway	1	16335	-	2	3258	132	1	-	1	19729
Poland	1	3	-	21505	19265	3936	1	-	-	44709
Portugal	24	-	-	2	5214	20627	1	1996	2985	30849
Romania	-	-	-	26003	3023	1387	-	-	-	30413
Serbia	-	-	-	-	397	14974	-	-	-	15371
Sweden	256	25	-	10	13261	11569	-	-	-	25122
Slovenia	544	-	-	10025	5565	2522	-	1	-	18657
Slovakia	-	-	-	-	4	16325	-	-	-	16329
Total	10172	34964	29878	112849	598632	894066	1000	2000	3000	

Table 21: Energy share of every technology per country, numeric representation, for target year 2030.

While offshore wind energy is split among several countries, with Belgium, Germany, Denmark, France, Great Britain, Croatia, Lithuania, Netherlands, Norway, Poland, Romania and Slovenia acquiring the largest share of it, WECs for the 2030 scenario appear to have clear preference, Italy and Portugal. Based on the production potential profiles of each technology (figure 26), Italy has available resource for all three WEC types, especially in the Adriatic Sea. In the system it is preferred for farshore WEC installation. Additionally, Portugal seems to have similar potential as Italy, and is preferred for nearshore and shallow WEC installation.

Generator	Country	Share [GW]
Bottom Fixed AC WTG	Great Britain	5.4
Bottom Fixed DC WTG	Norway	16.3
Floating AC WTG	France	28.7
Floating DC WTG	France	63.1
Onshore WTG	Great Britain	112.9
Solar	Italy	170.3
Farshore WEC	Italy	1.0
Nearshore WEC	Portugal	2.0
Shallow WEC	Portugal	3.0

Table 22: Highest installed capacities of generators in the 2030 model.

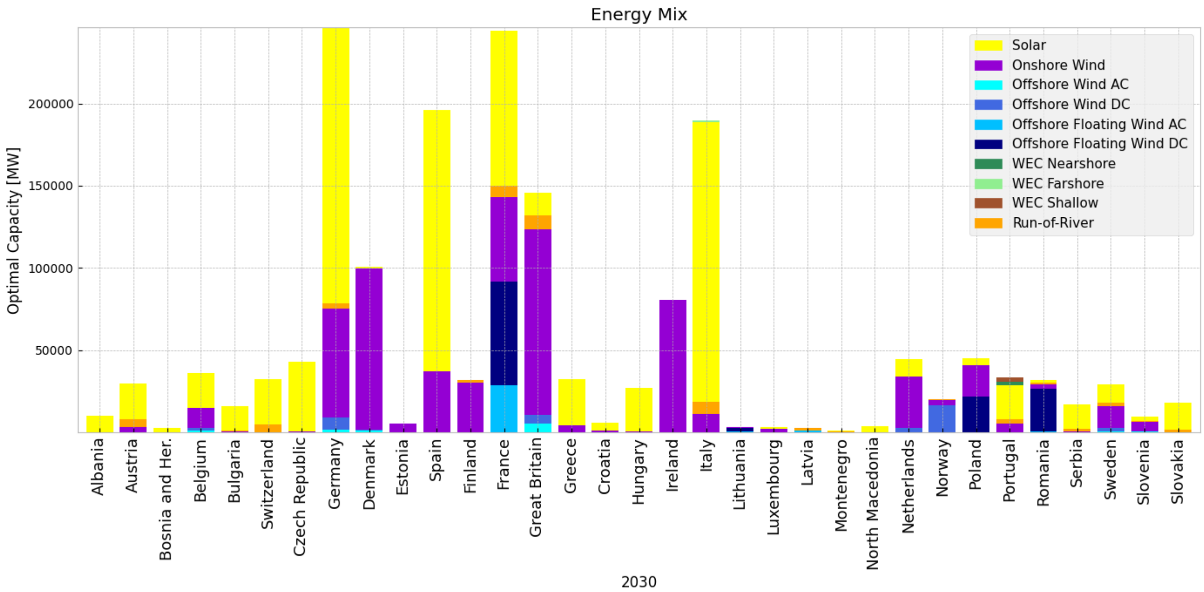

Figure 36: Energy share of every technology per country, visual representation, for target year 2030.

Table 21 is presented in terms of a stacked bar-chart visualization, for a better grasp on the amount and technology share of the system per country. In the overall installed capacity, highest of all are Germany and France, reaching almost 250GW of optimal capacity each. Following them are Spain, Italy with around 190GW each and Great Britain with around 140GW.

Next, the per-country/per-technology table for target year 2040 is presented.

Country	**B.Fixed AC WTG [MW]**	**B.Fixed DC WTG [MW]**	**Floating AC WTG [MW]**	**Floating DC WTG [MW]**	**Onshore WTG [MW]**	**Solar [MW]**	**Fars. WEC [MW]**	**Nears. WEC [MW]**	**Shal. WEC [MW]**	**Total [MW]**
Albania	-	-	-	-	-	10662	-	-	-	10662
Austria	-	-	-	-	3224	37755	-	-	-	40979
B. & Her.	-	-	-	-	87	4715	-	-	-	4802
Belgium	901	1411	-	-	15015	21199	-	-	-	38526
Bulgaria	-	-	-	1	703	16842	-	-	-	17546
Switzer.	-	-	-	-	86	27376	-	-	-	27462
Czech R.	-	-	-	-	339	46494	-	-	-	46833
Germany	1739	6990	-	-	67588	197506	-	-	-	273822
Denmark	1065	636	-	1	97897	1300	-	-	-	100899
Estonia	-	-	-	1	3434	130	-	-	-	3565
Spain	3	-	-	2	27084	186140	-	-	1474	214703
Finland	42	31	-	1	33319	410	-	-	-	33803
France	19835	-	34868	63071	17334	169064	-	-	-	304172

Great B.	5434	4948	-	-	113302	13462	-	-	-	137148
Greece	-	-	-	3	4113	43263	-	-	-	47379
Croatia	-	-	-	8604	788	5797	-	-	-	15189
Hungary	-	-	-	-	323	29173	-	-	-	29496
Ireland	25	1	13730	-	42652	40	-	-	969	57417
Italy	-	-	-	-	10882	170267	7000	-	6406	194553
Lithuania	-	-	244	2875	539	148	-	-	-	3805
Luxemb.	-	-	-	-	2370	1095	-	-	-	3465
Latvia	-	-	915	-	78	7	-	-	-	1000
Monten.	-	-	-	-	118	3612	-	-	-	3730
N. Maced.	-	-	-	-	37	7787	-	-	-	7824
Netherl.	129	2312	-	-	46750	10213	-	-	-	59404
Norway	1	22799	-	-	3258	132	-	-	-	26190
Poland	-	845	2	22987	16882	3936	-	-	-	44651
Portugal	25	-	-	-	5214	6525	-	15000	1150	27913
Romania	1	1	239	24799	3023	1387	-	-	-	29450
Serbia	-	-	-	-	397	17086	-	-	-	17483
Sweden	256	25	-	1267	13260	25028	-	-	-	39836
Slovenia	544	-	-	-	7548	2522	-	-	-	10614
Slovakia	-	-	-	-	4	18072	-	-	-	18076
Total	30000	40000	50000	115000	537645	1079146	7000	15000	10000	

Table 23: Energy share of every technology per country, numeric representation, for target year 2040.

Generator	Country	Share [GW]
Bottom Fixed AC WTG	France	19.8
Bottom Fixed DC WTG	Norway	22.8
Floating AC WTG	France	34.9
Floating DC WTG	France	63.1
Onshore WTG	Great Britain	113.3
Solar	Germany	197.5
Farshore WEC	Italy	7
Nearshore WEC	Portugal	15
Shallow WEC	Italy	6.4

Table 24: Highest installed capacities of generators in the 2040 model.

While some countries maintained their capacities for certain technologies (for example France which continues to have 63.1GW of Floating DC WTG), the technologies seem to increase in general. Significant changes are the rise of France's bottom fixed AC wind turbines (+19.8GW) and floating AC wind turbines (+6.2GW) together with around 75GW more solar energy, while its onshore wind energy drooped by 34.1GW. Added to the countries which now have offshore wind energy is Latvia with 0.9GW of floating AC wind turbines, and Sweden with 0.2GW of bottom fixed AC wind turbines and around 1.3GW of floating DC ones. An other country with major differences is Ireland which has an additional 13.7GW of floating AC wind turbines and almost 1GW of nearshore WECs. Wave generators have four clear candidates for their deployment, Spain for shallow water WECs in South-West Andalusia, Portugal for both nearshore and shallow WECs, Ireland for shallow water WECs in the South-East coast, and Italy for both farshore and shallow WECs.

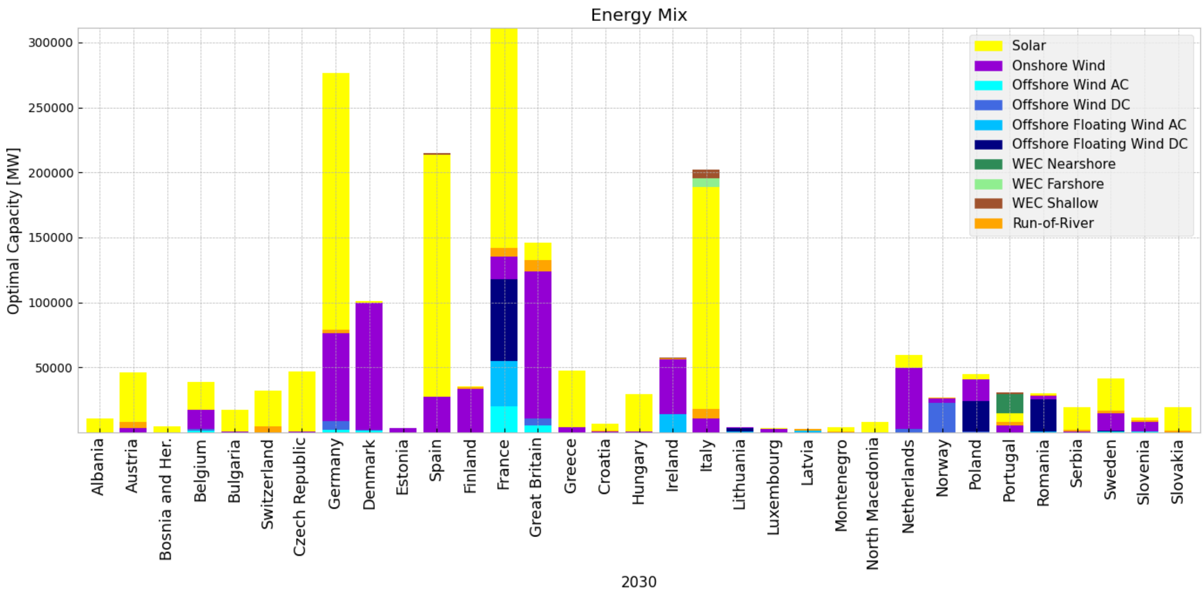

Figure 37: Energy share of every technology per country, visual representation, for target year 2040.

For 2040 most of the countries appear to increase their solar capacities, highest of which was the one of France followed by Germany (+29.4GW) and Spain (+27.2GW). An exception was Portugal, which has 14.1GW less solar energy compared to 2030. More detailed differences for each country's energy mix for the development trajectory 2030-2050 can be found in the Appendix. In the bar-chart visualization of the data above, one can observe the magnitude of the differences for certain countries. The load scaling in the model seems to affect Germany and France the most, since the both exceed the 250GW and 300GW required capacity threshold respectively.

Lastly, for 2050:

Country	B.Fixed AC WTG [MW]	B.Fixed DC WTG [MW]	Floating AC WTG [MW]	Floating DC WTG [MW]	Onshore WTG [MW]	Solar [MW]	Fars. WEC [MW]	Nears. WEC [MW]	Shal. WEC [MW]	Total [MW]
Albania	-	-	-	-	-	10662	-	-	-	10662
Austria	-	-	-	-	3224	37755	-	-	-	40979
B. & Her.	-	-	-	-	87	10012	-	-	-	10099
Belgium	4098	7283	-	-	2438	21198	-	-	-	35017
Bulgaria	-	-	-	4	703	18618	-	-	-	19325
Switzer.	-	-	-	-	86	27376	-	-	-	27461
Czech R.	-	-	-	-	339	50351	-	-	-	50690
Germany	1739	12450	-	-	54383	237051	-	-	-	305623
Denmark	1065	636	-	-	76263	1300	-	-	-	79264
Estonia	-	-	-	1723	316	130	-	1	-	2170
Spain	3	-	-	-	27084	196318	-	-	101	223507
Finland	42	31	-	16240	3118	410	-	-	-	19841
France	26154	1	38152	63636	17334	155035	3565	-	1	303877
Great B.	5434	4948	1	9919	62608	13462	-	-	-	96374
Greece	-	-	-	9058	4113	43263	-	-	-	56435
Croatia	-	-	-	-	788	6850	-	-	-	7638
Hungary	-	-	-	-	323	31654	-	-	-	31977
Ireland	25	1	41846	38887	4275	40	-	-	19897	104970
Italy	-	-	-	-	10882	170267	13435	-	-	194584
Lithuania	-	-	-	4108	539	148	-	-	-	4796
Luxemb.	-	-	-	-	2629	1095	-	-	-	3724
Latvia	-	-	-	1032	78	7	-	-	-	1117
Monten.	-	-	-	-	118	3612	-	-	-	3730

N. Maced.	-	-	-	-	37	8715	-	-	-	8752
Netherl.	614	2312	-	-	55342	10213	-	-	-	68481
Norway	1	27311	-	3569	3258	132	-	-	-	34271
Poland	-	-	-	44545	6267	3936	-	-	-	54748
Portugal	25	-	-	-	5214	1025	-	24999	-	31263
Romania	-	-	-	27253	3023	1387	-	-	-	31663
Serbia	-	-	-	-	397	19149	-	-	-	19546
Sweden	256	25	-	10025	13260	1417	-	-	-	24983
Slovenia	544	-	-	-	9531	2522	-	-	-	12597
Slovakia	-	-	-	-	4	19810	-	-	1	19814
Total	40000	55000	80000	230000	368059	1104922	17000	25000	20000	

Table 25: Energy share of every technology per country, numeric representation, for target year 2050.

Generator	Country	Share [GW]
Bottom Fixed AC WTG	France	26.1
Bottom Fixed DC WTG	Norway	27.3
Floating AC WTG	Ireland	41.8
Floating DC WTG	France	63.6
Onshore WTG	Denmark	76.3
Solar	Germany	237.1
Farshore WEC	Italy	13.5
Nearshore WEC	Portugal	25.0
Shallow WEC	Ireland	19.9

Table 26: Highest installed capacities of generators in the 2050 model.

The model appears to have settled on the countries which can accommodate offshore and marine renewables. A significant addition is Greece and Estonia which now has around 9.1GW and 1.7GW of floating DC wind turbines each. Due to the BAU minimum capacities set in the scenarios, the software trades a significant amount of onshore wind capacity to install offshore and marine technologies. Solar energy on the other hand, raises its numbers once again reaching 1105GW of infrastructure around the energy system.

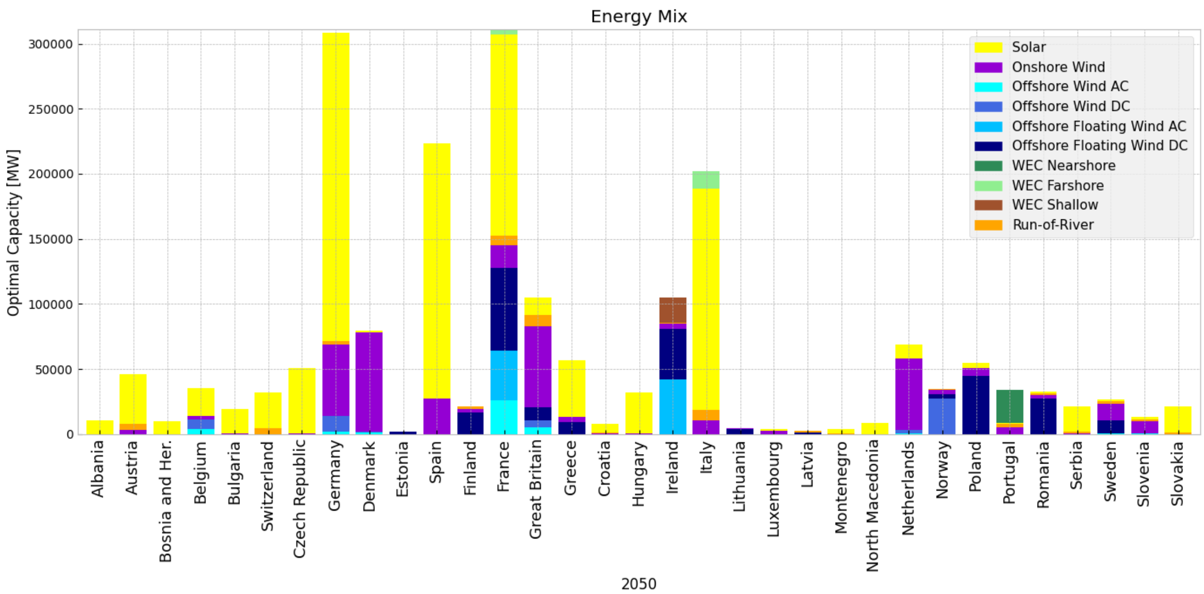

Figure 38: Energy share of every technology per country, visual representation, for target year 2050.

Since the optimal installed capacity of the generators of 2050's model is larger by only 56GW, minimal changes are observed in the capacity demand of each country. Germany now is the leader with 305GW of renewables, of which however a great proportion (237GW) is solar energy. In this model, France is suitable for almost 128GW of bottom fixed and floating WTGs, Ireland for 80GW of floating WTGs, followed by Poland with 44.5GW of floating WTGs in its economic zone in the Baltic Sea. For wave generators however, Spain's capacity has dropped significantly and France is now holding a great proportion of farshore devices (3.6GW), the rest of which are installed in Italy. Ireland still is a major contributor in wave energy with almost 20GW of shallow devices installed there and the same goes for Portugal which has 25GW of the nearshore one.

Figure 39 presents the total share of the renewable technologies in the energy system in terms of percentage. Solar energy followed by onshore wind energy are the dominating sources for all three scenarios. What is discussed above but is visually noticeable here is the drop of the share of onshore wind for target year 2050.

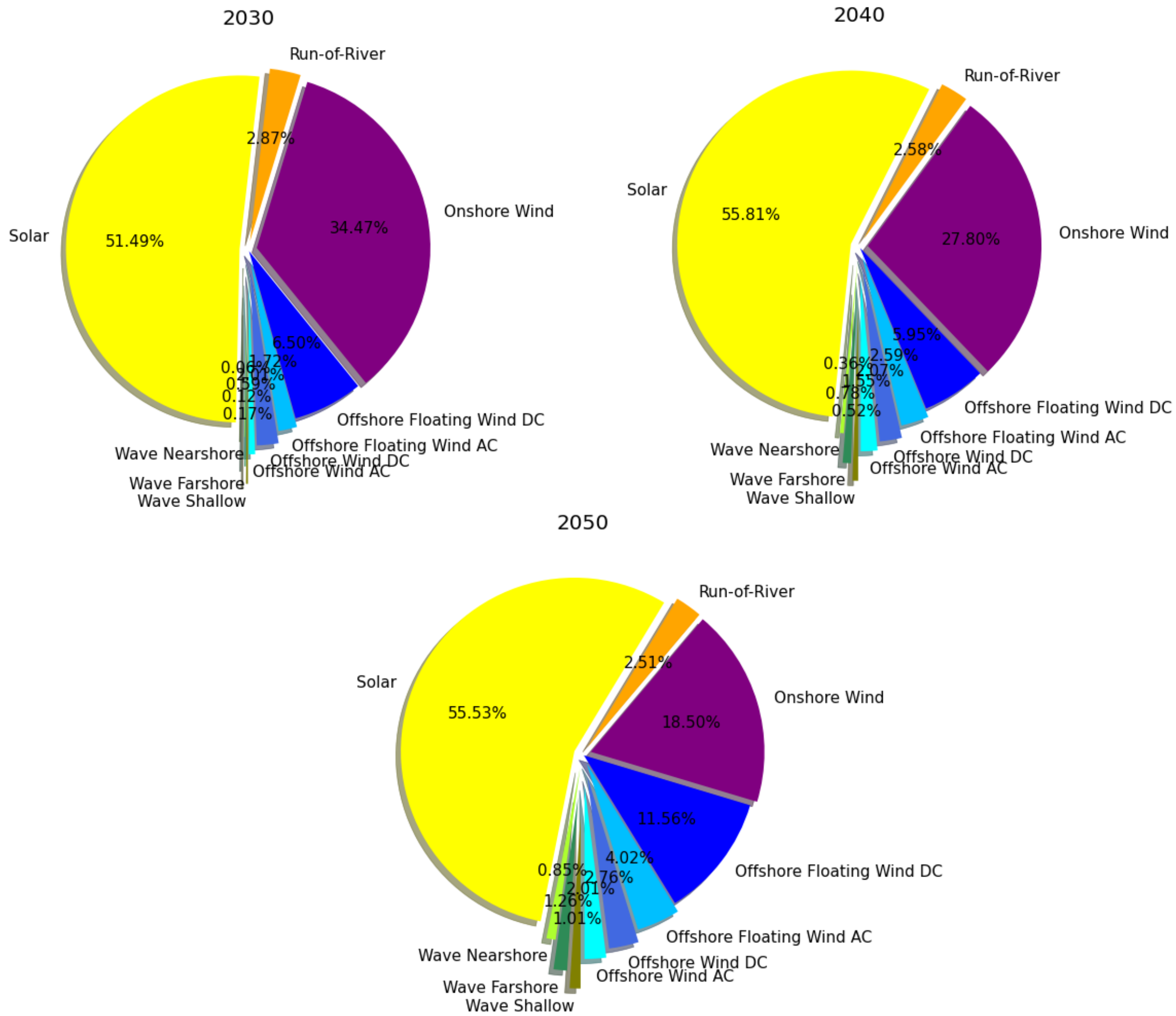

Figure 39: Share of each generator capacity for the three scenarios.

Adding up the storing units, the complete installation of components is presented in the following figure.

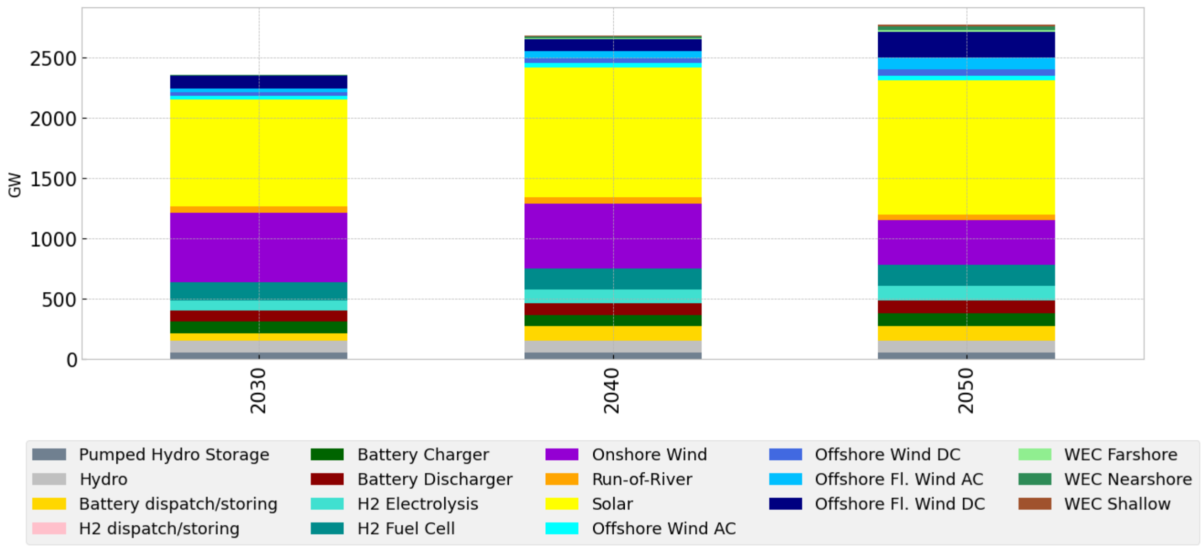

Figure 40: All technologies.

Figure 40 shows that the 2050 scenario has more total capacity of generators and storage systems in the than the 2040 and 2030 scenario, something that is anticipated since the energy demand is also advancing.

The complete 2050 generator configuration is presented in figure 41 followed by the corresponding maximum loads in figure 42.

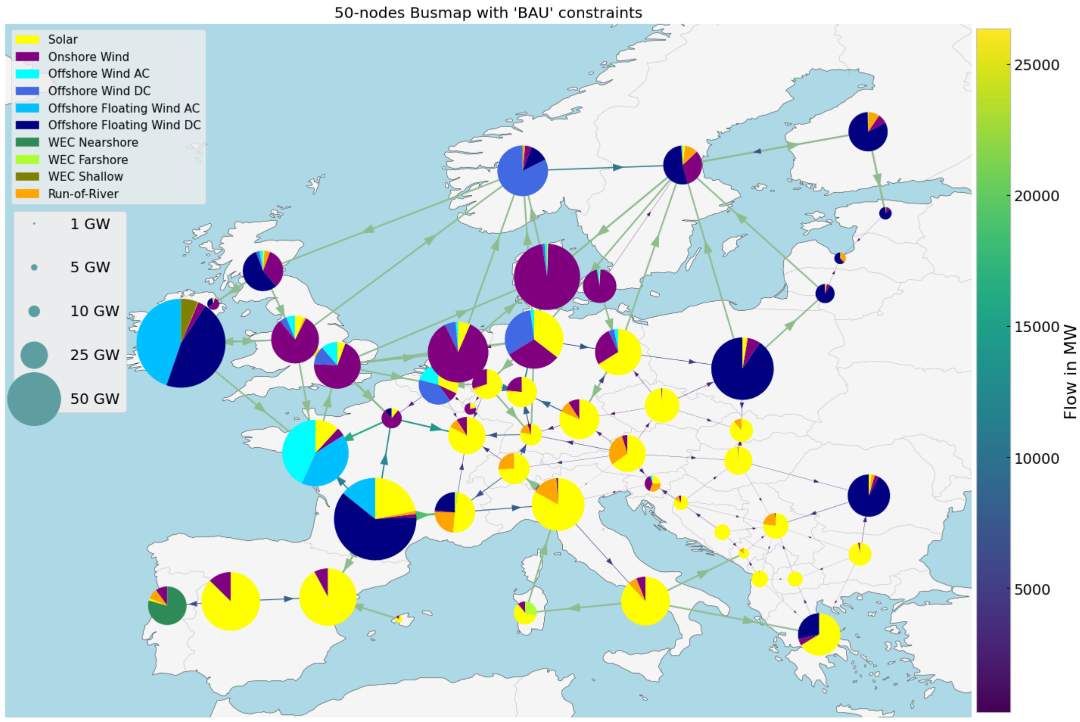

Figure 41: 50-nodes busmap of generators for year 2050.

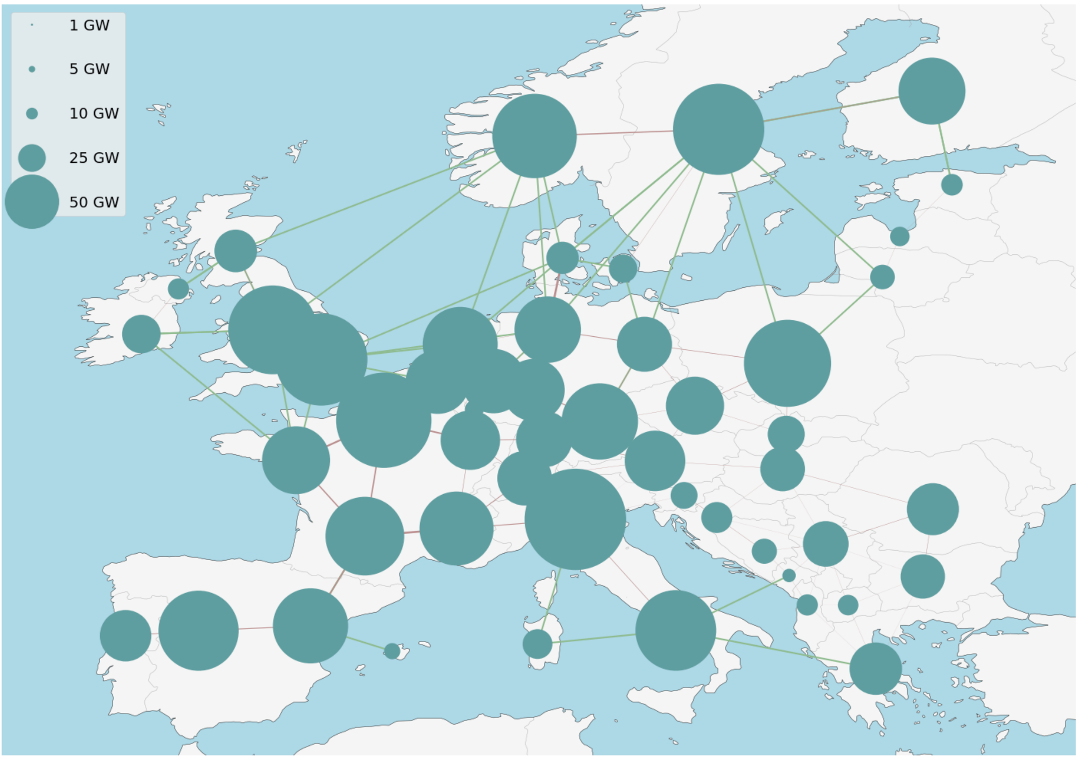

Figure 42: 50-nodes busmap of maximum loads for year 2050.

Lastly, figure 43 shows the maps which represent each technology installed for the target year 2050.

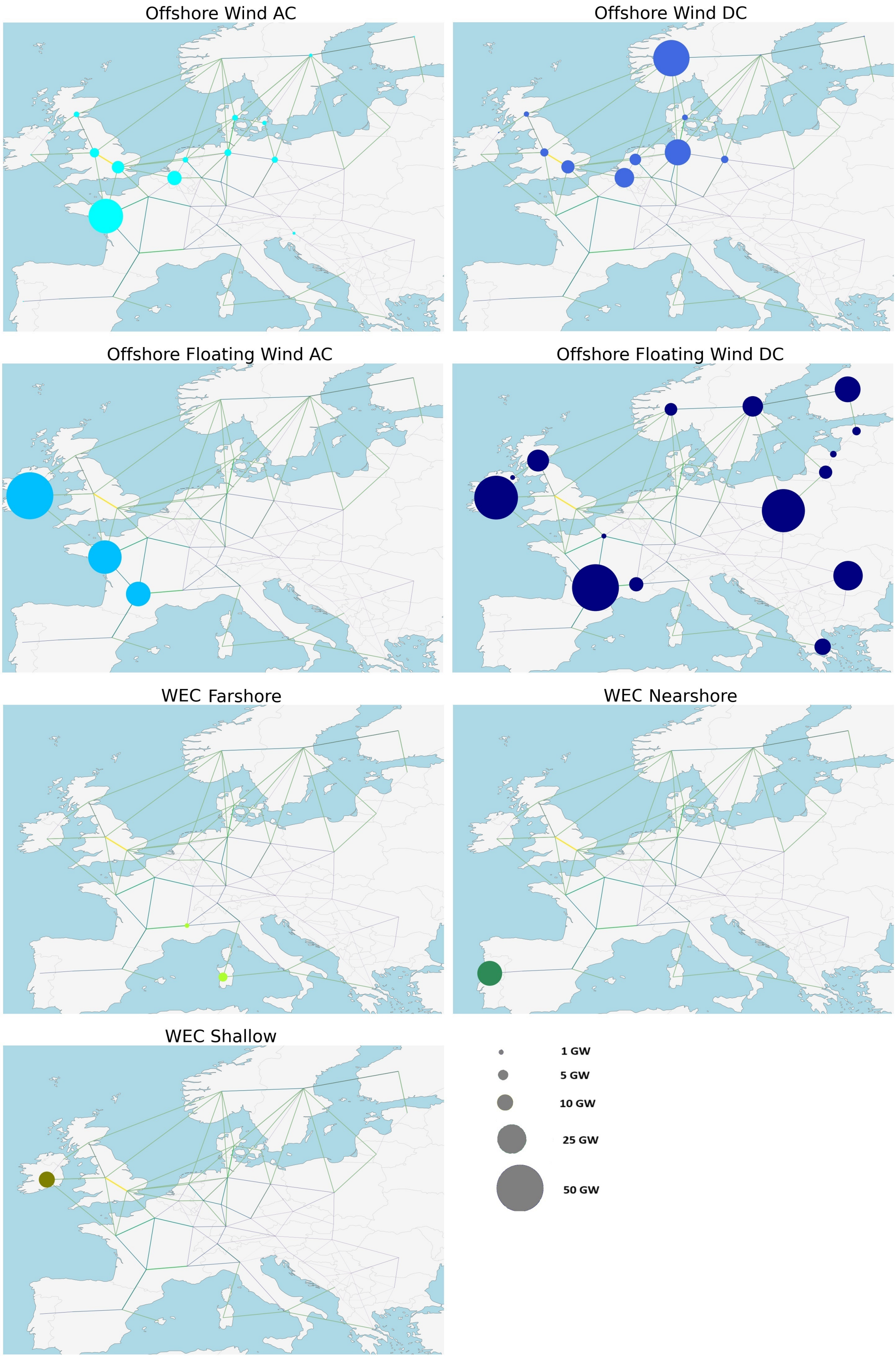

Figure 43: Generator capacities per bus for 2050.

4.4.3 Comparison of component capacity with a non-BAU 2050 scenario

In order to dwell into the decisions of the model by itself on the configuration of generators, the following table provides insight on a non-BAU scenario.

Carrier	BAU [GW]	Non-BAU [GW]	Difference [GW]
Offshore Wind AC	40.00	10.16	-29.84
Offshore Wind DC	55.00	30.75	-24.25
Offshore Fl. Wind AC	80.00	0.79	-79.21
Offshore Fl. Wind DC	230.00	104.41	-125.59
Onshore Wind	368.06	753.01	384.95
Solar	1104.92	1262.90	157.97
WEC Farshore	17.00	0.00	-17.00
WEC Nearshore	25.00	0.00	-25.00
WEC Shallow	20.00	0.00	-20.00
Total	1989.91	2211.93	222.02

Table 27: Difference in installed capacities between systems with and without BAU for the final 2050 scenario.

Even though offshore wind is reduced by a total of 259GW and the wave capacities did not make it at all into the system so another 62GW lost, the non-BAU system has significantly more total installation, reaching almost 2,212GW. Solar and onshore wind technologies are prevailing into the model, with DC floating wind following them. However, this greater capacity translates to around 21 billion € less in terms of annual costs for the non-BAU scenario, going from 178 to 157 billion €/a.

This is logical, since the objective function is a cost optimization function which aims to minimize system costs. The model will sacrifice diversity in the energy mix if it deems that energy supply will be guaranteed from cheaper sources like onshore solar and wind. However, in relation with the limitations of the model, it aggregates data of a single year and makes this year the baseline of the system construction. A satisfactory performance of the system for one year does not reassure that the system is ready for all possible scenarios. Integrating more energy sources into a system, especially a high-share renewable one, allows it to maintain some amount of supply when one carrier is failing, thus it enhances energy stability.

Type	Metric	BAU [GW]	Non-BAU [GW]	Difference [GW]
Line	HVAC	970.02	958.48	-11.54
	HVDC	165.52	158.48	-7.04
Storage Units	Battery Storage	122.55	165.18	42.63
	Hydrogen Storage	0.04	0.02	-0.02
	Pumped Hydro Storage	54.33	54.33	0.00
	Reservoir & Dam	102.22	102.22	0.00
Link	H2 electrolysis	123.97	181.14	57.16
	H2 fuel cell	169.87	224.86	54.99
	battery charger	103.50	118.34	14.84
	battery discharger	105.63	120.78	15.14
Energy capacity of general storage		BAU [GWh]	Non-BAU [GWh]	Difference [GWh]
Store	Battery Storage	601.73	741.28	139.55
	Hydrogen Storage	27110.40	36757.16	9646.76

Table 28: Capacity of the rest of the components.

4.4.4 Capacity factors

The following figure shows how the capacity factor of each technology is progressing in the model through time.

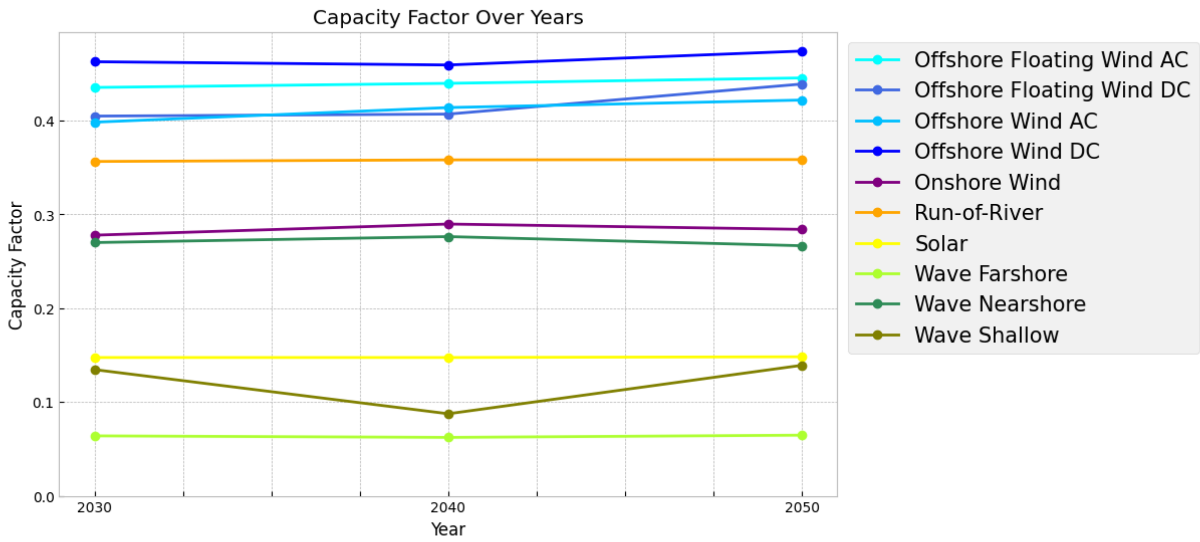

Figure 44: Capacity factors of each technology.

The highest capacity factor (CF) values are acquired by the offshore wind technologies, all surpassing the 0.4 threshold for the three scenarios, highest of which is the bottom fixed DC WTGs with a CF equal to 0.474 for the year 2050. Farshore wave energy has the smallest CF, and this is probably due to the ambitious capacity of $20MWkm^2$. Nearshore has the highest CF of the three WEC technologies, laying in the range of 0.267-0.276 for all scenarios. Nearshore WECs are installed exclusively in Portugal for the three scenarios. Shallow WECs show some fluctuation for the year 2040. What might cause this drop is the fact that the technology target for 2040 drives the model to install shallow WECs in 4 different regions (table 23), while for the 2030 and 2050 scenarios, its expansion is restricted into only one region, Portugal and Ireland respectively.

4.4.5 Transmission expansion

For all scenarios, the transmission lines in the system, as mentioned in the configuration section, are set to be expanded according to cost-optimal constraints under the total objective function. As a result, the model theoretically does not have a limit of expansions in terms of capacity. Choosing either cost or capacity constraints on line expansion is linked to the assumptions of the researcher on weather the availability of transmission line components is greater than the availability of energy generating components. Since the network is interconnected but relies solely on RES as the first line of energy generation, variability of energy supply is guaranteed. This means that the energy demand for regions with low intensity for a certain amount of period needs to be covered by energy provided through transmission lines from other regions. If the expansion of the electricity grid is limited and at the same time the demand is not met throughout the whole year, then it needs to be compensated by the installation of more generators. The matter suddenly becomes a question of weather the generator availability is adequate to create this model.

The network consists of 50 buses which are connected with 76 HVAC and 47 HVDC transmission lines, the total expansion of which in terms of capacity is presented by table 29.

<table>
<tr><th>Scenarios</th><th>Type</th><th>Existing Nominal Capacity [MW]</th><th>Optimal Nominal Capacity [MW]</th><th>Percentage</th></tr>
<tr><td rowspan="2">2030</td><td>HVAC</td><td rowspan="6">553269 [HVAC]
22691 [HVDC]</td><td>909512</td><td>64%</td></tr>
<tr><td>HVDC</td><td>160701</td><td>608%</td></tr>
<tr><td rowspan="2">2040</td><td>HVAC</td><td>920323</td><td>66%</td></tr>
<tr><td>HVDC</td><td>141284</td><td>523%</td></tr>
<tr><td rowspan="2">2050</td><td>HVAC</td><td>970018</td><td>75%</td></tr>
<tr><td>HVDC</td><td>165520</td><td>629%</td></tr>
</table>

Table 29: Total expansion of HVAC and HVDC transmission lines.

The cumulative expansion of the system in the transmission level for both types of lines and for the is 86% and 84% for years 2030 and 2040 respectively, while for the 2050 scenario line capacity almost doubles, reaching 98% of expansion compared to the extracted network of ENTSO-e of 2022.

Bellow, the expansion of each line used, is presented in two tables one for the HVAC lines 30 and one for the HVDC ones 31. The modelling starting point of each line is provided on the 1^{st} column and the finishing point on the 2^{nd} one. The other two columns present the existing and optimal capacities according to the model.

Start	End	Existing Nominal Capacity [MW]	2030 [MW]	2040 [MW]	2050 [MW]
Albania	Greece	1698	1698	1698	1698
	Montenegro	2190	3889	3349	2915
	North Macedonia	-	1149	750	719
	Serbia	2190	2190	2190	2190
Austria	Slovenia	3888	8445	8694	8149
	Switzerland	6792	6792	6792	6792
	Czech Republic	4379	6929	6766	6866
	Germany	5854	8648	8400	8102
	Germany	10189	10575	10648	10560
	Hungary	4379	6842	6672	6283
	Italy	492	804	758	791
Bosnia and Her.	Croatia	5362	6120	5362	5362
	Montenegro	2681	4033	3151	2685
	Serbia	2190	3406	2768	2512
Belgium	France	6792	7072	8791	9280
	France	2681	3973	4381	4818
	Luxembourg	983	2687	2868	3360
	Netherlands	6792	6792	8040	8216
Bulgaria	Greece	1698	1891	1847	1698
	North Macedonia	1698	2073	1985	1782
	Romania	6792	9322	9409	9134
	Serbia	1698	1991	1698	1879
Switzerland	Germany	27170	27170	27170	27170
	France	6346	13043	15148	16315
	France	3396	8352	8789	9947
	Italy	8267	18881	20539	21905
Czech Republic	Germany	3396	6160	6303	6133
	Germany	3396	7264	7597	7188
	Poland	4379	8295	7705	10033
	Slovakia	6077	6077	6077	6077
Germany	Germany	38609	38610	38610	38610
	Germany	1698	4060	4265	3678
	France	3888	6049	6914	7404
	Luxembourg	3441	3441	3441	3578
	Netherlands	10189	25929	28510	33953
	Germany	11172	11172	11172	11172
	Germany	17964	19692	21331	21565
	Germany	11172	11771	11567	13372
	Germany	21360	22978	23525	22995
	France	5586	13064	14249	16106
	Germany	12378	30538	32476	27994
	Germany	6792	18937	19424	17215
	Denmark	4379	48316	49435	38416
	Netherlands	3396	6225	6665	5510
	Poland	6792	14795	14771	13603
Denmark	Sweden	3396	3396	3396	3396

Estonia	Latvia	2011	2787	3070	2570
Spain	Spain	29717	29717	29717	30072
	Portugal	15059	15060	16106	18541
	France	4379	39436	31873	30259
Finland	Sweden	3396	10399	11296	11473
France	France	10725	34876	40660	44578
	France	13361	27708	32130	33383
	France	13138	28755	24022	27964
	France	14344	14345	14345	14345
	Italy	5586	15176	16900	18904
	France	24086	27291	28217	33397
	France	9250	36058	36744	43724
Great Britain	Great Britain	6792	6792	6792	6792
	Great Britain	32577	41289	34416	55530
	Ireland	983	2026	1475	4204
Greece	North Macedonia	3396	3396	3396	3396
Croatia	Hungary	6792	6792	6792	6792
	Serbia	1698	2567	2078	1958
	Slovenia	6077	8939	8734	8356
Hungary	Romania	3396	8975	7585	8103
	Serbia	1698	2781	2509	2457
	Slovakia	3396	8372	7363	8002
Italy	Italy	7284	9675	7651	9196
	Slovenia	2190	2472	2473	2490
Lithuania	Latvia	4022	4022	4022	4022
Montenegro	Serbia	2681	2681	2681	2681
North Macedonia	Serbia	3396	3396	3396	3396
Norway	Sweden	7284	13908	20375	24524
Poland	Slovakia	3396	7672	7181	9261
Romania	Serbia	5094	10612	10232	10521

Table 30: HVAC transmission lines of the network.

Some countries in the model are comprised of more than one bus. Domestic transmission lines start and finish to a bus which has the same country code. For example, Germany has a total of 8 connection lines which start and finish at other buses of Germany. A researcher can dive deeper into the power system analysis of a single country, by identifying which lines exist with it.

Since the three scenarios are independent from one another, there are cases in which lines have more capacity for years 2030 and 2040 compared with 2050. This happens because all scenarios have cost-optimal constraints and none of them has capacity expansion constraints. The different generator and storage system configurations of the three scenarios, for example the drop of onshore wind energy capacity and the rise of all of the rest of the capacities from 2030 to 2050, create different needs in terms of power transfer from one node to node. One solution to address this problem would be to perform limited expansion network optimization which would follow a linear increase of the capacity. More specifically, since the model of 2050 has almost double the line capacity of ENTSO-e grid, an equivalent simulation of a maximum of $\times 2$ of the existing line capacity constraint could be deliver similar results. An assumption about the two other scenarios could set a line expansion limit proportional to their generator minimum installation capacities. Limiting the line expansion could lead to a significantly larger need of generators.

Most of the HVAC lines have a higher optimal capacity than the existing one while the rest maintained their original capacity. The ones that stand out in the expansion are the line between Albania - North Macedonia, which did not exist previously, between Germany - Denmark, which is increased by 777%, and between Spain - France which is increased by 591%. Figure 41, apart from an overview of the generator provides also the average flow of electricity through the lines in the model for each direction

Start	End	Existing Nominal Capacity [MW]	2030 [MW]	2040 [MW]	2050 [MW]
Germany	Belgium	-	437	790	1423
	Germany	-	1	-	-
	Germany	-	2	-	-
	Germany	-	4624	4899	3946
	Norway	-	4	229	1092
	Germany	-	44	-	1
Denmark	Norway	1140	11095	7378	5827
	Germany	600	7413	6875	6744
	Denmark	600	1659	1833	1258
Spain	France	-	2	-	-
	Spain	400	579	618	712
Finland	Estonia	600	600	600	600
	Estonia	650	1170	1347	650
France	Spain	2000	2000	2000	2000
	Great Britain	-	2359	3168	2771
Great Britain	Great Britain	2200	2200	2200	2200
	Great Britain	2501	3474	2501	2501
	Great Britain	250	250	250	250
	France	-	1	-	278
	Ireland	500	28428	22250	43071
	Norway	-	778	974	2245
	Belgium	-	7804	8429	9062
	Germany	-	4112	3612	3207
	Denmark	-	7122	5488	3308
	France	2000	2000	2000	2000
	France	-	6647	6714	5682
	France	-	18	1	2
	Netherlands	1000	11036	5730	8563
Ireland	France	-	24867	17704	24351
	Great Britain	-	29	3	3
Italy	Switzerland	-	3	1	1
	Greece	500	532	595	2382
	Italy	1000	1000	2826	1679
	Montenegro	-	2041	1995	1781
	Italy	300	900	2100	1208
Lithuania	Sweden	700	909	966	1152
Netherlands	Denmark	-	5490	3473	2448
	Norway	700	700	2936	4494
Norway	Great Britain	-	5813	5880	5211
Poland	Lithuania	2000	2000	2000	2000
	Sweden	600	1532	3190	3851
Sweden	Germany	600	600	600	600
	Germany	-	1	-	1
Sweden	Denmark	250	250	250	250
	Denmark	300	6874	5577	3417
	Finland	800	800	800	800
	Finland	500	500	500	500

Table 31: HVDC transmission lines of the network. Values under 10MW are considered insignificant for the model and are not taken into account.

HVDC lines, however, appear to increase significantly, both in numbers and in capacity. With respect of the 2050 scenario, the model installs 14 new HVDC lines, most of which are overseas. Most of the new HVDC lines are installed in the North Sea, connecting most of the countries located around there. Higher in line expansion capacity were lines connecting Ireland to Great Britain and France reaching 43GW and 24GW respectively. Lines however between Baltic and Scandinavian countries appear to have a more limited expansion, the larger of which was between Poland and Sweden with a capacity higher by 3.1GW. On the south side of Europe

What is worth mentioning regarding modelling transmission lines is that the length of each line is equal to the distance between the centers of the nodes. This means that increasing the number of buses in the network will provide a better approximation of the length and capacity of each line since those will be divided into multiple pieces. This is crucial especially for overseas HVDC cables, a lot of which in this configuration need to cover large distances on land to connect the buses. HVDC underwater connections are costlier than onshore ones, not only due to capex and opex of the DC technology, but also due to the required employment of vessels and marine equipment. Ideally, a model should be able to approximate the exact underwater distance of such cables. An example is the HVDC line between Italy and Greece, which instead of being 910km in length, connecting Central Greece with the region of Napoli, it could be around 180km in length connecting the two closest points between the countries.

4.4.6 2050 storage system

Next, a table of each country's share of storage units is presented. General storage once again here refers to storing surplus energy produced from the generators on each node, which can be delivered to the system in a time of need. General storage refers to the energy capacity and is measured in MWh, as in the energy that they can contain, while the storage units refer to the power capacity of each type.

	Storage Units				**General Storage**	
Country	**H2 [MW]**	**PHS [MW]**	**Battery [MW]**	**Hydro [MW]**	**H2 [MWh]**	**Battery [MWh]**
Albania	0.30	-	3251.10	1493.70	367.10	2368.10
Austria	0.16	5044.30	160.86	3426.62	95.80	22488.40
B. & Her.	0.25	440.00	2359.90	1695.50	196.70	2023.10
Belgium	1.30	1308.00	401.43	12.78	763120.90	515.10
Bulgaria	0.37	864.00	886.85	2039.54	954.10	8300.30
Switzer.	0.20	4980.75	107.76	9181.98	111.20	13635.20
Czech R.	0.44	1155.00	5696.33	684.98	384.70	11384.50
Germany	5.00	7659.62	18279.96	189.50	2267618.40	45478.80
Denmark	2.48	-	2203.89	-	4614650.30	7249.30
Estonia	1.48	-	136.77	-	135.30	7469.80
Spain	0.44	8458.58	34370.10	15258.77	185.80	93710.80
Finland	1.17	-	13.59	1386.80	1404885.60	31590.50
France	3.39	4976.30	19440.50	8230.38	3090575.80	82416.70
Great B.	8.42	440.00	2466.06	138.30	4668418.60	32121.00
Greece	0.45	699.00	10570.18	2566.00	1018070.10	6596.10
Croatia	0.31	518.70	72.00	1327.62	207107.40	545.20
Hungary	0.42	-	3468.75	28.00	38.10	9608.90
Ireland	1.05	392.00	40.35	1.00	50.00	83282.60
Italy	1.03	7576.90	13805.36	4130.86	1005842.60	56572.20
Lithuania	1.15	900.00	17.92	-	1005620.30	10715.30
Luxemb.	1.13	2582.00	281.46	-	124.60	45037.60
Latvia	1.14	-	18.72	-	171.60	628.50
Monten.	0.27	-	928.00	362.96	1451747.10	640.50
N. Maced.	0.38	-	2413.02	-	1102.80	1478.50
Netherl.	1.39	-	298.47	-	1637429.70	34631.60
Norway	0.51	282.30	93.36	29541.50	536916.20	526.60
Poland	1.78	1706.00	1.31	239.51	2014033.20	23685.00
Portugal	0.06	2642.00	42.74	1520.40	2087431.60	7365.90
Romania	0.73	-	22.02	5636.88	30037.60	543.50
Serbia	0.29	614.00	354.86	790.10	112657.30	26340.70
Sweden	0.83	92.00	239.11	11978.72	336.40	503.20
Slovenia	0.20	180.00	53.02	118.00	944.20	471.80

Slovakia	0.56	822.45	52.30	241.90	1058440.50	32794.20
Total	39.06	54333.90	122548.03	102222.30	27110404.20	601726.20

Table 32: Storage units in the network.
Highest share per country:
Inter-temporal H2: Great Britain, 8.42MW
PHS: Spain, 8.5GW
Inter-temporal Battery: Spain, 34.4GW
Hydro: Norway, 29.5GW
Generic H2: Great Britain, 4,668GWh
Generic Battery: Spain, 93.7GWh

What can be noticed is that the technologies are employed from almost all of the countries. For pumped-hydro storage (PHS) and hydro dam storage, exceptions are countries like the Netherlands, or the Baltic countries, which have an terrain elevation disadvantage. PHS is a technique typically used in mountainous countries. Since hydro related storage and capacity is restricted in the model in terms of expansion, their results concern only existing infrastructure registered into the PyPSA carrier lists. North Macedonia, Montenegro and Romania have documented PHS and hydro capacities ([81],[82],[83]), however they are not included into the model.

4.4.7 Energy in the system

The following section will present the three scenarios in the model in terms of energy. Energy is calculated by the multiplication of the mean supply of each energy carrier with the number of snapshots in the model. Since the model has 1-hour resolutions this adds up to 8760 snapshots. Below, table 33 provides a break-down of each generator's annual energy production.

Generator	2030 [TWh]	2040 [TWh]	2050 [TWh]
Offshore Wind AC	35.49	108.76	147.81
Offshore Wind DC	141.71	160.92	228.41
Offshore Fl. Wind AC	113.92	192.57	312.15
Offshore Fl. Wind DC	400.13	409.91	884.39
Onshore Wind	1457.04	1364.40	915.75
Run of River	155.87	156.61	156.75
Solar	1154.76	1393.81	1434.69
WEC Farshore	0.56	3.82	9.63
WEC Nearshore	4.73	36.31	58.38
WEC Shallow	3.54	7.66	24.38

Table 33: Annual total energy production per generator per scenario in TWh.

Wave energy reaches a cumulative 92.4TWh of energy generation, with offshore wind generating more than 1572.5TWh. However, the theoretical maximum supply can be also calculated, to provide a greater perspective in the energy potential. Given the maximum installable capacities for offshore wind and wave energy, the following table is provided with respect to the 2050 scenario:

Clearly, the energy contained in waves, with respect to the configuration of these scenarios is more than enough for the demand of Europe ($\approx$ 4300TWh). Breaking down the supply of power even more, in the following bar-charts the supply rate of the generators is presented in an hourly basis for the final scenario of 2050. System supply refers to the active power injection from the power generating sources.

Carrier	Capacity Factor	Maximum capacity [GW]	Supply rate [GWh/h]	Annual energy generation [TWh]
Offshore Wind AC	0.422	1446	610	5342
Offshore Wind DC	0.474	871	413	3616
Offshore Fl. Wind AC	0.445	1371	611	5349
Offshore Fl. Wind DC	0.439	5509	2418	21182
Onshore Wind	0.284	11561	3284	28764
Solar	0.148	2406	357	3124
WEC Farshore	0.065	30810	1992	17451
WEC Nearshore	0.267	22363	5962	52223
WEC Shallow	0.139	3809	530	4643

Table 34: Theoretical maximum energy potential of the 2050 scenario.

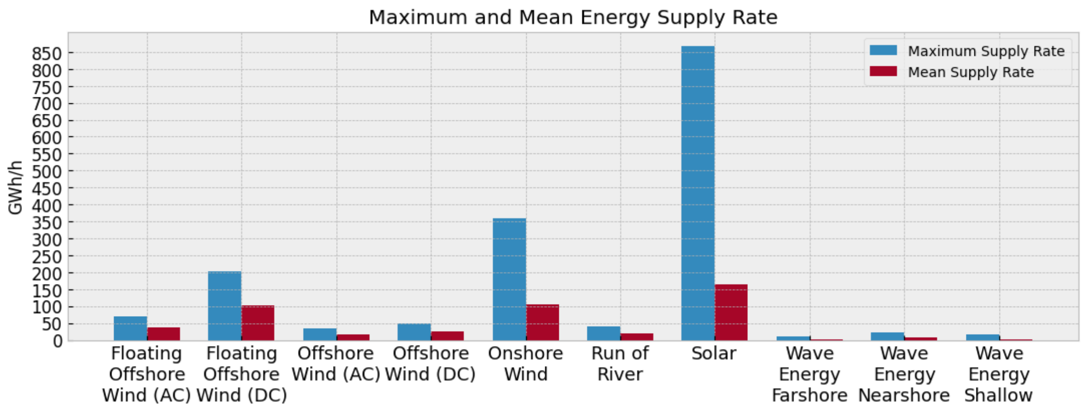

Figure 45: Supply rate of generators for year 2050.

It is obvious that due to the variability of the sources, there is quite a big difference between the maximum and average supply rate. Especially for solar energy, which constitutes more than 1100GW of capacity across the model, can deliver at times more than 850GWh per hour. However, taking into account night-time and averaging the supply over time, its mean energy delivery in the system is around 160GWh per hour, or 19% of the maximum. The differences between mean and maximum is smaller for the wind technologies, the ranges of which are around 50% for the offshore wind technologies and 30% for onshore wind. For WECs, the nearshore device is the most prominent averaging at 30% of the maximum, while the other two devices are bellow 15%.

Bellow there is the supply rate of the storage components.

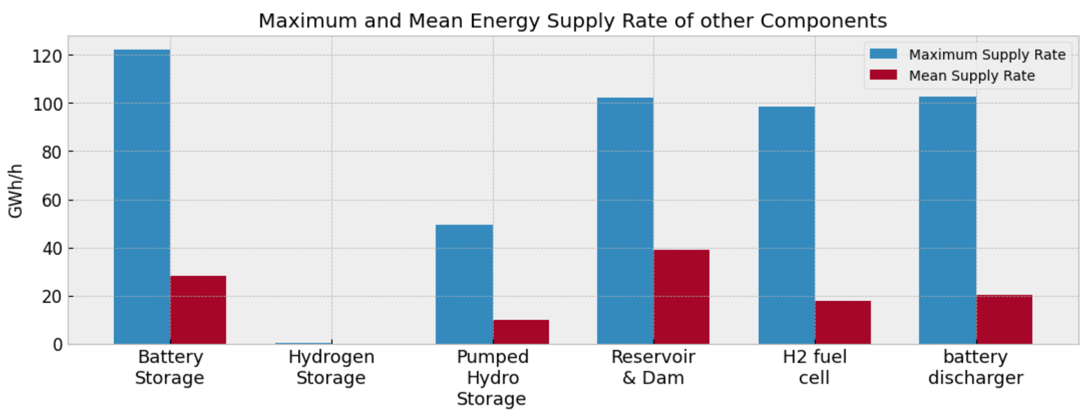

Figure 46: Supply rate of generators for year 2050. The first appearing "Battery Storage" and "Hydrogen Storage" units refer to the inter-temporal storage units while the last two refer to the generic storage units.

The average supply rate of the storage systems are all under 30GWh/h, except reservoir storage which is the most stable reaching 40GWh/h.

PyPSA incorporates two additional terms into the final energy system, curtailment and withdrawal of energy. Curtailment refers to the reduction of power production that may occur when there is excess generation from the renewable sources, hence the system cannot receive the full input of power. Withdrawal refers to the demand for electricity from other types of components which are essential to the network, in this case all of the operating components which are not classed as generators.

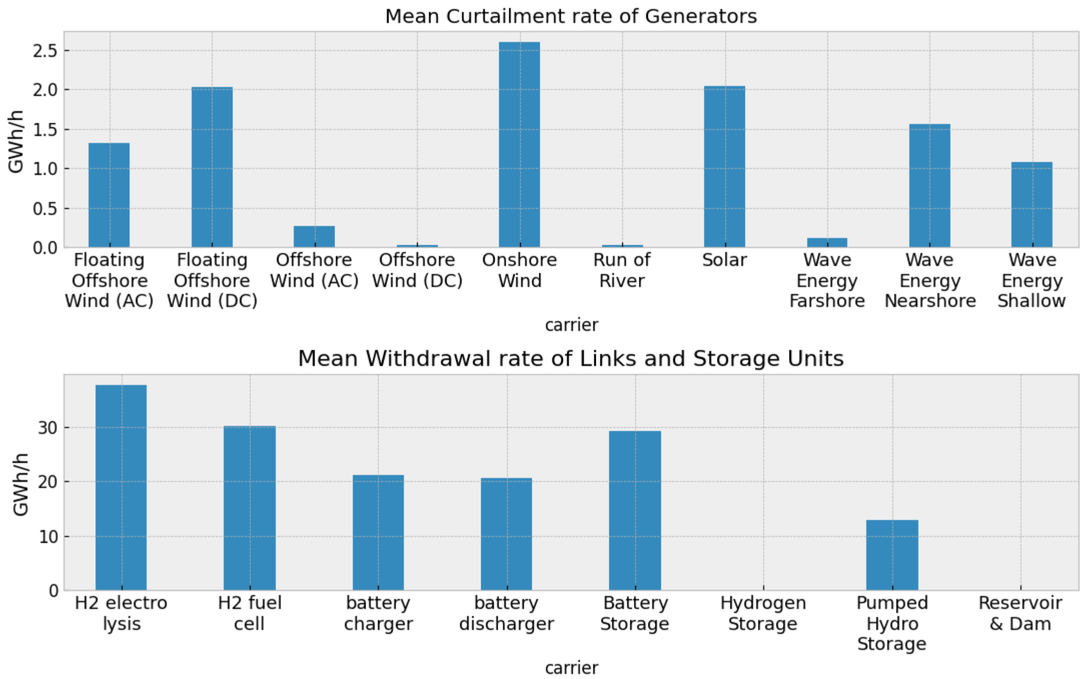

Figure 47: Mean curtailment and mean withdrawal of energy in the system.

Since reservoirs use the stored potential energy of water within their catchment area, their dispatch has theoretically zero electricity withdrawal.

Table 35 shows the annual contribution of energy by the storage components.

Type	Metric	2030 [TWh]	2040 [TWh]	2050 [TWh]
Storage Units	Battery dispatch	119.51	233.13	245.09
	Battery store	-124.61	-242.87	-255.35
	Hydrogen dispatch	1.08	0.02	0.05
	Hydrogen store	-2.36	-0.04	-0.11
	Pumped Hydro dispatch	90.72	83.46	84.69
	Pumped Hydro store	-121.44	111.54	-113.18
	Reservoir Dam dispatch	339.61	339.66	339.66
	Reservoir Dam store	0.00	0.00	0.00
Stores	H2 electrolysis	-201.56	-254.72	-264.63
	H2 fuel cell	116.90	147.74	153.49
	Battery charger	-159.19	-179.72	-181.12
	Battery discharger	155.97	176.09	177.51

Table 35: Annual total energy production per storage unit per scenario in TWh.

With the exception of H_2 inter-temporal performance, all of the components have a significant input of energy in the system.

Lastly, an overview of the generation of energy exclusively from the generators in table 36.

	2030 [TWh]	2040 [TWh]	2050 [TWh]
Load	3628.72	3958.60	4288.55
Generator Production	3467.75	3834.78	4172.35
Storage Unit Production	1184.56	1414.55	1446.29
Storage Unit Withdrawal	-1023.60	-1290.73	-1330.16
Total	3628.91	3958.96	4288.70
Generator Curtailment	165.52	104.67	96.61

Table 36: Annual total energy production per scenario in TWh.

The overall electrical generation trend seems to be almost completely linear, which is logical since the electricity load demand is linearly increasing for the three scenarios, by 10%, 20% and 30%. What else can be observed here is the power balance of the system. The yearly demand is covered entirely, with input and output of energy balanced. Curtailment of the generators is not part of the balance since it is not a part of the objective function.

4.4.8 Investment costs

As mentioned, the objective cost optimization is the global function that regulates the combination of the components in the system. This function provides the annual costs of the system. The following table shows the annual costs of each scenario.

	2030 [billion EUR/a]	2040 [billion EUR/a]	2050 [billion EUR/a]
Objective Costs	151.8	158.9	178.1

Table 37: Annual costs of energy system for each scenario.

In terms of expenditures in the model PyPSA uses six indexes: CAPEX and OPEX, Capital Cost of expansion, Marginal Cost of energy generation, Market Value and Revenue. CAPEX is calculated by simply multiplying the optimal capacity of each component by its corresponding capital cost of investment. OPEX on the other hand is the product of the power output and the variable cost of the components aggregated over a year. Capital costs of expansion refers to the average required capital upon increasing the capacity of an energy carrier by 1MW, and marginal cost refers to the average cost of the production of a 1 MWh by each carrier. Market value, also referred to as marginal price of electricity per bus, represents the economic value of electricity in the market at a specific point in space and time in terms of Euro/MWh. Market value is a revenue metric, and is different from LCOE, which is a per-unit metric of cost of generating electricity over the lifetime of the power plant. Market value is influenced mostly by operational costs of generators, transmission losses and energy demand. Lastly, by revenue PyPSA refers to the overall income per hour generated by the power system. Bellow, graphs with the values of each index per generator are presented.

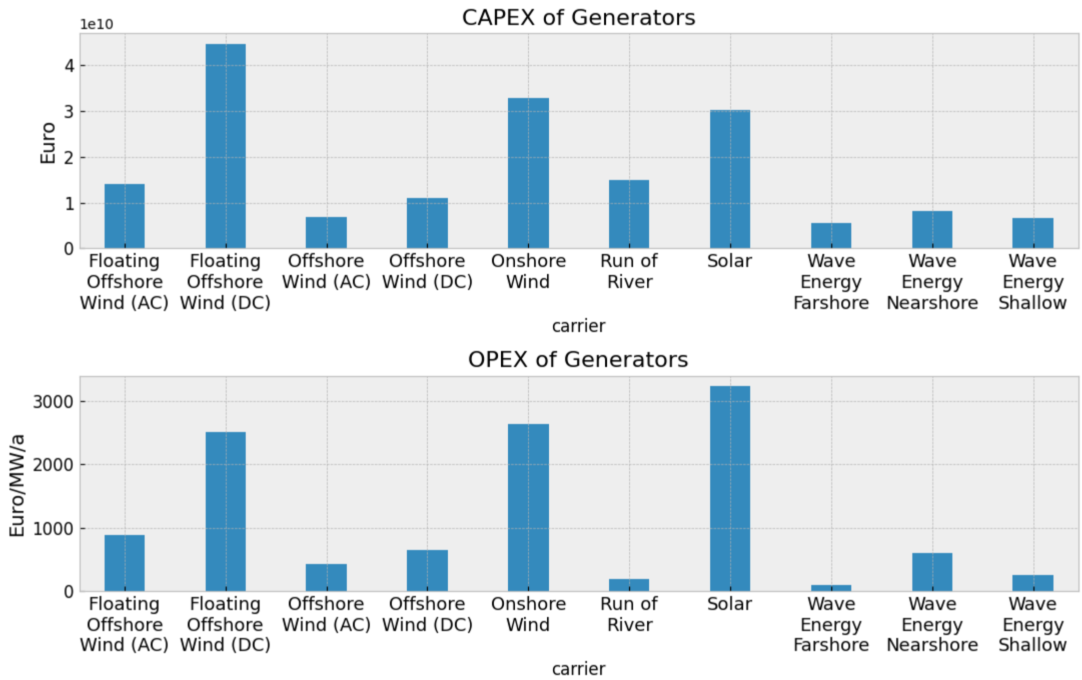

Figure 48: CAPEX and OPEX of generators for 2050 horizon.

The overall capital expenditures of all components in the system is 255.2 billion €. 15.2 and 6.9 billion € of those are related to HVAC and HVDC expansion respectively, while storage systems regard around 53 billion €. The rest 175 billion € refer to generators.

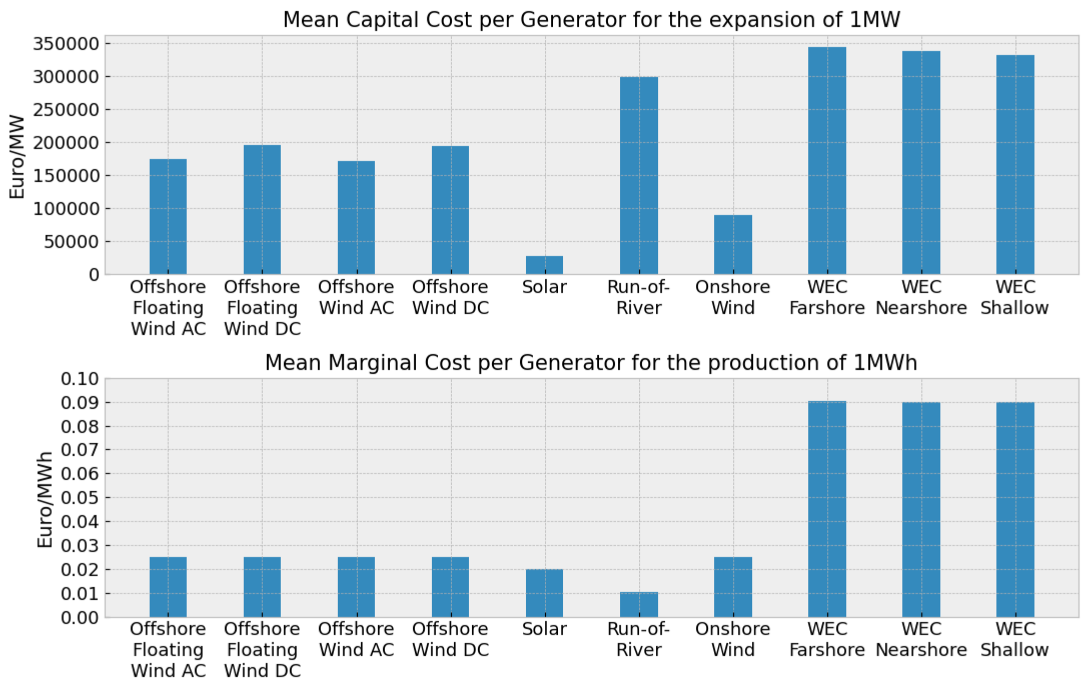

Figure 49: Mean capital and marginal costs of generators for 2050 horizon.

Wave energy here seems to have a disadvantage over the rest of the technologies both in capacity expansion and energy generation.

As mentioned, market value corresponds to the marginal price of electricity in each bus. Consecutively, revenue is calculated by simply multiplying the average supply of energy per generator, with this generator's mean market value.

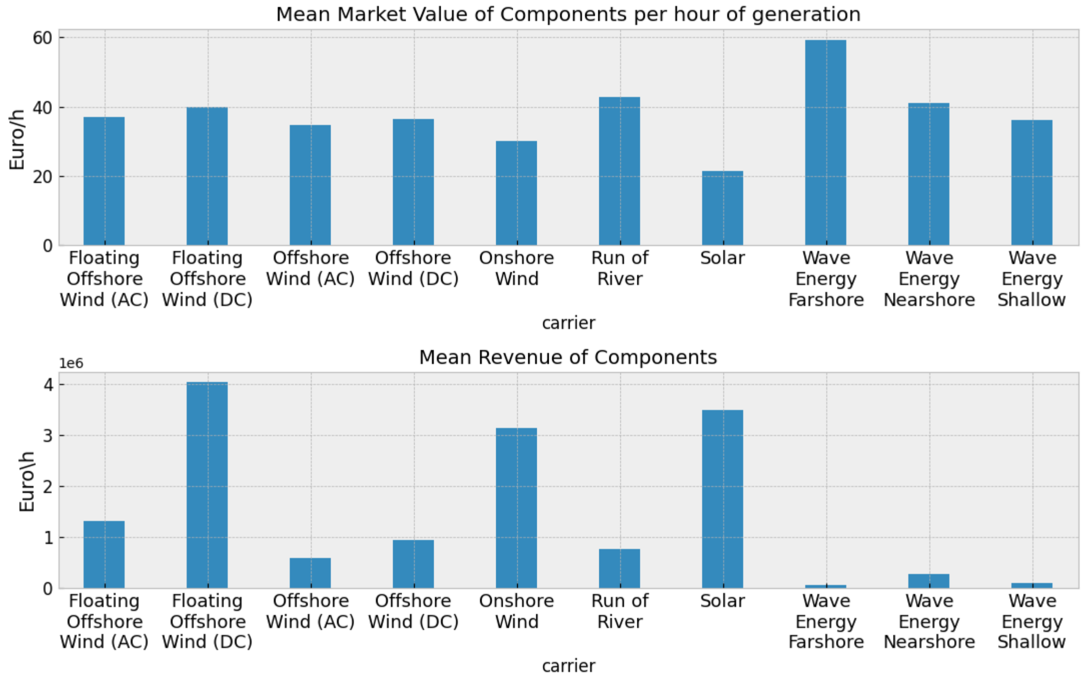

Figure 50: Mean market value and revenue of generators.

The limited installed capacity of wave converters produce a small final hourly revenue, despite high associated market values. The opposite can be witnessed for solar energy, which has a low market value, but its capacity make it highly profitable, indicating a general correlation between revenue and capacity. To calculate the annual revenue of the system, the hourly revenue is multiplied by the number of snapshots, those being equal to 8760. The results of annual revenue are presented below in table 38.

Type	Metric	Annual Revenue [billion €]
Generator	Floating Offshore Wind (AC)	11.55
	Floating Offshore Wind (DC)	35.38
	Offshore Wind (AC)	5.14
	Offshore Wind (DC)	8.32
	Onshore Wind	27.43
	Run of River	6.68
	Solar	30.58
	Wave Energy Farshore	0.57
	Wave Energy Nearshore	2.39
	Wave Energy Shallow	0.88
Line	HVAC	13.84
	HVDC	6.76
Storage Unit	Battery Storage	5.49
	Hydrogen Storage	0.01
	Pumped Hydro Storage	5.40
	Reservoir & Dam	32.52
Link	H2 electrolysis	2.71
	H2 fuel cell	15.20
	battery charger	0.73
	battery discharger	0.18
Store	Battery Storage	3.62
	Hydrogen Storage	2.27

Table 38: Annual revenue of all components in the network.

The overall maximum annual revenue of the power system is equal to 217.7 billion €.

5 Discussion

This section reflects on the comprehension of the dynamics inherent in the generated models. Apart from the establishment of the influence of temporal and spatial resolution for an energy model from a programming point of view, the goal is to understand the interactions between different components in the model and their final performance concerning 2050 scenario, in relation to the results provided. Emphasis is placed on evaluating the influence of offshore wind and wave energy sources on energy production, installable capacity, but also the general economic landscape within the model, drawing comparisons with existing literature. The discussion finally attempts to assess the feasibility of a fully renewable energy system.

Furthermore, region-specific insights into the behavior of the system are provided. This involves an examination of the roles of the selected technologies and the influence of a region's accessibility to water basins within the network. A critical aspect of this thesis is ensuring alignment with European directives, particularly those set for the target year 2050, since the 2030 and 2040 models are hypothetical scenarios. The discussion also involves the role of the transmission expansion into the system, and the integration of anti-variability measures to enhance stability, by assessment of the operating storage systems. These aspects collectively contribute to enhance the understanding of the model's performance and its relevance within the broader context of European energy objectives.

The initial findings from the results, featuring test models incorporating varied spatial and temporal resolutions, strongly suggest that an increased resolution in both space/network and time significantly enhances the ability of the model to properly introduce renewable generators offshore. The 25-hour resolution solar energy is represented very poorly under the daily aggregation of weather data. This implies an almost constant generation of solar energy, even in night-time, which does not correspond to reality. As a result, the overall system relies heavily on solar energy supply, and completely ignores both inter-temporal and generic battery storage. The situation drastically changes going from 24 to 1 hour of resolution where the system decreases solar installation by 150GW, while adding 413GW of total battery storage units (this number refers to the battery storage capacity and not the dispatch capacity of the technology). The higher resolution had noticeable differences in the capacities of almost all of the components in a beneficial way, hence the annual system cost showed a measurable decrease.

The attempt to increase the bathymetry resolution into the model however was almost insignificant for the results. By reviewing those results, the verdict was that when combining multiple space-related data into a single model, the final level of resolution shifts towards the one with the lowest resolution. This is clearly depicted in figure 28, where a significant amount of wave energy potential is lost under the $31,000m \times 31,000m$ resolution of ERA5 data, and the benefits of $460m \times 460m$ GEBCO 2023 bathymetry data are nonexistent. Places with a combination of promising resources, desirable bathymetry and reasonable distance from shore like Portugal, Spain, Italy and Ireland, are eventually overlooked, the model by itself does not install wave energy, and for this to happen, minimum capacity constraints need to be set.

With respect to the final scenario, the 2050 carbon-neutral fully-renewable scenario, and regarding wave energy, the minimum capacity constraints of 17GW, 25GW and 20GW for farshore, nearshore and shallow waters devices were not surpassed. This means that the share of wave energy is a bit larger than 3% in the energy mix of generators. This amount yields an annual 92.4TWh of electricity, the intensity of which however is lower during summer time. To achieve this capacity, wave energy must be deployed with a mean rate of 2.3GW per year. The farshore WEC's $20MW/km^2$, although it is the highest power density value of all three devices, obtained the lowest average capacity factor (CF=0.065). It is possible that the high density meant that the devices, all of which were installed in France and Italy, were interfering with one another, hindering the overall performance and generating large wake effects. By lowering the power density, the deployment of farshore WECs could be optimized to reach a CF closer to the other two WEC types.

Considering the installation potential and multiplying it by the corresponding average capacity factor throughout the year, wave converters could generate up to 17,451TWh of electricity from farshore regions, 52,223TWh from nearshore, and 4,643TWh from shallow waters. These numbers can not be summed up due to the fact that some regions between farshore and nearshore potential overlap, which means only one type of converter can be installed there. Those regions fall into the range of 50m and 80m of water depth. Nonetheless, on the one hand the results show a vast resource of wave energy in Europe, but on the other hand capacity factors still need to technologically advance to reach the values of wind and solar energy.

A similar optimal supply trend is observed for offshore wind energy as well, which yields a total of

1,573TWh, about half of which is generated by the floating DC turbines. This quantity constitutes 38% of the generation and corresponds into 405GW of installed capacity. Floating DC WTGs are by far the most installed, since their BAU constraint set a minimum boundary of 230GW, a capacity which was fulfilled. This, however, came with the largest amount of curtailment, it being equal to 17.5TWh, the highest of all offshore and marine technologies. Adding the wind's onshore capacity, wind supplied 2,489TWh per year, and the rest was covered by solar and run-of-river technologies. This amount of energy seems quite promising for the wind industry which in 2022 generated only 489TWh with a share of 18%, with 30GW being offshore while 225GW were onshore. Deployment rate however of offshore energy needs to advance from today's standards and reach an average of 13,9GW per year for the next 27 years.

It is hard to predict if Europe will be able to acquire this deployment rate of offshore wind. Onshore wind however, based on the model, would need only 143GW of additional power, which translates to a rate of 5.3GW per year. Since the focus shifts from onshore to offshore wind, the cumulative deployment rate of turbine manufacturing does not increase by a lot, moving from 16.7GW to 19.2GW per year.

Similarly to wave energy, the theoretical potential is again quite larger than the optimal. Up to 9,196GW of all offshore wind technologies can be installed 60% of which corresponds to floating DC turbines. Those WTGs have both the benefit of a wide range of installation depth, up to 250m, but also they have access to greater wind resource of farshore water regions, further than 30km offshore, allowed due to the DC output. Factoring in the average capacity factors of the model, electricity generation can reach 35,489TWh. This number, in contrast with the wave energy output, can be considered as the maximum, since every type of offshore WTG is installed in exclusive regions.

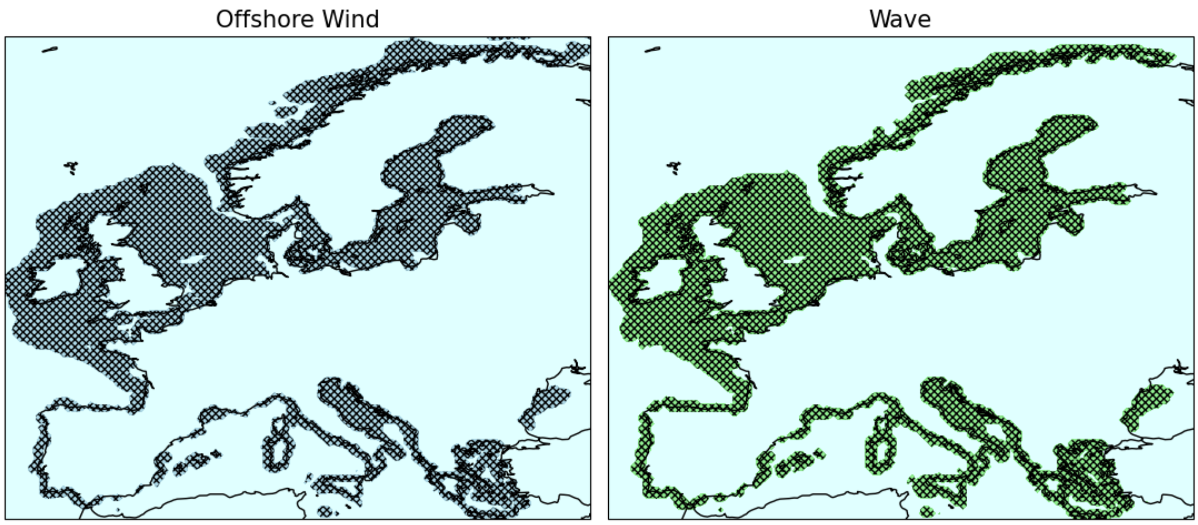

Figure 51: Offshore geographical potential for wind and wave installations. Offshore wind installations from 0 to 250m and maximum distance from shore at 100km, wave installations from 0 to 150m, and no distance from shore limits.

In this thesis the goal was to assess the total potential of marine and offshore technologies deployment. Because of this, and to explain better the lost potential due to the spatial resolution of the ERA5 dataset, no minimum distance from shore limits were set. This can be observed in figure 51, where the hatched offshore regions touch the land contours, leaving no space in between.

What is generally observed for the three scenarios, is that their minimum capacity constraints are surpassed only for the 2030 scenario, while for the other two, they are not. By constraining the model, the climate directive targets are logically met. Nevertheless, when the constraints are switched off, as shown in the 2050 non-BAU model offshore wind and wave energy are reduced by a cumulative 321GW of power, in favour of onshore wind and solar, disregarding energy supply diversity. The remaining 140GW of offshore wind and none of marine energy for 2050, both of which are quite far from the goals.

Since water dams are considered to be storage units in the model, their contribution is categorized as such and is not included in the generating capacities. The 102GW of reservoirs generated almost 340TWh of electricity zero withdrawal, followed by battery dispatch which can deliver up to 246.1TWh from a nominal capacity of 122GW. Generic battery storage on the other hand, with a storing capacity of around 105GW, contributed in total 177TWh into the system for the whole year, while its maximum charging energy capacity reached 601GWh. Nodal power shifting hydrogen technology was almost insignificant compared with all of the rest energy carriers. Regarding the generic hydrogen storage, it managed to save more than 27TWh of excess energy from generators, and gave 153.5TWh back to the system with the help of 170GW of installed fuel cell devices. Lastly, the 54GW of pumped-hydro storage supplied 84TWh.

By investigating the interaction of multiple components within the countries, the behaviour and limitations of the system can be approximated. This investigation aims to provide better understanding of the parameters into the model, giving insight on what needs to be done for it to optimize even more, given the available resources. By analyzing results on the behaviour of the system, a researcher can find reasoning behind the kind of expansion and can identify the areas where this expansion should happen. By extracting the resource profile based on the final nominal capacity of the generators, their intermittency can be estimated, easing the integration of anti-variability measures and ensuring the system's resilience to disruptions and its ability to provide a constant power supply.

5.1 Network configuration

Starting with the network resolution, a network's performance is obviously influenced by the density of its nodes. Increasing the network's number of buses, divides the same amount of space into more segments, thus each part, in this case the Voronoi cell, can more accurately represent the area of influence which it is derived from. Denser networks also facilitate the network from a transmission point of view. More specifically, energy can find alternative routes through neighboring nodes and can compensate for any inability of energy generation by the node in need. Additionally, with more nodes closer to the coastline contours, the connection distances can be estimated with greater detail, giving a good approximation of the percentage of onshore HVAC and underwater HVDC transmission lines.

Going from 37 to 50 nodes in the 2030 non-BAU scenario, rearranged the capacities of generators, boosting the overall capacity but at the same time cutting down the annual costs. Increasing the number of nodes, helped into visualizing the distribution of the generators over Europe. France for example upgraded from 1 national node to 5 smaller ones, clarifying that floating DC WTGs can be installed in the south of France. Also, with a greater proximity to the offshore resources, France gained a large portion of floating AC WTGs, previously ignored by the model.

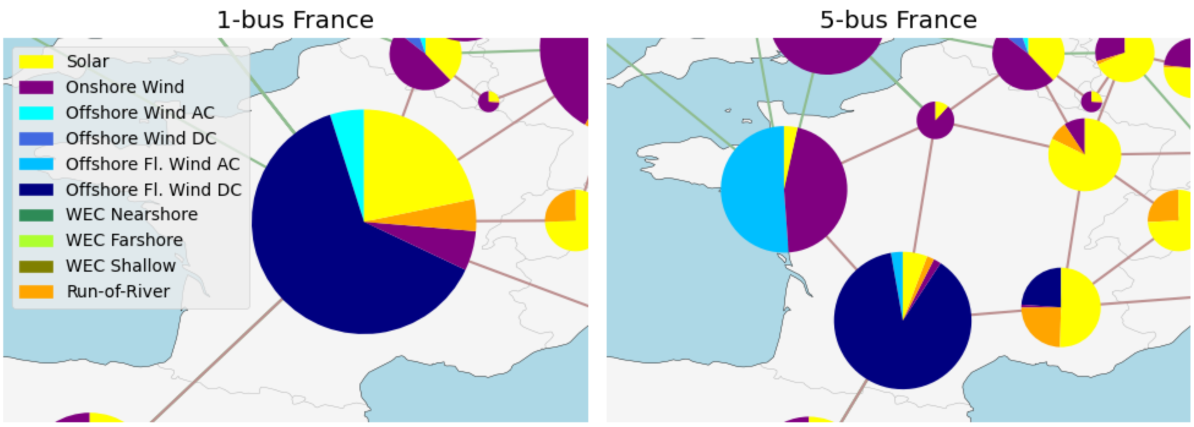

Figure 52: France with different number of buses, 1 for the left figure and 5 for the right figure.

A more accurate representation, will lead to greater estimation of the geographical constraints of the energy system and the transmission expansion. Regarding the last, the denser model, not only provided alternative routes for the energy to travel, but also brought coastal nodes closer together. This way it restricted the HVDC line expansion, a large portion of which is underwater. The overall cost of HVDC lines dropped from 7.52 billion€ to 6.66 billion€.

As mentioned, increasing the bus number requires exponentially larger computing power. Since the availability on that only allowed for a model scaled up to 50-nodes, there is still room for improving the results regarding this matter.

5.2 Validation and alignment with EU

Validating the energy trajectories of Europe to ensure sustainability and feasibility for all regions poses substantial challenges. Countries without proximity to water bodies face obvious limitations in harnessing certain renewable resources. A critical factor which will determine the success of an energy system, is maintaining energy stability across the entire system, particularly for countries situated far from offshore resources, with large terrain anomalies and with an inevitable small diversity into their own power mix. Balancing the synergy between generators, storage systems, and grid expansion is a complicated task, requiring careful consideration of the economic capabilities of each region. So far, the polices crafted to provide energy safety for the full system, emphasize in the integration of diverse energy sources, grid extension in length and capacity, and advancements in storage technologies. While those advancements might not be feasible for all regions at the same time, adaptable and supportive policies that take into consideration economic constraints can serve as a foundation for the goal fulfillment.

The climate directives of Europe were included in the PyPSA model as guides on the installed capacities of the generators for the target years. Since the scenarios in this thesis are all 100% renewable, the scenarios will be discussed in terms of deployment of the marine and offshore renewable technologies. The wave technology appeared in the model only with capacity constraints, when the offshore WTGs were present in all configurations.

What was observed in the results, was that the first target of 2030 was by far exceeded. The goal was to install 60 plus 50GW of offshore wind for Europe and UK. PyPSA however installed a total of 187GW of offshore wind turbines, 142GW of which were floating. The availability on the uninterrupted wind resources of deep waters meant that BAU minimum capacities were exceeded. In the context of this exact model, this validates the existence of the European wind turbine targets. Progressing towards the 2050 targets however, this changes as the installation reached only the lower boundaries of the constraints, hinting that the model probably harnessed all of its optimal existing potential, and now it is redirecting the remaining capacity wherever it damages the objective function the least. Performing a non-BAU 2050 scenario provides a better understanding on the extend of this damage. Wave energy capacity again dropped to 0GW, and wind energy was decreased from 405GW to only 146GW. One more time, the cost-optimization model prefers the less expensive solutions of relying on onshore solar and wind energy, with smaller transmission line expansion, 112GW of more storage capacity for all storage units, and 9,786GWh additional storing energy capacity.

Based on the above, and in the context of the models configuration and limitations, the European directives seems to overestimate the installable potential of offshore generators around Europe.

5.3 System behaviour

In this section, firstly, a general yearly behaviour of the components of all scenarios will be provided. Secondly, these operational data will be aggregated into a weekly average generational graph, in order to obtain the average behaviour of the system. Additionally, the performance of anti-variability measure is also presented. By analyzing the real-time balance of energy for specific regions in the model for the first three weeks of January and July, a general idea of the power supply can be formed.

5.3.1 Generators

The three scenarios have large differences in most of the generator capacities. Since the weather data input and load is the same for all of them, their behaviour can be compared with the installed capacity as a point of reference. Figure 53 presents 3-hourly aggregated data of the performance of each generator throughout the entire year. It is lowered in resolution to facilitate viewing of the data.

There are certain patterns that can be observed here and they seem to be related. Starting from January, with the progress of time, more daylight is available during the day. Solar energy is expected to depict a greater generation during summertime. What comes with this is the drop of power for all of the rest generators. They appear to have lower output during summertime. Farshore and shallow water WECs are affected the most by this, since they have multiple weeks without a significant operation output during summer.

Wind energy on the other hand seems to have a more consistent output profile. With the brown line as a reference (2050 scenario), the abundance of peaks by the offshore WTGs indicate that they reached the maximum output (88.55% of the nominal capacity, due to correction factor employed by PyPSA by default) multiple times throughout the year. Their average daily operation reached 180GW. While

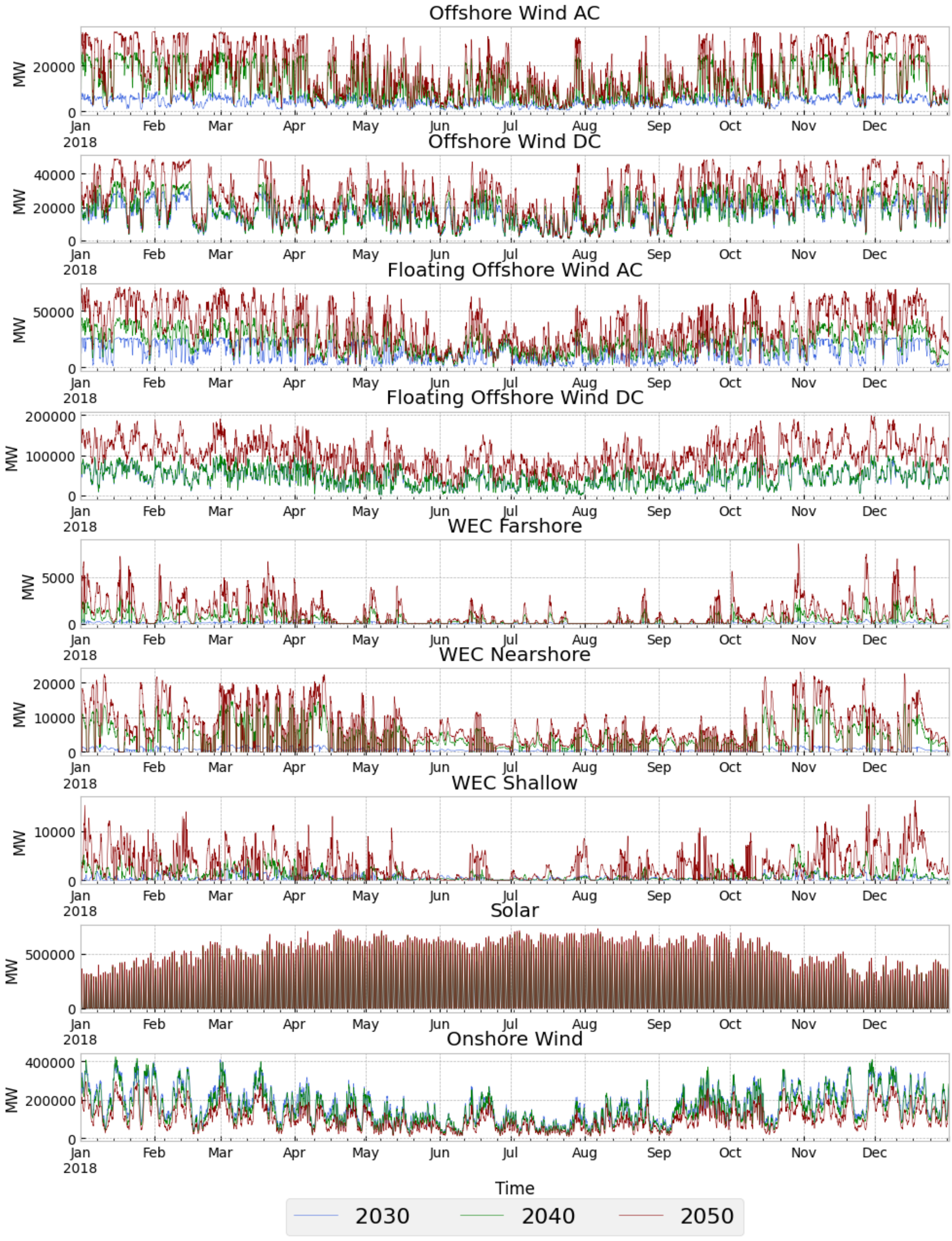

Figure 53: Generation time-series for each generator across a full year for all three scenarios.

the average daily operation of all WECs together was around 10GW, this dropped to only 6GW during summer time, while the farshore device was under 400MW.

Since wind is generated from solar energy, this patter follows the rules of nature. Winter time in general, creates a larger difference in the temperature gradients, something that generates more and faster winds, and since waves are generated by the winds, the same pattern is observed there too.

By stacking all of the generation time-series together and projecting them with the storage charging and discharging and the load time-series, the following figure presents the full year balance of all components in the energy system. The next set of plots refer to the 2050 scenario.

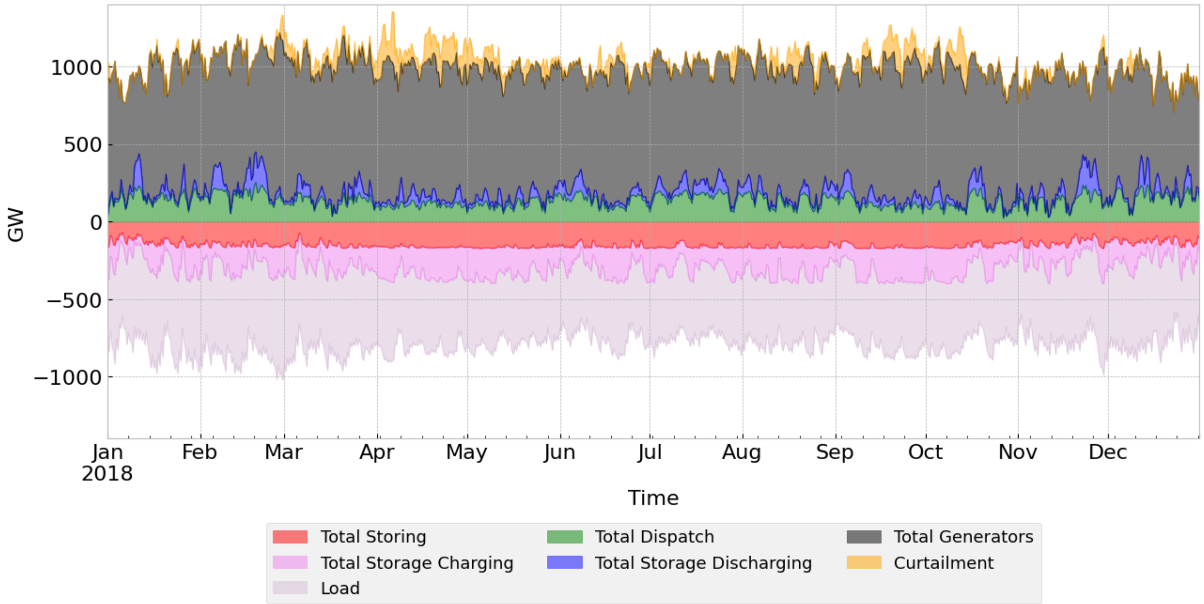

Figure 54: Full year system behaviour, 12-hour aggregation of data.

What is observed is that at all times, the sum of input of energy (positive values, excluding curtailment) is greater than the sum of output of energy (negative values). This is a sign of resilience of the model, which indicates that there is adequate energy at all times. Additionally, even though summer time provides less resources to the generators, electricity demand also drops, mitigating this problem. The weekly electricity load profile in general shows maximum demand during weekdays and drops during weekends. This is logical as weekdays are also workdays, industrial and commercial activities are typically increased. On a daily basis, what is observed is the drop of demand as the sun sets, something also related with industry, as the activity again drops in the evening.

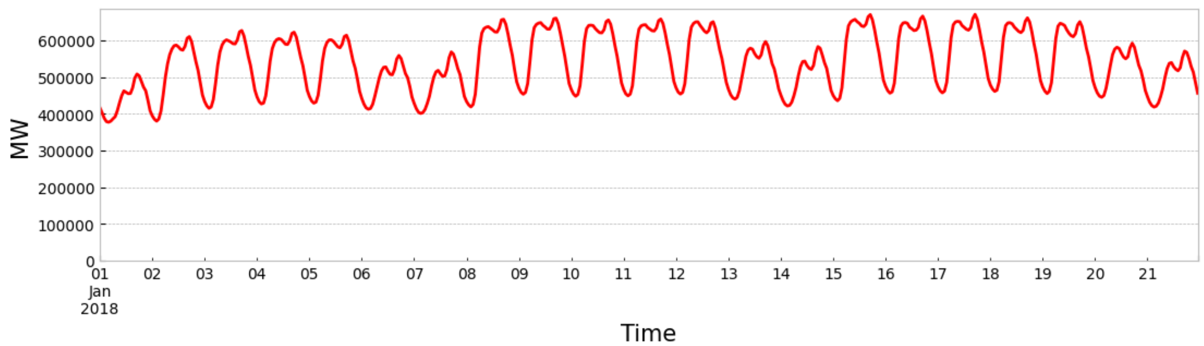

Figure 55: First 3 weeks of load time-series. Load is presented as positive in this figure.

The maximum recorded output of the generators occurred on the 28th of February, measuring 1019GW of all generators operating. At the same date the highest load was recorded as well, with a demand of 714GW of power. The inter-temporal dispatch of storage systems reached 254GW on the 19th of February, while their maximum charging day was 5th of May with 175GW. The difference in the dispatch/charging capacity time-series profiles derives from two reasons. Firstly, reservoir dam charging does not require input of energy from the system itself, thus it does not exist as a charging (negative) input. Secondly, charging duration is longer than discharging duration. In all of the tests done in this project, the nominal capacity of battery and hydrogen systems is greater for the discharging unit than the charging unit. This means that the higher output can be achieved due to the fact that the charging units operate for longer periods, increasing their state of charge. When the resource is created, it can be feed back to the system in greater capacity but for significantly shorter periods.

By observing figure 54, one can witness that the 'Total Storage Charging' and 'Total Storing' areas (pink and red colors) maintain a more rectangular shape compared with the dispatch ones, which show multiple peaks (blue and green colors). Lastly, the generic storage units were dispatching at a maximum of 259GW in the 19th of March, and storing at 201GW for the 21st of October. More information on the storage systems is given in section 5.3.2.

In order to have a clearer view on the behaviour of each generator, their time-series were sampled based on their mean value of every 168 snapshots, or exactly one week in the model, to generate a mean generation output profile. Firstly, the cumulative average generation is presented and secondly each generator individually.

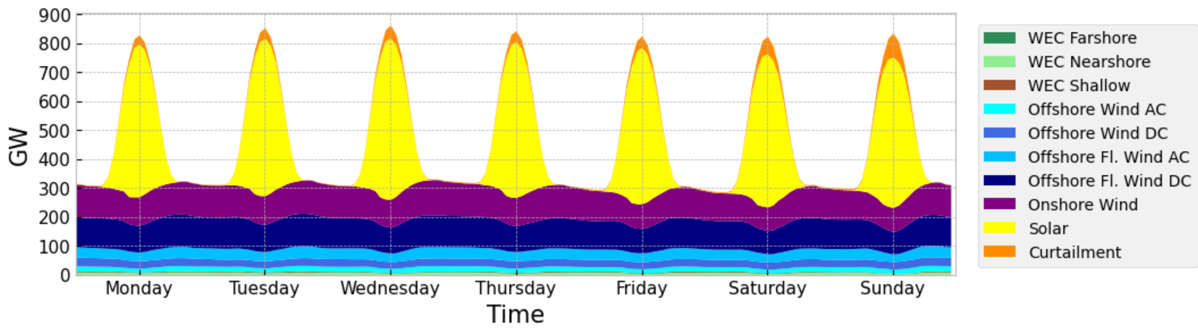

Figure 56: Mean generation of all generators for a representative week in the energy system.

	Mean supply rate [GWh/h]
Offshore Wind AC	16.9
Offshore Wind DC	26.1
Fl. Offshore Wind AC	35.6
Fl. Offshore Wind DC	101.0
Onshore Wind	104.5
Solar	163.8
WEC Farshore	1.1
WEC Nearshore	6.7
WEC Shallow	2.8

Table 39: Mean supply rate for generators.

The reader must be aware that this profile refers to the energy system as a whole, and does not apply into every region both in terms of generator diversity but in generator capacity as well. There are countries in Europe, most of them in the southern part, which from a generator point of view rely almost exclusively on solar energy. To understand the needs of each region, the researcher needs to clarify the characteristics of that specific region.

From the cumulative profile, it is clear that during the daylight, when the solar energy is at its maximum, wind and wave power drops to some extent. This drop is a phenomenon present in all types of generators, as figure 57 is showing. On average, of the total 773GW of nominal power wind generators, around 300GW operate in a regular basis, about 39%. For wave energy this is equal to around 9GW of the 62GW, or around 14%.

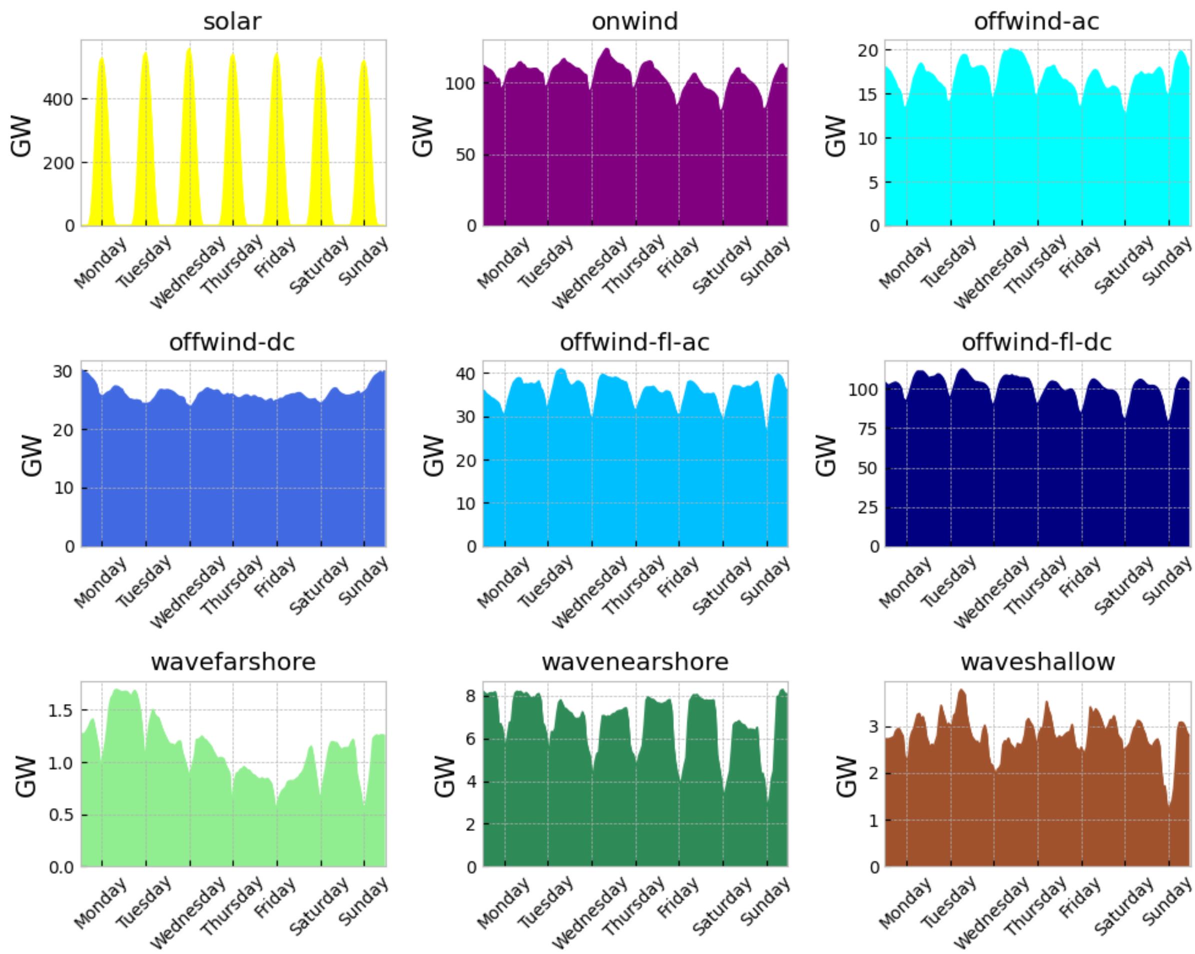

Figure 57: Mean production of each generator individually for a representative week.

A noteworthy conclusion drawn from this figure is that, despite onshore WTGs having 138GW more capacity than floating DC WTGs, their mean output is nearly identical. This suggests that the offshore resource is performing well. The irregularity on wave energy is due to the fact that their well performing days are quite scarce, resulting in an uneven sample.

The next image presents the theoretical maximum output of the system, by aggregating every maximum recorded production per generator for every 168 snapshots, or a week. The result seems quite optimistic, suggesting that for perfect conditions, with minimum curtailment and a simultaneous maximum operation of all generators, those can reach up to 1600GW of power during the day and 770GW of power during the night. This is equal to 80% and 39% of the total installed capacity for day and night periods. It is worth mentioning that their corresponding average outputs are 810GW (40%) and 280GW (14%).

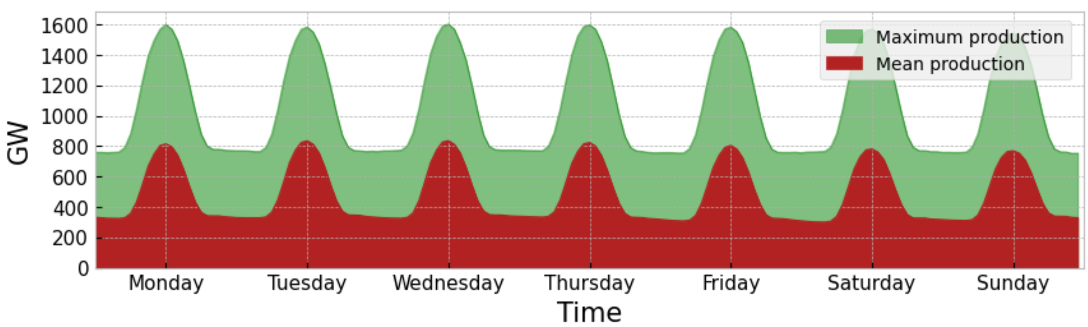

Figure 58: Maximum and mean aggregated production of the generators in the system for a representative week.

Next, the yearly production profile of each wind generator type on a single plot is presented. Each generator is presented individually, so the plot does not have a stacked area style.

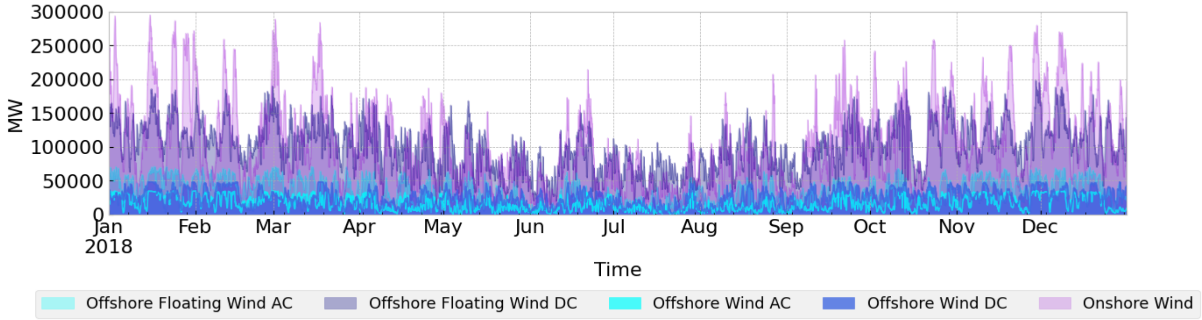

Figure 59: Wind annual operation by each type for 2050.

The deficiency of wind resource from April to August is present for all wind energy types. Production ramps-up again by the end of August.

WECs on the other hand manage to maintain the same levels of operation during April too, and only after do they show lack of resource.

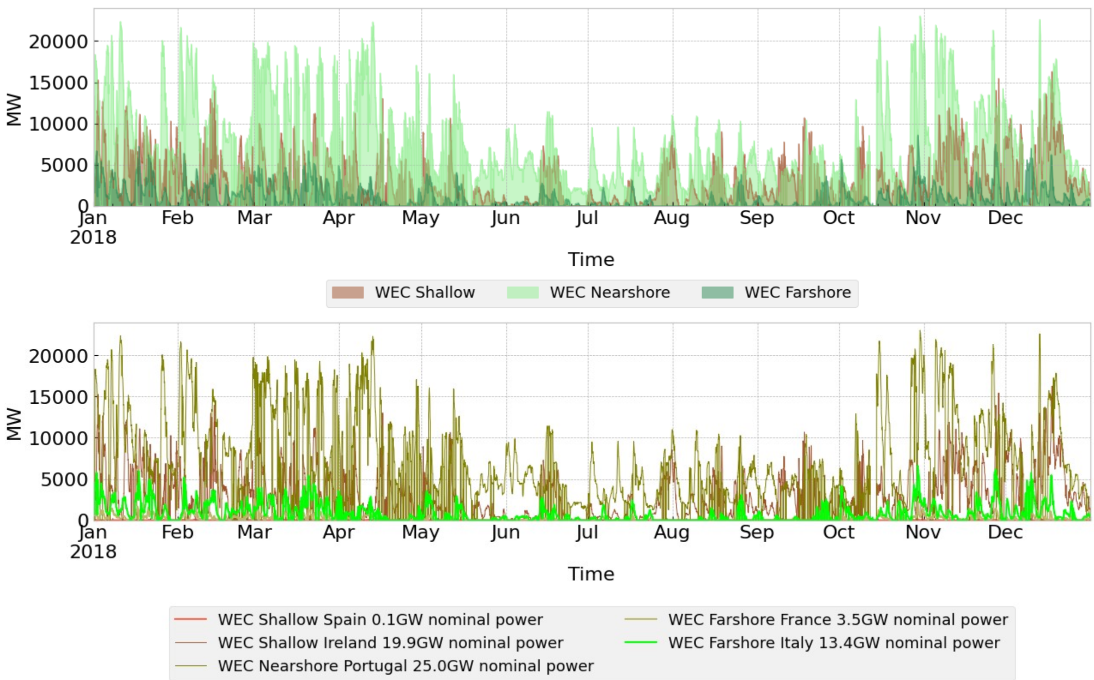

Figure 60: Yearly generation of WECs (top), per installed WEC (bottom).

Since WECs in the system are installed in only 5 regions, a separate plot can show how each region is performing. The performance is influenced by the installed capacity and the related capacity factor. Thus, WECs in Portugal and Ireland, which are in nearshore and shallow waters respectively, stand out from the other three locations, followed by the Italian farshore devices, which however have a low capacity factor.

The following table provides a summary of the most productive day of each generation type according to the 2018 weather data.

	Capacity [GW]	Date
Offshore Wind AC	35.3	28-11-2018
Offshore Wind DC	48.7	30-11-2018
Fl. Offshore Wind AC	71.0	17-11-2018
Fl. Offshore Wind DC	198.5	30-11-2018
Onshore Wind	295.3	15-01-2018
Solar	732.4	06-08-2018
WEC Farshore	8.6	29-10-2018
WEC Nearshore	23.0	29-10-2018
WEC Shallow	16.3	17-12-2018

Table 40: Maximum production recorded.

With solar energy as an exception, all of the maximums where achieved by the end of October until January.

5.3.2 Storage Systems

Coming back to the anti-variability measures of the energy system, this section focuses on their behaviour and overall performance. A first glance of their contribution was given in the previous section, however in this section the storage types are analyzed individually.

Similarly with the generators, a weekly mean operational profile is provided. Staring with the inter-temporal storage units, figure 61 shows charging and discharging of the units typically happens on specific hours during the day.

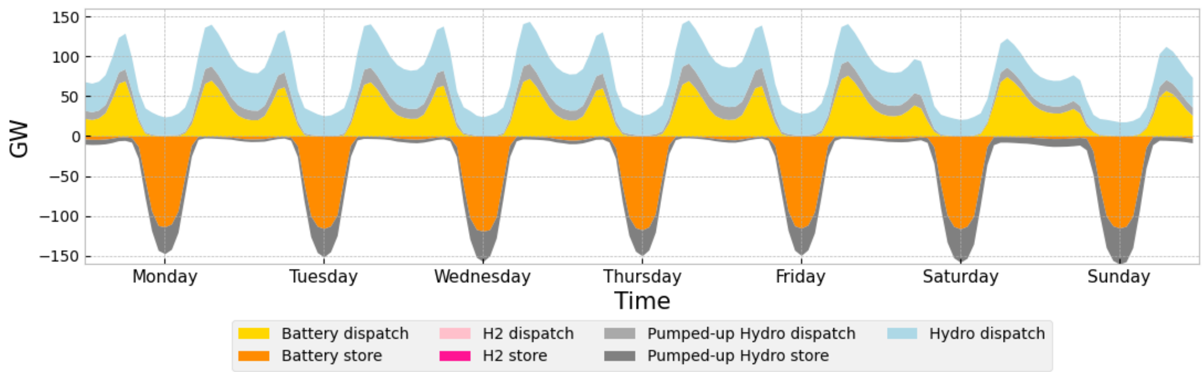

Figure 61: Mean operation of the storage units for a representative week in the energy system.

	Mean supply rate [GWh/h]	Mean withdrawal rate [GWh/h]
Battery	28.0	29.1
H2	5.6	13.4
PHS	9.7	12.9
Hydro	38.8	-

Table 41: Mean supply and mean withdrawal rate for inter-temporal storage units.

Since generators are the ones which provide the energy for the storage units to operate, an opposite-looking profile is observed here. High generator output during the day, which has the benefit of solar energy is covering both the load and the charging of the storage systems, with the exception of hydro energy. During daylight, hydro energy source is the only one delivering power into the system. When the sun starts to go down, the generators have reduced production, so the electricity demand is covered by the storage units, until the sun is completely gone. Since load drops during nighttime, the contribution of the storage systems is no longer as big, and at the same time there is some excess of power from the generators, which they appear to help the storage units recover a small amount of additional energy.

When human activities start to increase, storage units start again to provide energy to the system, until solar energy is operating once again in a desired capacity.

Next, the behaviour of each inter-temporal storage unit is shown. On the top subfigure, the state of charge of each unit type is shown and on the bottom one the dispatch and storing of energy.

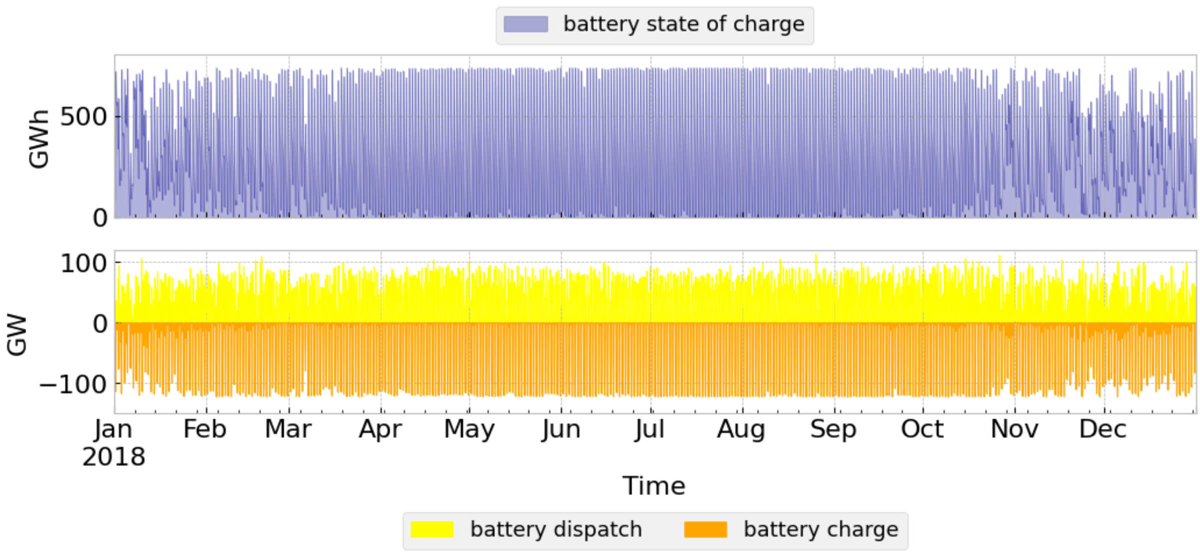

Figure 62: Battery time-series across the full year.

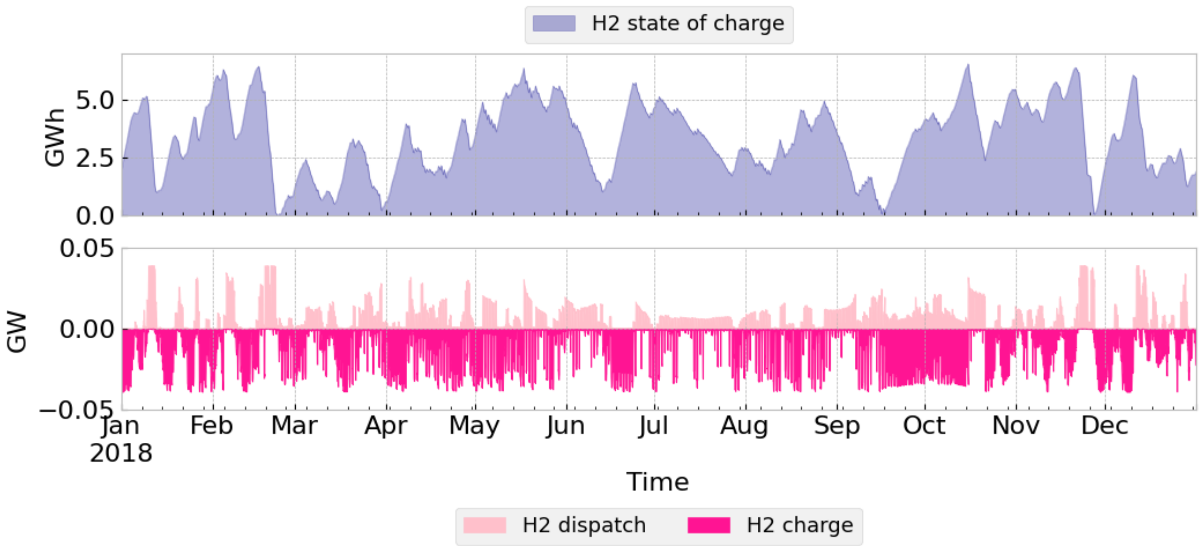

Figure 63: H2 time-series across the full year.

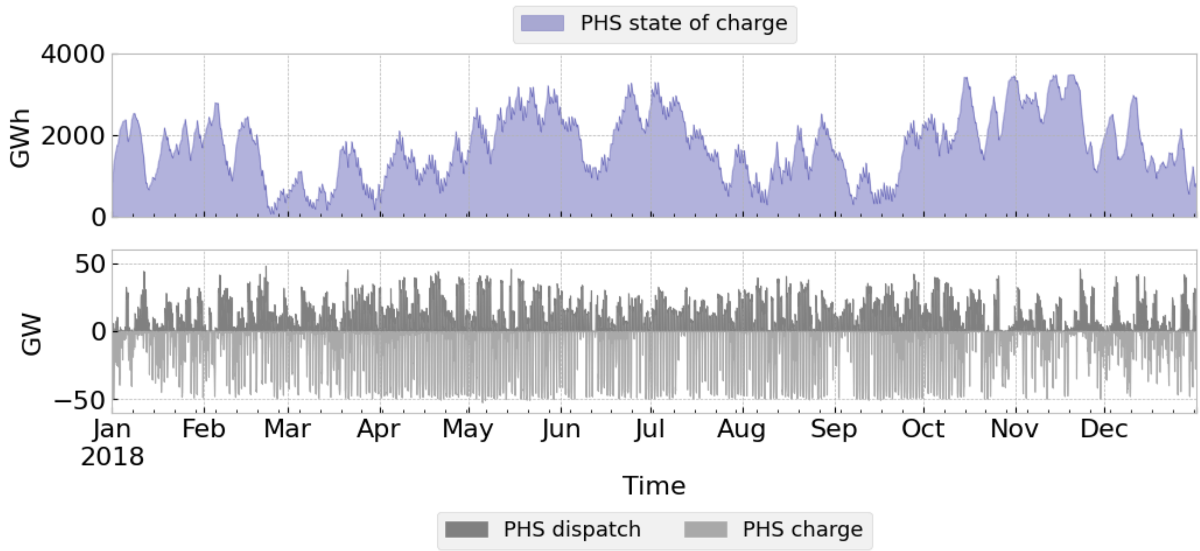

Figure 64: Pumped-up Hydro storage time-series across the full year.

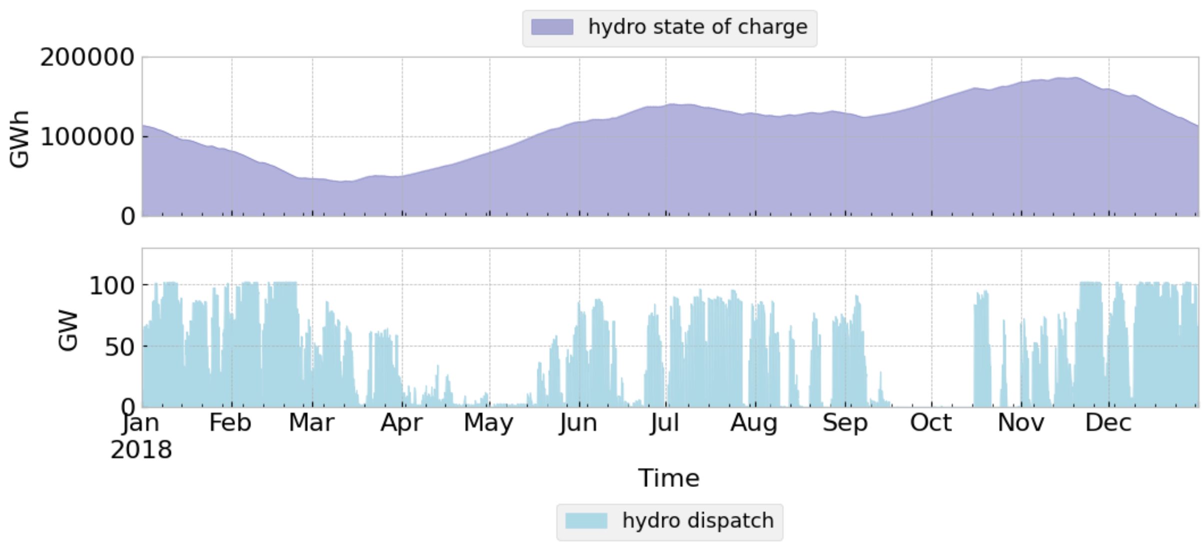

Figure 65: Hydro dam time-series across the full year.

The figures suggest that the amount of charging time is greater than the amount of dispatch time. Battery has the most constant fluctuations during the year, following the supply of solar power into the system. Hydrogen and pumped-up hydro storage have more irregularities in their power delivery but they both a noticeable drop of operation during winter time. Hydro power, operates in a maximum power mostly from the end of fall time until winter, while in spring its contribution drops significantly, probably due to factors related with precipitation levels. With the exception of batteries, the state of charge of the units is mostly above zero, indicating that the periods where the storage unit reserve is entirely drained very occasional.

Next, the behaviour of the rest of the storage systems is presented, namely generic battery and H2 storage.

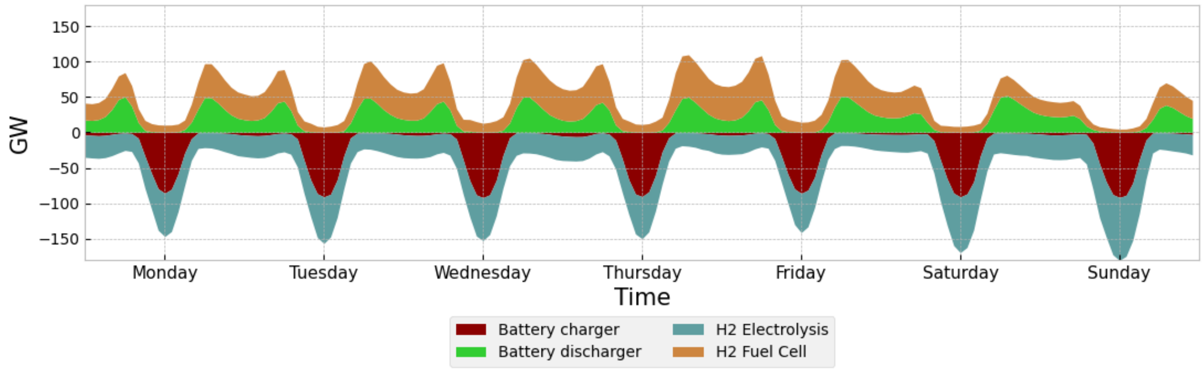

Figure 66: Mean operation of the generic storage units for a representative week in the energy system.

	Mean supply rate [GWh/h]	Mean withdrawal rate [GWh/h]
Battery	20.3	21.1
H2	17.5	37.8

Table 42: Mean supply and mean withdrawal rate for generic storage units.

The patters of charging and discharging are almost identical, which is logical since the system takes advantage of the excess of solar power here as well.

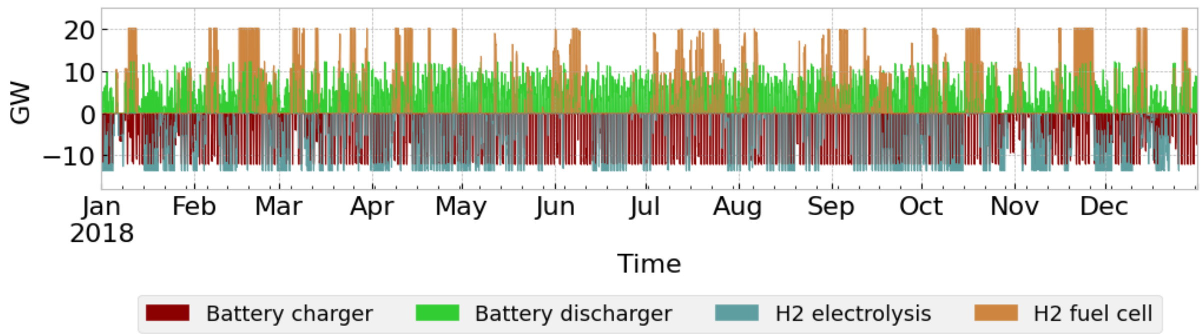

Figure 67: Generic storage system time-series across the full year.

Again, one can observe that the dispatch of energy is more irregular and shorter in duration than the charging of the units.

Lastly, an 'average day' profile of the system is provided for an even more general overview of the system.

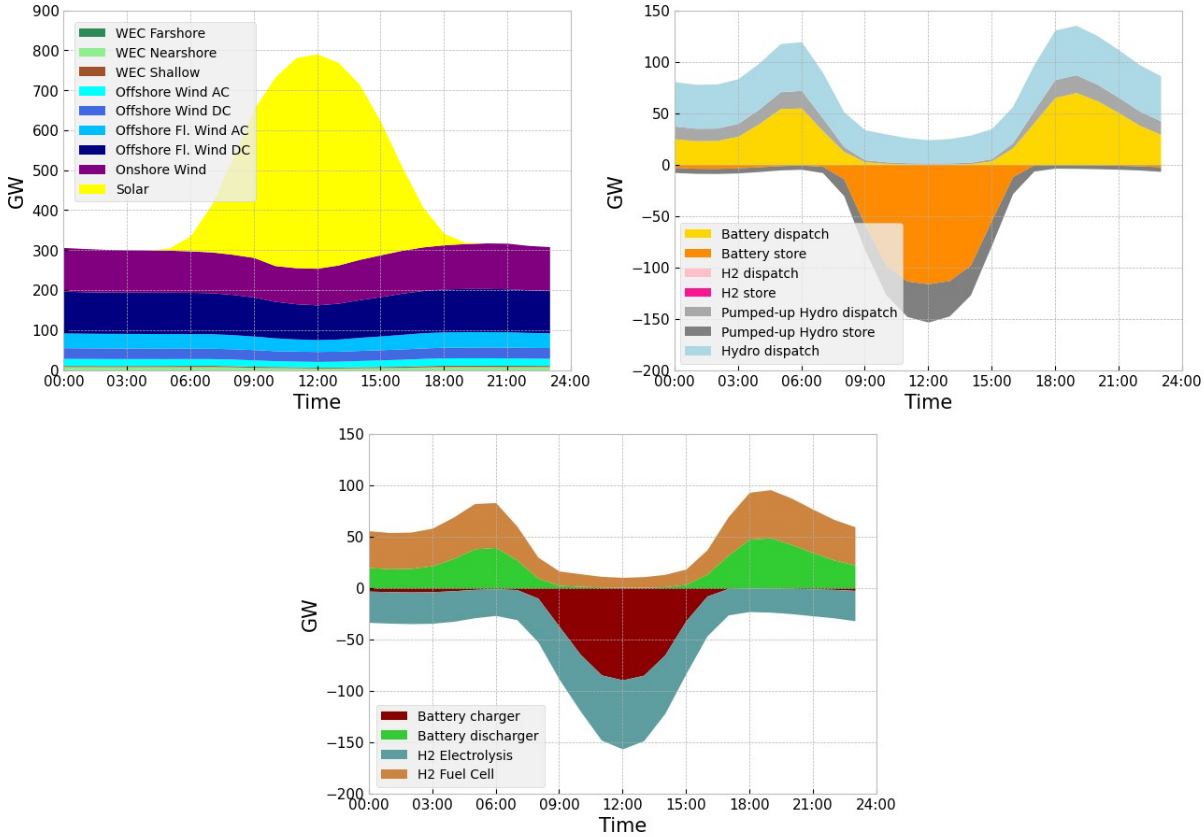

Figure 68: Mean aggregated production of the components in the system for a representative day.

The average solar activity starts at around 05:30 in the morning and stops at 18:30. In between this time-margin is when battery and pumped-up hydro charge, while the rest of the time are discharging.

5.4 Regional behaviour of the system and geographic constraints

In this section, the focus shifts into country specific component configurations. For each region there are two figures representing the first three weeks of January and July, for a reference between winter and summer behaviour. Starting with Italy which has large loads and small energy mix diversity.

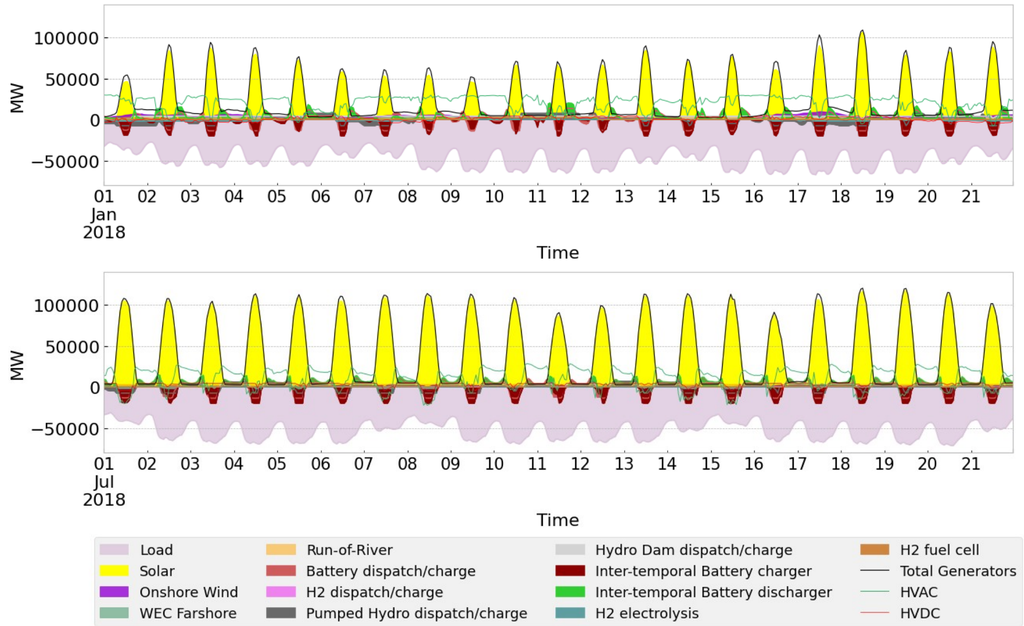

Figure 69: Italy power balance between 2018-01-01/2018-01-21 (top) and 2018-07-01/2018-07-21 (bottom).

It can be observed that both in winter and summer, solar energy plays a crucial role on meeting the energy demand. While solar energy is in a high output, a small amount of it recharges the battery systems, and when the sun sets, Italy is using some of its battery stored energy. The rest is imported through the HVDC lines. The 13.4GW of farshore WECs in Italy operated in a maximum of around 5GW. A country with greater diversity is France which incorporates 7 of the 10 generator types including AC and DC floating WTGs and farshore WECs.

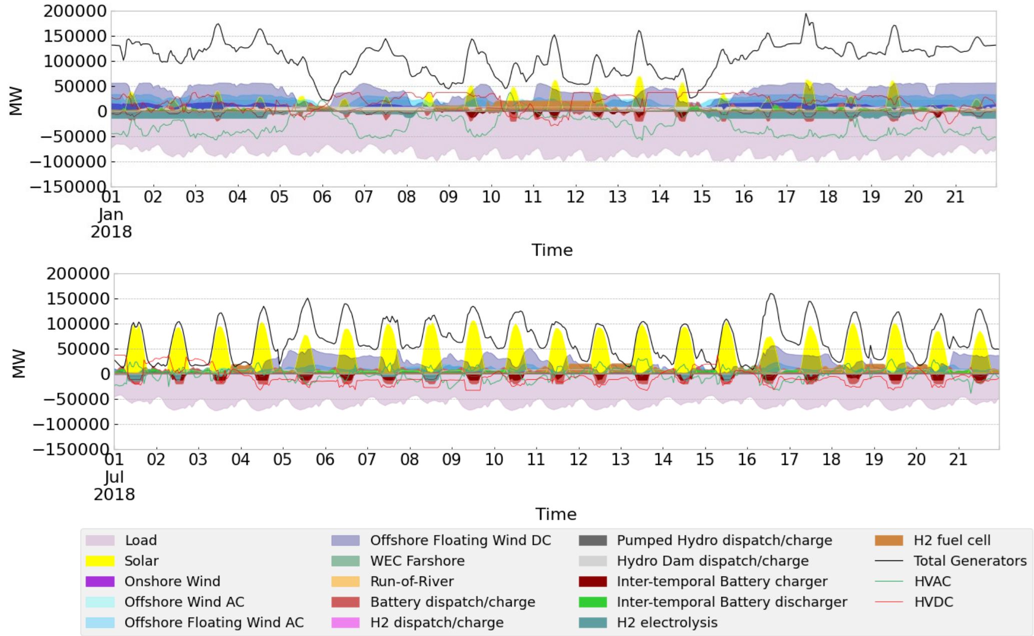

Figure 70: France power balance between 2018-01-01/2018-01-21 (top) and 2018-07-01/2018-07-21 (bottom).

During winter, solar activity is significantly less than during summer. The offshore wind and marine devices seems promising as they operate on more than 100GW during night time and the total energy produced exceed the demand for most of the times. In times of need, France imports energy from neighbouring countries, via its 18 line connections. When including those into the power balance, the net exchange of energy results into 51.5TWh of imported energy, the sum of 52.4TWh of export and 103.9TWh of import. The annual energy load was 551.2TWh. In the 2050 model, France has a total capacity of 310.8GW of renewables, more double than 2022 capacity according to IRENA [84], which also produced 95MT of CO_2 from the electricity, heating and industrial sector.

Next we investigate the behaviour of the components for a country without any access on offshore resources, Hungary.

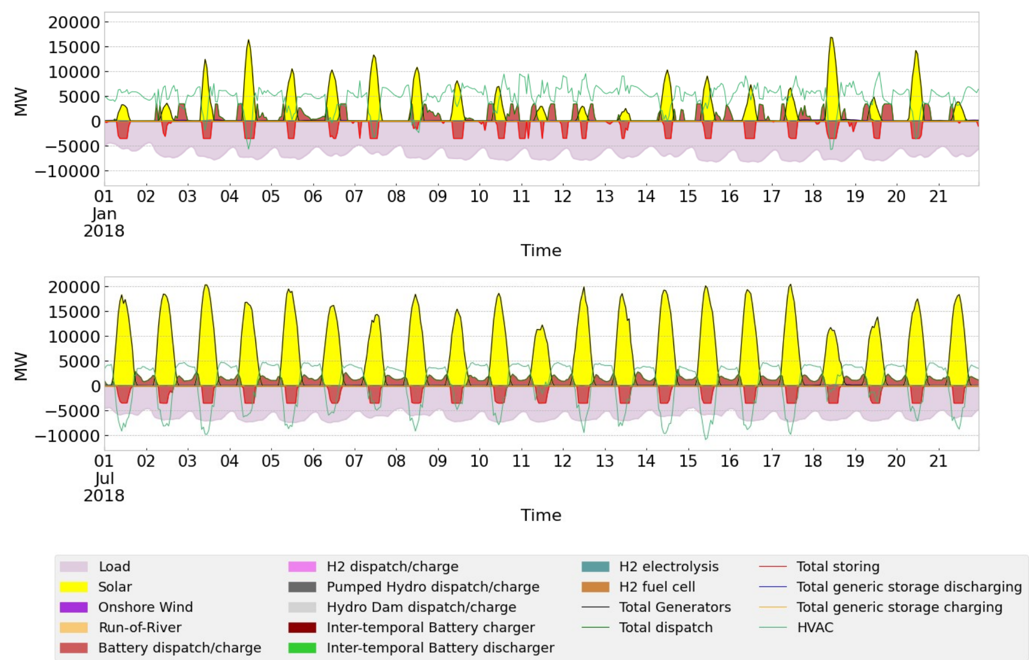

Figure 71: Hungary power balance between 2018-01-01/2018-01-21 (top) and 2018-07-01/2018-07-21 (bottom).

The lack of offshore renewables is immediately recognizable as Hungary imports a lot of energy during the winter time-frame, especially when solar power is not operating. This makes Hungary highly dependable to the energy abundance of the neighbouring countries. In total, the country's import are as high as 28.7TWh, or 56% of the total energy demand, while the exports are only 3.8Twh. However a lot of the neighbouring countries of Hungary, with a very high share of solar power, also do not have access in water bodies, complicating the task of power distribution even more. Summer period also shows a similar problem, with import of electricity on a daily basis during the nighttime, and significant amount of export during the daylight. Generic battery storage appears to be Hungary's second main resource.

Looking into Ireland will give a reasonable perspective on how the shallow WECs perform.

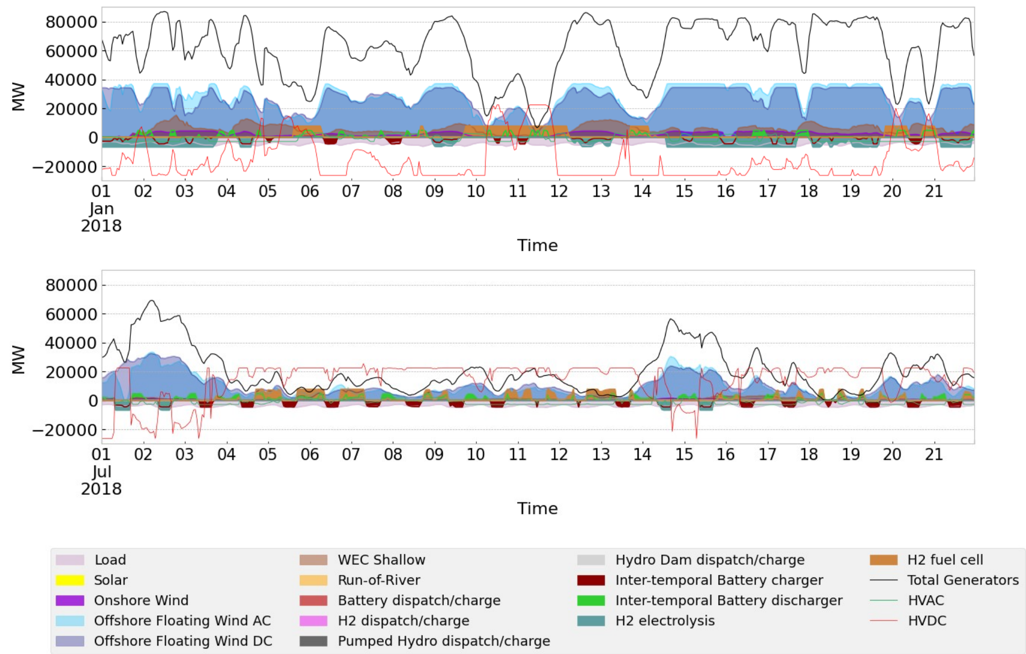

Figure 72: Ireland power balance between 2018-01-01/2018-01-21 (top) and 2018-07-01/2018-07-21 (bottom).

From the graphs above we observe that apart from the two floating WTG types, the wave converter has an impressive contribution on the mix during winter time, reaching at peak 15GW of the 20GW installed. Both AC and DC floating WTGs operate regularly at their maximum capacities, indicated by the flat line reaching around 40GW and 36GW of capacity accordingly. The total energy generated, allows Ireland to export a large amount of electricity during winter through HVDC lines, most of which is imported by Great Britain. In summer however, wave converters are non operational for the most part. We can see that for the first three weeks of July, WECs recorded almost 0 operational time and Ireland ends up importing a significant amount of energy, reaching the maximum capacity of transmission lines frequently. Observing the period between the 4^{th} and $14^t h$ of July however, comparing the net result of input in the bus of Ireland (between approximately 25GW-45GW) with the consumption of load, battery and H_2 electrolysis on this bus (≈10GW), a possible conclusion is that Ireland serves also as an in-between node of energy transfer between France and Great Britain.

Next we investigate Great Britain.

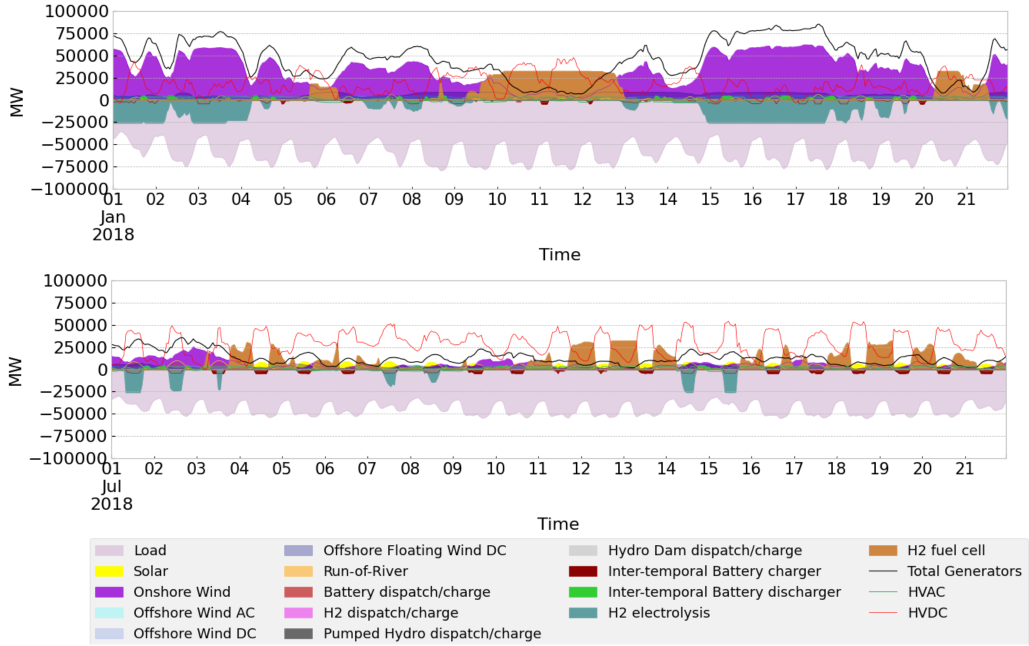

Figure 73: Great Britain power balance between 2018-01-01/2018-01-21 (top) and 2018-07-01/2018-07-21 (bottom).

Great Britain relies heavily on onshore wind generation, while at the same time is covering part of its energy with H_2, with electrolyzers and fuel cells, and through import. GB is a major importer in Europe requiring an additional 178.4TWh of electricity distributed almost evenly throughout the year. The exports are only 5.1TWh. The large capacity of onshore wind appears to be insufficient during summer, where hydrogen units need to operate on an almost daily basis. GB can store up to 4668GWh of energy via H_2.

Next, regarding Portugal, which is the was the country with all of the installed nearshore WECs, showed a promising behaviour of its energy mix. Their share is 80% of the total energy mix.

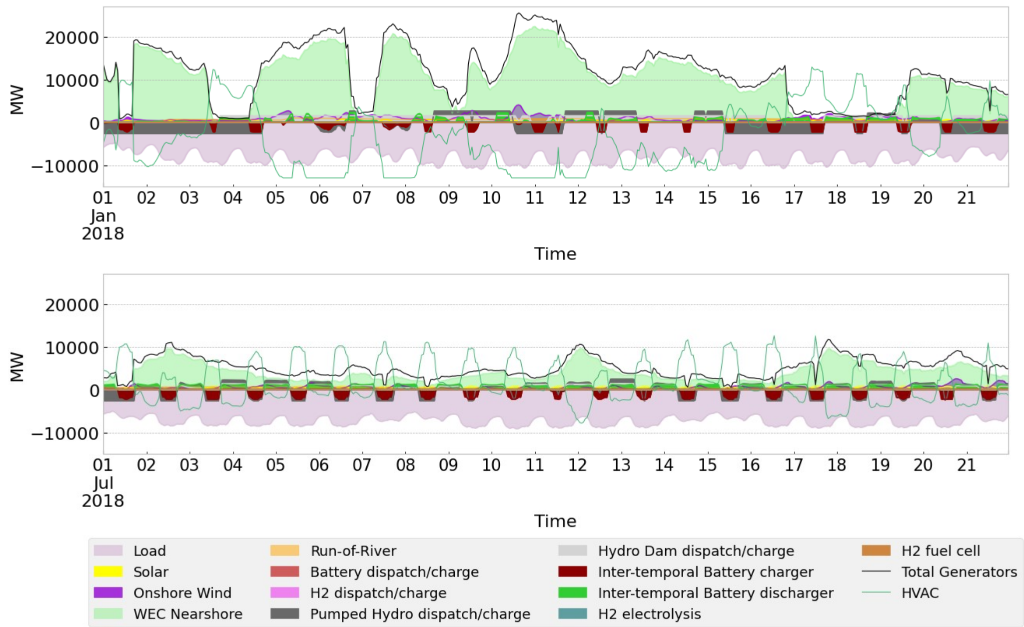

Figure 74: Portugal power balance between 2018-01-01/2018-01-21 (top) and 2018-07-01/2018-07-21 (bottom).

In general, Portugal exported 9TWh more than what it imported for a total of 31.4TWh. Wave converters generate enough electricity for the most part of winter, while on summer their contribution drops by a lot. Portugal retrieves on importing energy from Spain on a daily basis, some of which is used for battery and pumped-up hydro storage during the daylight. Those are being dispatched when the sun goes down. Wave energy still has some high output days in summer, enabling Portugal of exporting energy to Spain.

Lastly, we focus on a country with a high share of floating turbines, Poland, more than 82%.

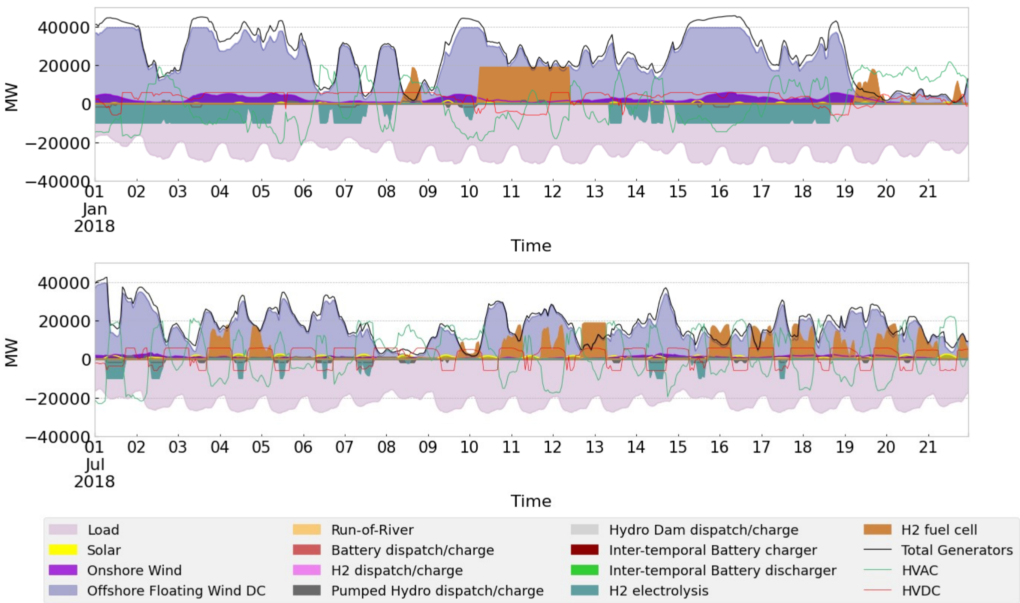

Figure 75: Poland power balance between 2018-01-01/2018-01-21 (top) and 2018-07-01/2018-07-21 (bottom).

We observe that the generation of floating DC WTGs is more reliable during January both in terms of power capacity and power duration. With onshore wind complimenting the production whenever possible, and a limited contribution of solar energy during the summer, Poland's annual import was 45.0TWh while the export is 62.8TWh, something consolidates the feasibility of high-share offshore wind energy in the mix.

All time-series indicate a decline in both demand and generation, with solar power being the exception, as it remains relatively more reliable during the summer. The model's installation preferences reveal a clear division in Europe. The southern part heavily relies on solar energy, while the northern part integrates various technologies, taking advantage of the shallow waters of the North Sea and the Baltic Sea. Wind resources are predominant in the north, complemented by the installation of shallow water wave converters. However, there are exceptions to this trend, such as Greece and Romania, where there is a notable presence of DC floating wind turbines in the Aegean and the Black Sea. Nearshore and farshore WECs are prominent in southern Portugal, southern France, and Sardinia.

Considering the economic incentives in each region allows for an better interpretation of the behavioural analysis. Nations with substantial industrial activity, high GDP, and large populations are also the ones to exhibit a diverse energy mix. These countries can likely tackle the complexities of the energy system and transition their energy mix optimally. In contrast, nations with limited economic growth in terms of GDP or population may find it are mostly required to invest into the less expensive alternative of high share of solar energy accompanied by an significantly expanded grid and storage units.

5.5 Economic analysis of a renewable energy system

From the findings on the financial expenditure for this project, it is apparent that the 230GW of floating DC WTGs require 48% more capital compared to the 1105GW of solar energy, amounting to approximately 44.7 billion €. Note that this capital includes the fabrication costs of the turbines, underwater cables and connections to the main grid, and substation costs, while it does not include initial installation costs, foundation and decommissioning expenditures. This CAPEX aligns with expectations given their distinct mean capital cost of expansion. Offshore WTGs, both farshore DC and nearshore

AC turbines, exhibit a mean capital cost of expansion of less than 200,000 €/MW and 180,000 €/MW, respectively. In contrast, solar installations have a mean cost below 35,000 €/MW. Despite this, the mean hourly revenue generated by floating DC wind generators is 4 million €, significantly surpassing the 3.0 million € from solar sources. Consequently, this establishes a market value of 40/ €h, which is 10 € higher than that of solar energy. Ultimately, the marginal cost of generation for offshore WTGs is only 0.005 €/MWh more than that of onshore turbines.

Wave energy presents a higher capital cost for the model in terms of expansion expenses. Those exceed 330,000 €/MW for all WECs, resulting in a marginal cost of energy around 0.09 €/MWh. The cumulative capital investment amounts to 14.4 billion €, despite their lower installed capacity. Worth noting is that this investment contributes to an annual output of 92.4TWh, with operational costs below 600 €/MW/a or 21.6 million €/a. This results in a promising mean market value, the highest observed in the model, capable of reaching up to 59/ €h for the farshore device. The other two devices are closer to 40/ €h, roughly matching offshore wind turbines. These indicators suggest that when wave converters operate, they have a financial benefit. Their disadvantages lie on their operational time during the year, which is lower than the rest of the technologies.

The marginal costs mentioned above are the the main factors which shape the final locational marginal price (LMP). LMP is an index of the average cost of energy in relation to each region's mix of generators, transmission expansion and storage unit dispatch.

Comparing the 2030 and 2050 scenarios in figure 76, we can safely assume that the additional offshore and wave devices increase the overall cost of energy in the network.

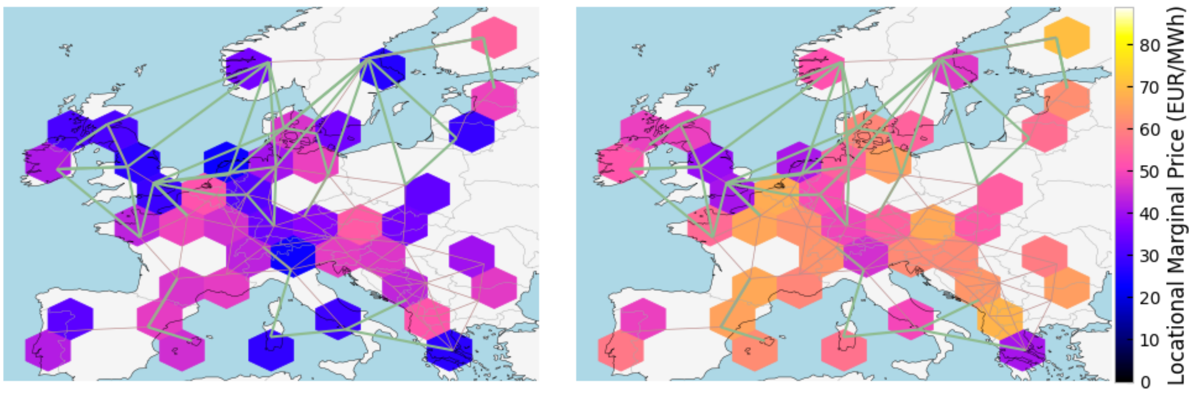

Figure 76: Locational marginal prices for 2030 and 2050 scenarios.

As the model undergoes the deployment of more offshore renewables, by integrating a diverse energy system, the marginal prices of electricity in each bus is also experiencing fluctuations. The expansion of offshore renewables, transmission grid and anti-variability measures, is a large investment project that has an immediate effect on the end user of the energy. Note that according to IEA (International Energy Agency) the marginal prices for Europe in 2018 were in the range of 40-65 €/MWh [85]. The 2050 scenario marginal pricing of electricity does not fall very far from those records, but it still increases the range to 40-75 €/MWh.

The scenarios of this project included energy equity constraints that were set to 70%. This means that every country must be able to produce on average at least 70% of its consumption. There is possibility that by lowering this constraint and allowing more frequent trade of energy between the nodes, will enable greater expansion of the transmission system, which was 98% for the 2050 scenario. However, since the models were not free on choosing the installation capacities per technology, we witness that some regions have a significant disadvantage of energy cost compared to other.

Capacity factors and energy mix play a pivotal role on the shaping of the marginal price. Greece and Romania will be compared in respect to those. Romania has a share of 84% floating DC WTGs with an average capacity factor of 0.34, while the rest of the demand is covered by solar, r-o-r and onshore wind capacity. Greece uses the same types of generators (15MW DC floating WTG), which are only 16% with a capacity factor of 0.27, while solar is almost 76% and has a better efficiency throughout the year. The combination of those two factors cause the marginal price of Greece to be 20 € less than the one for Romania, since solar energy has a more predictable periodic generation of power and feeds the storage units more systematically. Coupling this source with battery back-up allows Greece to decrease the regional cost of energy.

Comparing countries with installed WECs, Ireland and Portugal are the best candidates, since they have 19% and 73% of wave converters in their mix respectively. The corresponding capacity factors are 0.19 for Ireland and 0.33 for Portugal. Ireland however exhibits a more diverse mix, including onshore wind with CF=0.34, floating offshore AC WTGs with CF=0.51, and DC ones with CF=0.54. At the same time Ireland has the benefit of two connections to Great Britain, which has 62GW of onshore wind operating in an average CF equal to 0.37 and one to North France, which has a variety of generation types available. Portugal only has one alternative of import and that is Spain. As a result, Ireland manages to obtain a marginal price of around 15 € less than Portugal.

In figure 77 we observe that the sum of all wave energy generators in the system curtail a very large portion of energy compared to offshore wind turbines. This damages the economic performance of wave generators, since curtailment translates into lost revenue opportunity. Note that in Portugal, the curtailment of the nearshore WEC devices was equal to 13.7TWh (23%), and for Ireland the it was 9.4TWh for the farshore WECs (39%). Since the goal of a feasible energy system is to maintain the stability of supply and low cost dispatch, the system decides that the fluctuating output of wave energy creates congestion issues to the grid more often than wind energy does. In theory, more storage units could be build in regions where WECs are installed to take advantage of the curtailed energy. Since the objective of the model is to minimize costs, taking into account lifetime of the components together with energy sufficiency and transmission expansion, the model itself decides that, meeting the demand can be achieved by occasional imports, and wave energy can serve the model as a back-up source.

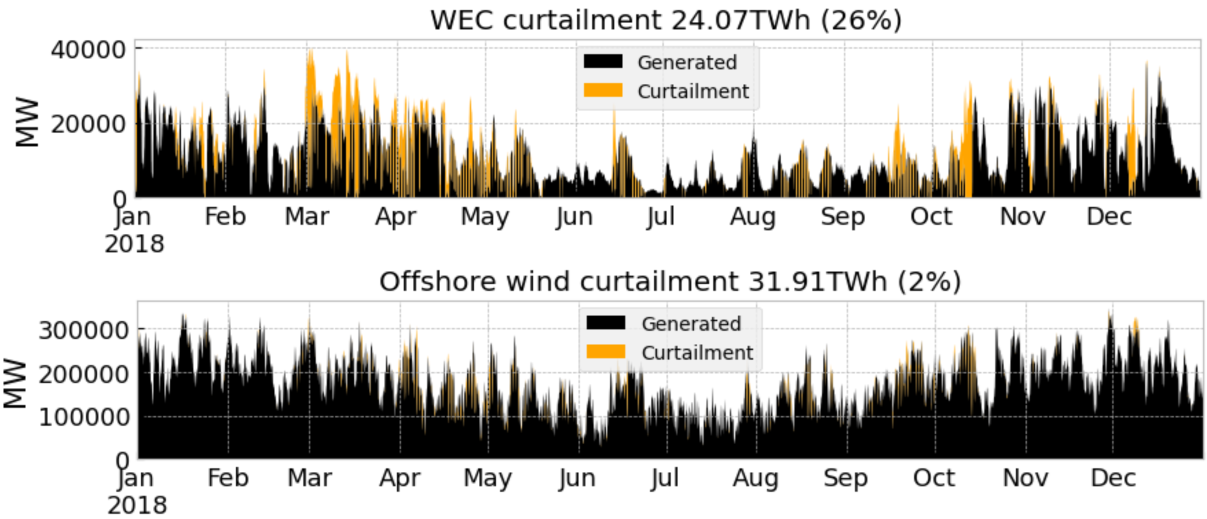

Figure 77: Curtailment of WECs and Offshore WTGs with their percentage of curtailed energy with respect to the generated one‘.

PyPSA implements shadow prices into the objective function, derived from the marginal costs of generation of each component in order to calculate locational marginal prices. Since the marginal cost of wave energy is almost 4 times higher than the rest, curtailing WECs is the most economic option. This however does not mean that wave energy is not beneficial. A renewable energy system, by its nature requires significantly more capacity than what it needs in theory. This justifies the installation of almost 1990GW of nominal generator power, while the maximum recorded load for the 2018 dataset at any moment was around 715GW. Dealing with the intermittency of the supply, means redirecting the source somewhere else so that supply can be fulfilled. Inevitably, there will be periods for which the supply needs to be complemented with storage dispatch or import through transmission lines, and other periods for which the grid can not absorb all of the generating power. As the cost of renewables continues to decrease over time, the cost of curtailment decreases as well. Optimizing energy management systems in a power network can probably mitigate the influence of the variability of RES.

6 Conclusions

In this concluding section, we delve into a combination of findings derived from the modeling and exploration of fully renewable energy system. Through an analysis of energy generation, system behavior, transmission expansion, and economic results, we aim to solidify key elements that shed light on the effectiveness, challenges, and future prospects of the modelled network scenarios with respect to the limitations of the used software. We will assess the feasibility of the 100% renewable energy system, as a result of the software's processes and the inputs used to create it, by attempting to give answers to the research questions that drove us to investigate it in the first place.

How does the modeling of a power system vary with different spatial and temporal resolutions, considering time as the iterations of the optimization process and space as the spatial resolution of the network and the bathymetry?

During the initial work on this research we tested two different network configurations, three different time-steps of power flow optimization iterations, and we tried to implement the high fidelity GEBCO2023 bathymetry dataset into the model. While reaching the ceiling of the available computational power, with a maximum network density to 50-nodes of hourly resolution, we obtained a noticeable decrease in the overall annual expenditure by 1.2% for the 2030 scenario, even though the nominal generator capacity increased by 1.4%. Significant was the decrease of the length and cost of the underwater fractions of the HVDC lines, which was possible since the denser network brought the nodes closer together. Since offshore technology deployment is highly dependant on the depths at which it needs to be installed, the latest GEBCO2023 data substituted the previously used GEBCO2014 data. Unfortunately, the high resolution bathymetry data were not able show their merits, as they were overshadowed by the low resolution ERA5 weather data and only marginally did they show some benefits in installation. The model calculates the renewable potential energy by filtering the space with both spatial data. Conclusively, the final resolution shifts towards the lower inputted one. This clearly impacted wave energy availability, which was entirely overlooked by the model, and only when considering minimum capacity constraints was it included into the mix.

Can we validate the targets of 300GW of offshore wind and 40 GW of marine capacity at the European Union, and an additional 150GW at Great Britain for 2050?

The models under investigation were inspired by the European ambition of transitioning towards a carbon neutral energy system. Focusing on the deployment of marine and offshore wind technologies, we followed the European Union's and Great Britain's climate change directives to set minimum targets of wave and wind capacity future deployment with respect to three target years, 2030, 2040 and 2050. Setting those goals as minimum constraints into the model and with respect to the 2030 scenario, the findings were initially positive for offshore wind energy, as the needs by EU and GB were met and surpassed by a great extend. The model installed more than 187GW of offshore wind power, while the goal was only 110GW, generating 691TWh/a. Wave energy however, was only able to acquire the minimum goal of 6GW in total installation, generating less than 0.5% of the total annual energy (8.25TWh). Moving towards the 2050 scenario, both offshore wind and wave energy technologies reached only their minimum capacities, 405GW and 62GW respectively, indicating that the model probably harnessed all of the economically viable potential of the technologies, and only because of capacity constraint does it reach those high shares of wind and wave energy. Their contribution was 1,572.5TWh for offshore wind and 92.4TWh for wave energy. However, based on the configurations of each energy type, the available energy potential around Europe for wave was more than 52,000TWh for the nearshore WECs alone, multiple times larger than the energy demand which is estimated to be around 4300TWh. Offshore wind resource potential is also quite large reaching a cumulative 35,000TWh.

The yearly potential however is not the only criteria of generator deployment into an energy system. The purpose of energy system modelling with PyPSA's workflow algorithms is to obtain the optimal distribution of generation and ensure energy equity throughout the year with respect to a cost-minimizing objective function. Supply stability in the energy model is influenced by the tuning of the technical characteristics that define its final potential. In this research, we set relatively high power densities for wave converters, which resulted into the lowest average capacity factors (CF) of all generators. The very optimistic $20MW/km^2$ capacity of farshore WECs obtained a CF equal to 0.065 ($CF_{OWTGs} \approx 0.40$).

With the device being a 750kW Pelamis P2, its investment costs were also high since there are roughly 27 devices in every km^2. Adding to this the fact that wave energy in the model is active in a quite unsteady manner, resulted into a high marginal cost of generation and large amount of curtailment.

Wind energy also had a very optimistic power density, it being $8MW/km^2$ for bottom fixed wind turbine generators (WTGs) and $9MW/km^2$ for floating ones derived from high rated turbine models. Their performance was higher and steadier than the wave converters, resulting into low marginal costs and small curtailment. Observing 2030 scenario results, we can safely assume that the model desires the uninterrupted high value resource of the farshore winds. However, more optimization could be achieved if specific power densities could be set for specific regions for both wind and wave energy, which would bring down the costs. In general the model showed a clear preference on where every energy type is deployable. It roughly divided the continent into a mainly solar power plant (south) and a mainly wind power plant (north). The northern part also accommodated most of the offshore wind capacity and farshore wave converters. This was found to be reasonable since the North and Baltic Seas have a combination of large wind resource and desirable bathymetry, which facilitate the installation of offshore WTGs.

From an economic perspective, it is difficult to justify the goals set by the European countries. Performing unconstrained versions of the scenarios showed that solar and onshore wind energy will always be dominant in the mix, as they are relatively inexpensive and when coupled with storage systems and unlimited transmission expansion, they can be highly reliable. The unconstrained model deems reasonable that based on the provided data energy demand can be met with a significantly lower share of offshore wind and wave devices into the mix. Nevertheless, the less versatile the energy mix, the more fragile supply stability becomes. Cost-optimal solving methods have limitations, in the sense that the modeling of a scenario is based on a specific reference year. This means that it may yield solutions that are impractical for alternative weather and load years. A greater level of supply safety can be achieved by integrating more generators, both in type and capacity.

What is the role of Wave and Offshore Wind energy technologies in the context of a 2050 carbon-neutral scenario?

The developments on the PyPSA-Eur framework allowed for floating wind and wave converters to participate in a European system model with respect to 2030, 2040 and 2050 horizons. This addition, allowed the model to have access to the undisturbed wind speeds of the deep sea, and the untapped energy contained into waves. Those technologies were initially assessed for their installation potential and then they were integrated into the model.

As previously stated, the model clearly found the potential of farshore wind resources to be advantageous, with installations exceeding 111GW of floating and 35GW of bottom fixed DC WTGs for the 2030 scenario. Despite the 'Business As Usual' minimum capacity constraints setting the installation target at 285GW for these WTG types, the unconstrained 2050 scenario still incorporated 135GW. This demonstrates the model's preference for the more expensive far offshore wind energy, even in a cost optimization context. By analyzing the generation time-series of the wind generators, we confirmed that production is affected strongly by the seasonality of the physical resource. However, operations of close to maximum nominal capacity during fall, winter and spring were reached multiple times, justifying their total installed capacity. Their average daily operation reached 180GW.

Wave power did not exhibit the same promising performance as wind power. Although the energy potential contained in waves around Europe is immense, their installation happened only in 5 countries, Portugal (25GW), Spain (0.1GW), France (3.5GW), Italy (13.4GW) and Ireland (19.9GW). Seasonality significantly impacted the device's performance, resulting in entire weeks where they could not contribute to the system. The average daily operation of all wave energy converters (WECs) combined was approximately 10GW, which dropped to only 6GW during the summer. Specifically, the farshore device contributed less than 0.4GW during the summer, while the nearshore device had a larger contribution, averaging around 4.1GW, and the shallow one was approximately 1.3GW. A possible conclusion is that the role of the marine renewables in this model which installed them based on cost-optimal functions, is auxiliary. Despite their better performance during colder periods, wave converters are viewed as a backup source of power, being the first to be curtailed due to their marginal costs of electricity ($\approx$ 0.09 €/MWh).

In a broader context, the significance of wave energy goes beyond capacity metrics. While wave power installations may induce larger operational costs, once in operation their market value is high. The key lies in identifying regions where feasible installation is possible, enabling the deployment of wave energy devices and justify their role. Unfortunately, the potential of wave power within the model could not be fully realized due to spatial resolution constraints in wave data resulting in an underestimation of the resource. It is noteworthy that, despite wind data having same resolution, their consistency solidified more confidence on them by the model. When considering the relatively low visual impact of wave converters, them being submerged or slightly above the surface, they gain a distinct advantage with respect to public acceptance. If a greater level of resolution could be achieved to get closer to a real-world scenario, WECs could significantly contribute to the development of a diversified and sustainable energy system.

All in all, not all nations can take advantage of the oceanic resource. The role of marine and offshore renewables is intertwined with the role of land and overseas transmission expansion. In this manner, the model effectively increases the availability of wave and offshore wind technologies on the network. With a 2050 scenario for which the line capacity is almost twice the current capacity, we concluded that the network requires quite an upgrade in order to be able to carry out the demanded power flow.

What is the role of anti-variability measures on a fully-renewable energy system and its contribution on electricity supply stability?

By analyzing the generational time-series of the model we realized that energy supply stability in this network would not be possible without storage systems. We witnessed multiple times in which the dispatch of energy from inter-temporal power-shifting units reached the maximum during the year, also indicated by their state of charge every time it was equal to 0. On an average daily basis, their capacity surpassed 100GW, including the less demanding weekends. It was observed that the sum of all storage units suggested an operational profile for which dispatch happens mostly during the early hours in the morning and the later hours of the evening. An exception was the hydro dams which have an almost constant daily operational capacity. Note that some countries, like the ones in Scandinavia, depend on reservoir storage for a large part of generation, since the weather patterns there allow it. This dispatch matched the deficiency of the generators during these periods, in which solar power does is not able to contribute into the system due to lack of sunlight.

What else was observed, was that during summer, where the wind and wave resource is dramatically less, storage units, excluding batteries, kept a positive state of charge. This suggests that the model guarantees energy safety and is able to cover a possible shortage. Batteries had a daily pattern of charging and discharging, which was also influenced by their maximum 6-hour dispatch time. A verdict out of this behaviour is that, battery storage is heavily reliant on solar power and both of their operations are somewhat supplementary. Wind power also appeared to contribute to the charging of the units during the less demanding night-time periods.

In conclusion, the integration of more storage units in a 100% renewable energy system appears to be a critical point of its feasibility. With regions away from offshore wind and wave resources, storage units provide energy in times of need, otherwise wasted or curtailed.

What are the geographic constrains that affect the deployment of Marine and Offshore technologies?

It is apparent that the additional technologies used on these models have obvious geographical constraints regarding water depth and proximity to land, the energy resource available, and the combinations of the above in order to create viable solutions for their deployment. Those however are inputs, and are a part of literature study. The question on geographic constraints of the model, refers only to the effect of the geographic characteristics around Europe on the deployment of marine and offshore technologies by analyzing the behaviour of a complete energy model.

In general, offshore devices are not implementable in the entirety of the network for obvious reasons regarding the vicinity of some nodes to water basins but also the availability of resource of the basins themselves. This is where the transmission line expansion comes to facilitate the delivery of energy towards the more entrapped regions, providing an alternative to accomplish the zero-carbon emitting electricity sector.

We constrained the model as to be mandatory for each country to acquire a generator capacity of at least 70% of its power demand, but we did not impose any transmission expansion limits. It was assumed that this will enhance energy security, by installing more generators than it would normally do, and set a country-specific lower goal of installed power. This constraint potentially can increase the predictability of the energy costs and can mitigate the vulnerability by supply disruptions and geopolitical tensions in a real-world scenario.

When we dived into country-specific analysis of the interaction of the components, we realized that some regions rely on solar-battery energy sources, and large imports of energy. Those regions belong mostly to the central and southern part of Europe. This part is characterized by less access to water bodies and a more mountainous terrain. Even with the power equity constraints, we witnessed that the high power capacity does not translate into high energy generation, resulting in large energy imports via AC and DC lines. The geomorphological anomalies increase the overall roughness of the terrain. This was probably the reason why the model was less confident on deploying onshore WTG and installing large amounts of solar power instead. These high-share solar energy mixes have significant drawbacks during winter time, where solar power appeared to be quite unstable and insufficient, even during day-light.

The geographical constraints of the model, suggest that energy dependability of landlocked countries on their neighbours is still high. Transmission expansion, both onshore and offshore, is the key for overcoming supply difficulties. If an increase of the transmission lines by a factor of two could be achieved, the system could overcome its geographical constraints.

What is the verdict of the economic assessment of a 100% Renewable Power System.

Lastly, the economic assessment and discussion of the 2050 model, suggests a mostly balanced pricing of electricity around Europe, not very far from the energy market standards of 2018. With a few countries obtaining prices around 40 €/MWh and most of them around 60 €/MWh, we concluded that from an economic point of view, the end user will sense a slight increase of cost, with the benefits of a clean energy generation.

In general, the capital investment was found to be influenced by the power density of each device. While a higher power density corresponds to more devices, it doesn't necessarily translate to increased energy output. Generation is strongly affected by capacity factors, the lowest of which were obtained by wave converters. This was found to be the reason why the model calculates a very high capital cost and a quite small revenue. A potential solution to this challenge could involve reducing the power density, thereby enhancing the wave farm's capacity factor and subsequently reducing the initial investment costs.

As previously mentioned, the model employs a strategy of reducing power within the network by giving priority to curtailing wave converters, due to their high marginal cost. The evaluation of the economic feasibility of wave energy is subject to uncertainty, stemming from the underestimation of the resource potential. By comparing the 2030 and 2050 scenarios we expected that locational prices would rise, as the deployment of more offshore technologies increased. This situation raises questions about the justification for developing a potentially more expensive energy system. Nevertheless, it highlights the benefit of diversifying the energy mix, providing access to a wider range of resources.

6.1 Limitations and future outlook

A major struggle of this report was integrating high fidelity data, in order to increase the resolution of the network analysis. So far we used the $31,000m \times 31,000m$ ERA5 weather data for the wind, wave and solar resource, which pose significant limitations on the approximation of the potential. Noticeable improvements could be witnessed if higher resolution data such as the CERRA weather reanalysis dataset with a horizontal resolution of $5,000m \times 5,000m$ could be integrated into the model. Furthermore, the Marine Renewable Energies Lab (MREL) of TU Delft is developing a high-fidelity wave dataset, closer to the resolution of GEBCO2023, which could be the watershed of marine energy. This way the software will view the coastline with greater clarity, and less potential would be overlooked.

Additional improvement could also be achieved by increasing the network resolution itself, going beyond 50-buses networks and representing the grid with greater clarity. This would require significantly more computing capacity, given the fact that we maintain the 1-hour resolution of snapshots. It is expected that overseas transmission lines would be reduced, something that is beneficial for the development, as it diminishes the expenses and provides more alternative routes for the power flow.

A vital part of power system analysis is the configuration of the technologies. For our model we selected an optimistic capacity density for the generators that yielded quite low average capacity factors for the wave converters. While our assumptions indicate specific results on the role of each renewable technology, more experimentation to further optimize the technologies could reveal greater availability of the resources.

In addition to this, a major limitation of the model is the single-device representation of each energy carrier. Extra branches that enable the model to use more turbines or wave converters could increase capacity factors, and reduce marginal costs.

This model is the product of developments on the PyPSA-Eur model framework (employing the PyPSA workflow) that made it possible for the energy system to consider wave and farshore wind energy technologies. Addition of more proven technologies could unlock a more inclusive pathway of the energy transition. Those technologies could be floating solar power, tidal, ocean thermal energy conversion (OTEC) etc. Note that each type would require unique developments and assumptions in the software.

References

[1] European Commission. *European Climate Law*. 2020. URL: https://climate.ec.europa.eu/eu-action/european-climate-law_en.

[2] Valentina Vannucchi and Lorenzo Cappietti. "Wave Energy Assessment and Performance Estimation of State of the Art Wave Energy Converters in Italian Hotspots". In: *Sustainability* 8.12 (2016). ISSN: 2071-1050. DOI: 10.3390/su8121300. URL: https://www.mdpi.com/2071-1050/8/12/1300.

[3] Treaty on the Functioning of the European Union. *Article 191 (ex Article 174 TEC)*. 2008. URL: https://eur-lex.europa.eu/LexUriServ/LexUriServ.do?uri=CELEX%3A12008E191%3AEN%3AHTML.

[4] European Union. *Regulation (EU) 2021/1119 of the European Parliament and of the Council of 30 June 2021 establishing the framework for achieving climate neutrality and amending Regulations (EC) No 401/2009 and (EU) 2018/1999 ('European Climate Law')*. 2020. URL: https://eur-lex.europa.eu/legal-content/EN/TXT/?uri=CELEX%3A32021R1119.

[5] Gregor Erbach. *European Climate Law*. 2021. URL: https://www.europarl.europa.eu/RegData/etudes/BRIE/2020/649385/EPRS_BRI(2020)649385_EN.pdf.

[6] European Union. *Mid-century zero emissions strategy for the EU*. 2023. URL: https://www.europarl.europa.eu/legislative-train/theme-resilient-energy-union-with-a-climate-change-policy/file-mid-century-zero-emissions-strategy-for-the-eu.

[7] European Union. *Fit for 55*. 2018. URL: https://www.consilium.europa.eu/en/policies/green-deal/fit-for-55-the-eu-plan-for-a-green-transition/.

[8] European Commission. *Renewable Energy – Recast to 2030 (RED II)*. 2018. URL: https://joint-research-centre.ec.europa.eu/welcome-jec-website/reference-regulatory-framework/renewable-energy-recast-2030-red-ii_en.

[9] European Commission. *REPowerEU*. 2022. URL: https://commission.europa.eu/strategy-and-policy/priorities-2019-2024/european-green-deal/repowereu-affordable-secure-and-sustainable-energy-europe_en.

[10] European Commission. *World Energy Technology Outlook to 2050*. 2007. URL: https://ec.europa.eu/commission/presscorner/detail/en/MEMO_07_2.

[11] UK Government. *Offshore Wind Net Zero Investment Roadmap*. 2023. URL: https://assets.publishing.service.gov.uk/government/uploads/system/uploads/attachment_data/file/1167856/offshore-wind-investment-roadmap.pdf.

[12] European Commission. *Offshore renewable energy*. 2020. URL: https://energy.ec.europa.eu/topics/renewable-energy/offshore-renewable-energy_en.

[13] European Evironment Agency. *Share of energy consumption from renewable sources in Europe*. 2021. URL: https://climate-energy.eea.europa.eu/topics/energy-1/renewable-energy/indicators/share-of-energy-consumption-from-renewable-sources-in-europe.

[14] WindEurope. *Wind energy in Europe: 2022 Statistics and the outlook for 2022-2026*. 2023. URL: https://windeurope.org/intelligence-platform/product/wind-energy-in-europe-2021-statistics-and-the-outlook-for-2022-2026/.

[15] D.P. Schlachtberger, T. Brown, S. Schramm, and M. Greiner. "The benefits of cooperation in a highly renewable European electricity network". In: *Energy* 134 (2017), pp. 469–481. ISSN: 0360-5442. DOI: https://doi.org/10.1016/j.energy.2017.06.004. URL: https://www.sciencedirect.com/science/article/pii/S0360544217309969.

[16] WindEurope. *Wind energy in Europe: 2022 Statistics and the outlook for 2022-2026*. 2022. URL: https://eur-lex.europa.eu/legal-content/EN/TXT/?uri=CELEX:52020DC0301.

[17] European Assosiation of Storage of Energy. *Energy Storage Targets 2030 and 2050*. URL: https://ease-storage.eu/publication/energy-storage-targets-2030-and-2050/.

[18] Intergovernmental Panel on Climate Change (IPCC). "Summary for Policymakers". In: *Global Warming of 1.5°C: IPCC Special Report on Impacts of Global Warming of 1.5°C above Pre-industrial Levels in Context of Strengthening Response to Climate Change, Sustainable Development, and Efforts to Eradicate Poverty.* Cambridge University Press, 2022, pp. 1–24.

[19] Arshad Raza, Raoof Gholami, Reza Rezaee, Vamegh Rasouli, and Minou Rabiei. "Significant aspects of carbon capture and storage – A review". In: *Petroleum* 5.4 (2019), pp. 335–340. ISSN: 2405-6561. DOI: https://doi.org/10.1016/j.petlm.2018.12.007. URL: https://www.sciencedirect.com/science/article/pii/S2405656118301366.

[20] IRENA. *Renewable Power Generation Costs in 2022.* 2023. URL: https://www.irena.org/Publications/2023/Aug/Renewable-Power-Generation-Costs-in-2022.

[21] Eurostat. *Renewable energy statistics.* 2022. URL: https://ec.europa.eu/eurostat/statistics-explained/index.php?title=Renewable_energy_statistics#Share_of_renewable_energy_more_than_doubled_between_2004_and_2022.

[22] WindEurope. *Wind energy in Europe: 2022 Statistics and the outlook for 2023-2027.* 2022. URL: https://windeurope.org/intelligence-platform/product/wind-energy-in-europe-2022-statistics-and-the-outlook-for-2023-2027/#:~:text=28%20February%202023-,Overview,new%20wind%20capacity%20in%202022..

[23] Technical University of Denmark (DTU Wind Energy). URL: https://globalwindatlas.info/en.

[24] Zhiyu Jiang. "Installation of offshore wind turbines: A technical review". In: *Renewable and Sustainable Energy Reviews* 139 (2021), p. 110576. ISSN: 1364-0321. DOI: https://doi.org/10.1016/j.rser.2020.110576. URL: https://www.sciencedirect.com/science/article/pii/S1364032120308601.

[25] European Commission. *An EU Strategy to harness the potential of offshore renewable energy for a climate neutral future.* 2020. URL: https://eur-lex.europa.eu/legal-content/EN/TXT/?uri=COM:2020:741:FIN&qid=1605792629666.

[26] EMODnet. URL: https://ec.europa.eu/maritimeaffairs/atlas/maritime_atlas/#lang=EN;p=w;bkgd=5;theme=89:0.75,88:0.75;c=1034567.5360353943,6856196.402968529;z=4.

[27] WindEurope. *Europe can expect to have 10 GW of floating wind by 2030.* 2022. URL: https://windeurope.org/newsroom/news/europe-can-expect-to-have-10-gw-of-floating-wind-by-2030/.

[28] Ocean Energy Europe. *Ocean Energy Key trends and statistics 2022.* 2023. URL: https://www.oceanenergy-europe.eu/category/publication-library/.

[29] Kester Gunn and Clym Stock-Williams. "Quantifying the global wave power resource". In: *Renewable Energy* 44 (2012), pp. 296–304. ISSN: 0960-1481. DOI: https://doi.org/10.1016/j.renene.2012.01.101. URL: https://www.sciencedirect.com/science/article/pii/S0960148112001310.

[30] Tom Brown. "Transmission network loading in Europe with high shares of renewables". In: *IET Renewable Power Generation* 9.1 (2015), pp. 57–65.

[31] ENTSO-e. 2023. URL: https://www.entsoe.eu/data/map/downloads/.

[32] Kangyin Dong, Gal Hochman, Yaqing Zhang, Renjin Sun, Hui Li, and Hua Liao. "CO2 emissions, economic and population growth, and renewable energy: Empirical evidence across regions". In: *Energy Economics* 75 (2018), pp. 180–192. ISSN: 0140-9883. DOI: https://doi.org/10.1016/j.eneco.2018.08.017. URL: https://www.sciencedirect.com/science/article/pii/S0140988318303256.

[33] Tim Tröndle, Johan Lilliestam, Stefano Marelli, and Stefan Pfenninger. "Trade-Offs between Geographic Scale, Cost, and Infrastructure Requirements for Fully Renewable Electricity in Europe". In: *Joule* 4.9 (2020), pp. 1929–1948. ISSN: 2542-4351. DOI: https://doi.org/10.1016/j.joule.2020.07.018. URL: https://www.sciencedirect.com/science/article/pii/S2542435120303366.

[34] Emil H. Eriksen, Leon J. Schwenk-Nebbe, Bo Tranberg, Tom Brown, and Martin Greiner. "Optimal heterogeneity in a simplified highly renewable European electricity system". In: *Energy* 133 (2017), pp. 913–928. ISSN: 0360-5442. DOI: https://doi.org/10.1016/j.energy.2017.05.170. URL: https://www.sciencedirect.com/science/article/pii/S0360544217309593.

[35] T.W. Brown, T. Bischof-Niemz, K. Blok, C. Breyer, H. Lund, and B.V. Mathiesen. "Response to 'Burden of proof: A comprehensive review of the feasibility of 100% renewable-electricity systems'". In: *Renewable and Sustainable Energy Reviews* 92 (2018), pp. 834–847. ISSN: 1364-0321. DOI: https://doi.org/10.1016/j.rser.2018.04.113. URL: https://www.sciencedirect.com/science/article/pii/S1364032118303307.

[36] Patrick Moriarty and Damon Honnery. "Feasibility of a 100% Global Renewable Energy System". In: *Energies* 13 (2020), n/a. DOI: https://doi.org/10.3390/en13215543. URL: https://www.mdpi.com/1996-1073/13/21/5543.

[37] Peng Hou, Jiangsheng Zhu, Kuichao Ma, Guangya Yang, Weihao Hu, and Zhe Chen. "A review of offshore wind farm layout optimization and electrical system design methods". In: *Journal of Modern Power Systems and Clean Energy* 7.5 (2019), pp. 975–986. DOI: 10.1007/s40565-019-0550-5.

[38] Francisco Bañuelos-Ruedas, César Angeles-Camacho, and Sebastián Rios-Marcuello. "Methodologies Used in the Extrapolation of Wind Speed Data at Different Heights and Its Impact in the Wind Energy Resource Assessment in a Region". In: *Wind Farm*. Ed. by Gastón O. Suvire. Rijeka: IntechOpen, 2011. Chap. 4. DOI: 10.5772/20669. URL: https://doi.org/10.5772/20669.

[39] Lin Lu, Hongxing Yang, and John Burnett. "Investigation on wind power potential on Hong Kong islands—an analysis of wind power and wind turbine characteristics". In: *Renewable Energy* 27.1 (2002), pp. 1–12. ISSN: 0960-1481. DOI: https://doi.org/10.1016/S0960-1481(01)00164-1. URL: https://www.sciencedirect.com/science/article/pii/S0960148101001641.

[40] A. Martinez and G. Iglesias. "Mapping of the levelised cost of energy for floating offshore wind in the European Atlantic". In: *Renewable and Sustainable Energy Reviews* 154 (2022), p. 111889. ISSN: 1364-0321. DOI: https://doi.org/10.1016/j.rser.2021.111889. URL: https://www.sciencedirect.com/science/article/pii/S1364032121011564.

[41] Barry Johnston, Aoife Foley, John Doran, and Timothy Littler. "Levelised cost of energy, A challenge for offshore wind". In: *Renewable Energy* 160 (2020), pp. 876–885. ISSN: 0960-1481. DOI: https://doi.org/10.1016/j.renene.2020.06.030. URL: https://www.sciencedirect.com/science/article/pii/S0960148120309241.

[42] Srinivasan Santhakumar, Gavin Smart, Miriam Noonan, Hans Meerman, and André Faaij. "Technological progress observed for fixed-bottom offshore wind in the EU and UK". In: *Technological Forecasting and Social Change* 182 (2022), p. 121856. ISSN: 0040-1625. DOI: https://doi.org/10.1016/j.techfore.2022.121856. URL: https://www.sciencedirect.com/science/article/pii/S0040162522003808.

[43] Anders Myhr, Catho Bjerkseter, Anders Ågotnes, and Tor A. Nygaard. "Levelised cost of energy for offshore floating wind turbines in a life cycle perspective". In: *Renewable Energy* 66 (2014), pp. 714–728. ISSN: 0960-1481. DOI: https://doi.org/10.1016/j.renene.2014.01.017. URL: https://www.sciencedirect.com/science/article/pii/S0960148114000469.

[44] Aaron Du. *Semi-Submersible, Spar and TLP – How to select floating wind foundation types?* 2021. URL: https://www.empireengineering.co.uk/semi-submersible-spar-and-tlp-floating-wind-foundations/.

[45] ENERDATA. *Offshore wind goes floating*. 2022. URL: https://www.enerdata.net/publications/executive-briefing/floating-offshore-wind-evolution.html.

[46] Marine Renewable Energies Lab (MREL). URL: www.tudelft.nl/ceg/mrel.

[47] Carbon Trust. *Floating offshore wind market technology review*. 2022. URL: https://www.carbontrust.com/our-work-and-impact/guides-reports-and-tools/floating-offshore-wind-market-technology-review.

[48] Muhammad Asif Hanif, Farwa Nadeem, Rida Tariq, and Umer Rashid. "Chapter 7 - Power generation by ocean energy". In: *Renewable and Alternative Energy Resources*. Ed. by Muhammad Asif Hanif, Farwa Nadeem, Rida Tariq, and Umer Rashid. Academic Press, 2022, pp. 359–430. ISBN: 978-0-12-818150-8. DOI: https://doi.org/10.1016/B978-0-12-818150-8.00002-2. URL: https://www.sciencedirect.com/science/article/pii/B9780128181508000022.

[49] Nicolas Guillou, George Lavidas, and Georges Chapalain. "Wave Energy Resource Assessment for Exploitation—A Review". In: *Journal of Marine Science and Engineering* 8.9 (2020). ISSN: 2077-1312. DOI: 10.3390/jmse8090705. URL: https://www.mdpi.com/2077-1312/8/9/705.

[50] IRENA. *Wave Energy: Technology brief.* 2014. URL: https://www.irena.org/publications/2014/Jun/Wave-energy.

[51] Wanan Sheng. "Wave energy conversion and hydrodynamics modelling technologies: A review". In: *Renewable and Sustainable Energy Reviews* 109 (2019), pp. 482–498. ISSN: 1364-0321. DOI: https://doi.org/10.1016/j.rser.2019.04.030.

[52] Seongho Ahn, Kevin A. Haas, and Vincent S. Neary. "Wave energy resource classification system for US coastal waters". In: *Renewable and Sustainable Energy Reviews* 104 (2019), pp. 54–68. ISSN: 1364-0321. DOI: https://doi.org/10.1016/j.rser.2019.01.017. URL: https://www.sciencedirect.com/science/article/pii/S1364032119300279.

[53] George Lavidas. "Developments of energy in EU–unlocking the wave energy potential". In: *International Journal of Sustainable Energy* 38.3 (2019), pp. 208–226. DOI: 10.1080/14786451.2018.1492578. URL: https://doi.org/10.1080/14786451.2018.1492578.

[54] Simon P. Neill and M. Reza Hashemi. "Chapter 5 - Wave Energy". In: *Fundamentals of Ocean Renewable Energy.* Ed. by Simon P. Neill and M. Reza Hashemi. E-Business Solutions. Academic Press, 2018, pp. 107–140. ISBN: 978-0-12-810448-4. DOI: https://doi.org/10.1016/B978-0-12-810448-4.00005-7.

[55] Hongzhou He, Quanyou Qu, and Juyue Li. "Numerical Simulation of Section Systems in the Pelamis Wave Energy Converter". In: *Advances in Mechanical Engineering* 5 (2013), p. 186056. DOI: 10.1155/2013/186056. URL: https://doi.org/10.1155/2013/186056.

[56] Silvia Bozzi, Adrià Moreno Miquel, Alessandro Antonini, Giuseppe Passoni, and Renata Archetti. "Modeling of a Point Absorber for Energy Conversion in Italian Seas". In: *Energies* 6.6 (2013), pp. 3033–3051. ISSN: 1996-1073. DOI: 10.3390/en6063033. URL: https://www.mdpi.com/1996-1073/6/6/3033.

[57] Chad Augustine, Richard Bain, Jamie Chapman, Paul Denholm, Easan Drury, Douglas G. Hall, Eric Lantz, Robert Margolis, Robert Thresher, Debra Sandor, Norman A. Bishop, Stephen R. Brown, Glenn F. Cada, Fort Felker, Steven J. Fernandez, Alan C. Goodrich, George Hagerman, Garvin Heath, Sean O'Neil, Joshua Paquette, Suzanne Tegen, and Katherine Young. "Renewable Electricity Futures Study. Volume 2. Renewable Electricity Generation and Storage Technologies". In: (June 2012). DOI: 10.2172/1219712. URL: https://www.osti.gov/biblio/1219712.

[58] S. Astariz and G. Iglesias. "The economics of wave energy: A review". In: *Renewable and Sustainable Energy Reviews* 45 (2015), pp. 397–408. ISSN: 1364-0321. DOI: https://doi.org/10.1016/j.rser.2015.01.061. URL: https://www.sciencedirect.com/science/article/pii/S1364032115000714.

[59] Mirko Previsic and Julia Chozas. "International Levelised Cost of Energy for Ocean Energy Technologies". In: (May 2015). DOI: 10.13140/RG.2.2.34304.38407.

[60] Jonas Hoersch, Fabian Hofmann, David Schlachtberger, and Tom Brown. "PyPSA-Eur: An open optimisation model of the European transmission system". In: *Energy Strategy Reviews* 22 (2018), pp. 207–215. DOI: 10.1016/j.esr.2018.08.012. eprint: 1806.01613.

[61] OPSD - Open Power System Data. URL: https://open-power-system-data.org/.

[62] Fabian Gotzens, Heidi Heinrichs, Jonas Hörsch, and Fabian Hofmann. "Performing energy modelling exercises in a transparent way - The issue of data quality in power plant databases". en. In: *Energy Strategy Reviews* 23 (Jan. 2019), pp. 1–12. ISSN: 2211467X. DOI: 10.1016/j.esr.2018.11.004. URL: https://linkinghub.elsevier.com/retrieve/pii/S2211467X18301056 (visited on 12/03/2018).

[63] Copernicus. URL: https://cds.climate.copernicus.eu/cdsapp#!/dataset/reanalysis-era5-single-levels?tab=overview.

[64] GEBCO. *Gridded Bathymetric Data.* URL: https://www.gebco.net/data_and_products/gridded_bathymetry_data/version_20141103/.

[65] Fabian Hofmann, Johannes Hampp, Fabian Neumann, Tom Brown, and Jonas Hörsch. "atlite: A Lightweight Python Package for Calculating Renewable Power Potentials and Time Series". In: *Journal of Open Source Software* 6.62 (2021), p. 3294. DOI: 10.21105/joss.03294. URL: https://doi.org/10.21105/joss.03294.

[66] T. Brown, J. Hörsch, and D. Schlachtberger. "PyPSA: Python for Power System Analysis". In: *Journal of Open Research Software* 6.4 (1 2018). DOI: 10.5334/jors.188. eprint: 1707.09913. URL: https://doi.org/10.5334/jors.188.

[67] Henrik Lund, Finn Arler, Poul Alberg Østergaard, Frede Hvelplund, David Connolly, Brian Vad Mathiesen, and Peter Karnøe. "Simulation versus Optimisation: Theoretical Positions in Energy System Modelling". In: *Energies* 10.7 (2017). ISSN: 1996-1073. DOI: 10.3390/en10070840. URL: https://www.mdpi.com/1996-1073/10/7/840.

[68] Georgios Savvidis, Kais Siala, Christoph Weissbart, Lukas Schmidt, Frieder Borggrefe, Subhash Kumar, Karen Pittel, Reinhard Madlener, and Kai Hufendiek. "The gap between energy policy challenges and model capabilities". In: *Energy Policy* 125 (2019), pp. 503–520. ISSN: 0301-4215. DOI: https://doi.org/10.1016/j.enpol.2018.10.033. URL: https://www.sciencedirect.com/science/article/pii/S0301421518306864.

[69] Gurobi Optimization, LLC. *Gurobi Optimizer Reference Manual*. 2023. URL: https://www.gurobi.com.

[70] ZENODO. *GridKit extract of ENTSO-E interactive map*. DOI: 10.5281/zenodo.55853.

[71] Hans Hersbach, W Bell, P. Berrisford, Andras Horányi, Muñoz-Sabater J., J. Nicolas, Raluca Radu, Dinand Schepers, Adrian Simmons, Cornel Soci, and Dick Dee. *Global reanalysis: goodbye ERA-Interim, hello ERA5*. eng. Apr. 2019. DOI: 10.21957/vf291hehd7. URL: https://www.ecmwf.int/node/19027.

[72] Nicolas Guillou, George Lavidas, and Bahareh Kamranzad. "Wave Energy in Brittany (France)mdash;Resource Assessment and WEC Performances". In: *Sustainability* 15.2 (2023). ISSN: 2071-1050. DOI: 10.3390/su15021725. URL: https://www.mdpi.com/2071-1050/15/2/1725.

[73] Matias Alday G., Vaibhav Raghavan, and George Lavidas. "Analysis of the North Atlantic offshore energy flux from different reanalysis and hindcasts". English. In: *Vol. 15 (2023): Proceedings of the European Wave and Tidal Energy Conference*. Vol. 15. The 15th European Wave and Tidal Energy Conference, EWTEC 2023 ; Conference date: 03-09-2023 Through 07-09-2023. EWTEC, 2023. DOI: 10.36688/ewtec-2023-140. URL: https://ewtec.org/ewtec-2023/.

[74] European Marine Energy Centre (EMEC). *PELAMIS WAVE POWER*. URL: https://www.emec.org.uk/about-us/wave-clients/pelamis-wave-power/.

[75] *Vestas V90-3.0*. URL: https://en.wind-turbine-models.com/turbines/603-vestas-v90-3.0.

[76] National Renewable Energy Laboratory. *NREL Turbine Archive*. URL: https://nrel.github.io/turbine-models/index.html.

[77] George Lavidas and Kornelis Blok. "Shifting wave energy perceptions: The case for wave energy converter (WEC) feasibility at milder resources". In: *Renewable Energy* 170 (2021), pp. 1143–1155. ISSN: 0960-1481. DOI: https://doi.org/10.1016/j.renene.2021.02.041. URL: https://www.sciencedirect.com/science/article/pii/S0960148121002093.

[78] Silvia Bozzi, Marianna Giassi, Adrià Moreno Miquel, Alessandro Antonini, Federica Bizzozero, Giambattista Gruosso, Renata Archetti, and Giuseppe Passoni. "Wave energy farm design in real wave climates: the Italian offshore". In: *Energy* 122 (2017), pp. 378–389. ISSN: 0360-5442. DOI: https://doi.org/10.1016/j.energy.2017.01.094. URL: https://www.sciencedirect.com/science/article/pii/S0360544217301019.

[79] Daniela Benites-Munoz, Luofeng Huang, and Giles Thomas. "Optimal array arrangement of oscillating wave surge converters: An analysis based on three devices". In: *Renewable Energy* 222 (2024), p. 119825. ISSN: 0960-1481. DOI: https://doi.org/10.1016/j.renene.2023.119825. URL: https://www.sciencedirect.com/science/article/pii/S0960148123017408.

[80] Eero Vartiainen, Gaëtan Masson, Christian Breyer, David Moser, and Eduardo Román Medina. "Impact of weighted average cost of capital, capital expenditure, and other parameters on future utility-scale PV levelised cost of electricity". In: *Progress in photovoltaics: research and applications* 28.6 (2020), pp. 439–453.

[81] Ljubomir Tančev. "Dams and Reservoirs in Macedonia". In: *Encyclopedia of Lakes and Reservoirs*. Ed. by Lars Bengtsson, Reginald W. Herschy, and Rhodes W. Fairbridge. Dordrecht: Springer Netherlands, 2012, pp. 186–191. ISBN: 978-1-4020-4410-6. DOI: 10.1007/978-1-4020-4410-6_150. URL: https://doi.org/10.1007/978-1-4020-4410-6_150.

[82] Helena Huđek, Krešimir Žganec, and Martin T. Pusch. "A review of hydropower dams in Southeast Europe – distribution, trends and availability of monitoring data using the example of a multinational Danube catchment subarea". In: *Renewable and Sustainable Energy Reviews* 117 (2020), p. 109434. ISSN: 1364-0321. DOI: https://doi.org/10.1016/j.rser.2019.109434. URL: https://www.sciencedirect.com/science/article/pii/S1364032119306422.

[83] Gabriela Costea, Martin T. Pusch, Doru Bănăduc, Diana Cosmoiu, and Angela Curtean-Bănăduc. "A review of hydropower plants in Romania: Distribution, current knowledge, and their effects on fish in headwater streams". In: *Renewable and Sustainable Energy Reviews* 145 (2021), p. 111003. ISSN: 1364-0321. DOI: https://doi.org/10.1016/j.rser.2021.111003. URL: https://www.sciencedirect.com/science/article/pii/S1364032121002938.

[84] IRENA. *ENERGY PROFILE France*. URL: https://www.irena.org/-/media/Files/IRENA/Agency/Statistics/Statistical_Profiles/Europe/France_Europe_RE_SP.pdf.

[85] IEA. *Real-Time Electricity Tracker*. URL: https://www.iea.org/data-and-statistics/data-tools/real-time-electricity-tracker?from=2018-1-1&to=2018-12-31&category=price.